THESIS FOR THE DEGREE OF DOCTOR OF PHILOSOPHY (PHD)

Protein phosphatases regulate the activity of nitric oxide synthase and the barrier function of endothelial cells

by Róbert Károly Bátori

Supervisor: Prof. Dr. Ferenc Erdődi

UNIVERSITY OF DEBRECEN

DOCTORAL SCHOOL OF MOLECULAR MEDICINE

DEBRECEN, 2018

TABLE OF CONTENTS

ABBREVIATIONS

AEBSF	4-(2-Aminoethyl)benzenesulfonyl fluoride
AJ	Adherens junction
ADP	Adenosine diphosphate
AMPK	Adenosine-monophosphate activated kinase
AKAP	A-kinase anchoring protein
ALI	Acute lung injury
APT-1	Acyl-protein thioesterase 1
ATP	Adenosine-triphosphate
ATPγS	Adenosine 5′-O-(3-thio) triphosphate
β-NADH	β-Nicotinamide adenine dinucleotide
BH4	(6*R*-)5,6,7,8-tetrahydrobiopterin
BPAEC	Bovine pulmonary artery endothelial cells
BSA	Bovine serum albumin
cAMP	3',5'-cyclic adenosine monophosphate
Cav-1	Caveolin-1
CaM	Ca^{2+}/calmodulin
CaMKII	CaM-dependent protein kinase II
cDNA	Complementary DNA
CDK-2	Cyclin-dependent kinase-2
cGMP	3',5'-cyclic guanosine monophosphate
CLA	Calyculin-A
CPI-17	C-kinase potentiated Protein phosphatase-1 Inhibitor of 17 kDa
Cys	Cysteine
DAF-2 DA	4,5-diaminofluorescein diacetate
DARPP-32	cAMP-regulated phosphoprotein of 32 kDa
DMEM	Dulbecco's modified Eagle’s medium
DNA	Deoxyribonucleic acid
DTT	Dithiothreitol
EBM-2	Endothelial basal medium-2
EC	Endothelial cells
ECIS	Electric cell-substrate impedance sensing
ECL	Enhanced chemiluminescence
eEF1A1	Translation elongation factor 1-α 1
EDTA	Ethylenediaminetetraacetic acid
EGCG	(-)-epigallocatechin-3-O-gallate
EGF	Epidermal growth factor
EGM-2	EC growth medium
EGTA	Ethylene glycol-bis(β-aminoethyl ether)-N,N,N',N'-tetraacetic acid

EIA	Enzyme immunoassay
eNOS	Endothelial nitric-oxide synthase
EPAC1	Exchange factor directly activated by cAMP 1
FA	Focal adhesion
FAD	Flavin adenine dinucleotide
FAK	Focal adhesion kinase
FBS	Fetal bovine serum
FMN	Flavin mononucleotide
GBPI	Gastrointestinal- and brain-specific PP1 inhibitor
GEF	Guanine nucleotide exchange factor
GJ	Gap-junction
GST	Glutathione *S*-transferase
HEPES	4-(2-hydroxyethyl)-1-piperazineethanesulfonic acid
HEK	Human embryonic kidney
HLMVEC	Human lung microvascular endothelial cells
HPAEC	Human pulmonary artery endothelial cells
HRP	Horseradish-peroxidase
HUVEC	Human umbilical vein endothelial cells
I1	Inhibitor-1
I2	Inhibitor-2
IEJ	Interendothelial junction
ILK	Integrin-linked kinase
iNOS	Inducible nitric-oxide synthase
JAM-A	Junctional Adhesion Molecule-A
KEPI	C-kinase enhanced PP1 inhibitor
Kf	Filtration coefficient
L-Arg	L-Arginine
67LR	67 kDa laminin receptor
Leu	Leucine
L-NAME	N_{ω}-nitro-L-arginine-methyl ester
L-NOARG	N^{G}-nitro-L-arginine
LPS	Lipopolysaccharide
M20	20 kDa small subunit of myosin phosphatase
MAPK	Mitogen-activated protein kinase
MC-LR	Microcystin-LR
MDPK	Myotonic dystrophy protein kinase
MEM	Minimum Essential Medium
MLC20	20 kDa regulatory light chain of myosin II
MLCK	Myosin light chain kinase
MOPS	3-(*N*-morpholino)propanesulfonic acid

MP	Myosin phosphatase
MYPT1	Myosin phosphatase target subunit 1
NADPH	Nicotinamide adenine dinucleotide phosphate
NF-κB	Nuclear factor kappa-light-chain-enhancer of activated B cells
nNOS	Neuronal nitric-oxide synthase
NM-II	Non-muscle myosin II
NO	Nitric oxide
OA	Okadaic acid
P2YK	Proline-rich tyrosine kinase 2
PAK	p21-activated kinase
PBS	Phosphate-buffered saline
PBST	PBS-Tween20
PEI	Polyethylenimine
PFA	Paraformaldehyde
PHI-1	Protein phosphatase holoenzyme inhibitor-1
PHI-2	Protein phosphatase holoenzyme inhibitor-2
PKA	cAMP-dependent Protein kinase
PKC	Protein kinase C
PKG	cGMP-dependent Protein kinase
PLA	Proximity ligation assay
PMA	Phorbol-12-myristate-13-acetate
PP1	Protein phosphatase type 1
PP2A	Protein phosphatase type 2
PP2B	Calcineurin
PP1cδ	PP1 catalytic subunit δ
PPM	Metal ion dependent phosphatases
PPP	Phosphoprotein phosphatases
PSP	Ser/Thr phosphatases
PVDF	Polyvinylidene difluoride
qPCR	Quantitative PCR
Rac-1	Ras-related C3 botulinum toxin substrate 1
Raf-1	RAF proto-oncogene serine/threonine-protein kinase
ROCK	Rho-A associated protein kinase
SDS-PAGE	Sodium dodecyl sulfate–polyacrylamide gel electrophoresis
Ser	Serine
SDS	Sodium dodecyl sulfate
sGC	Soluble guanylyl cyclase
siRNA	Small interfering RNA
SNO	S-nitrosothiol
Src	Proto-oncogene tyrosine-protein kinase Src

TBS	Tris-buffered saline
TCA	Trichloroacetic acid
TER	Transendothelial electrical resistance
Thr	Threonine
TJ	Tight junction
TM	Tautomycin
TNFα	Tumor necrosis factor-α
Tyr	Tyrosine
VE	Vascular endothelial
VEGF	Vascular endothelial growth factor
ZIPK	Zipper-interacting protein kinase
ZO-1	Zonula occludens-1
ZO-2	Zonula occludens-2

INTRODUCTION

The endothelial monolayer lines the lumen of blood vessels and serves as a semi-permeable membrane between the interior vascular compartment and the underlying tissues. Endothelial cells (EC), therefore contribute to the regulation of important physiological processes including but not limited to normal tissue-fluid homeostasis, host-defense reaction, blood flow regulation, and angiogenesis [1]. In response to inflammatory stimuli, the endothelial barrier can become compromised leading to severe and frequently fatal diseases. Although endothelial dysfunction is a common process in several diseases, the pharmacological options for treatment remain suboptimal. Thus, a better understanding of the precise mechanisms regulating the endothelial function is imperative.

Nitric oxide (NO), produced by endothelial nitric oxide-synthase (eNOS), is a major mediator of several key functions of the endothelium such as the regulation of a proper vascular tone and blood flow, smooth muscle cell proliferation and migration, leukocyte adhesion, platelet aggregation and angiogenesis [2]. Maintenance of the semi-permeable endothelial barrier properties also requires a basal level of NO [3]. The activity of eNOS and consequently the extent of NO production is regulated by protein-protein interactions, its cellular localization, the expression level of eNOS and reversible phosphorylation/dephosphorylation at serine (Ser), threonine (Thr) and tyrosine (Tyr) residues. The inhibitory phosphorylation of eNOS at Thr495 is a major determinant of eNOS activity. The kinases responsible for phosphorylation of this site such as protein kinase C (PKC) and Rho-A activated kinase (ROCK) are well characterized. However, the phosphatases that dephosphorylate phospho-Thr495, and the phosphatase holoenzymes responsible for eNOS regulation are poorly explored. Protein phosphatase-1 (PP1), -2A (PP2A) [4-5] and -2B (PP2B) [6-7] have been implicated in eNOS dephosphorylation in a site-specific manner. Both PP1 and PP2A exist in the cells in various holoenzyme forms, however, there is very limited information on the ones which are involved in eNOS dephosphorylation.

The endothelial barrier function is also dependent upon the activation of actomyosin contractile machinery, intercellular gap formation, and cytoskeletal reorganization. Phosphorylation of the regulatory myosin light chains (MLC20) which is triggered by Ca^{2+}/calmodulin-dependent MLC kinase (MLCK) and/or ROCK [8], is a key mechanism underlying

EC contraction and barrier dysfunction [9]. Dephosphorylation of phospho-MLC20 is mediated by the myosin phosphatase (MP) holoenzyme, which is barrier protective. MP consists of PP1cδ catalytic subunit, the myosin phosphatase target subunit-1 (MYPT1) and a 20 kDa subunit (M20) [10]. The activity of the MP holoenzyme is regulated by phosphorylation/dephosphorylation of the MYPT1 regulatory subunit at Ser and Thr residues. Phosphorylation of Thr696 and Thr853 by ROCK [11] inhibits the activity of PP1 catalytic subunit (PP1c), while phosphorylation of the adjacent Ser695 and Ser852 by cAMP-dependent protein kinase (PKA) prevents the inhibitory phosphorylation by ROCK [12]. Alternatively, MP activity is regulated by the dephosphorylation of MYPT1 via PP2A and PP2B [13-14]. It has been reported that a green tea polyphenol (-)-epigallocatechin-3-O-gallate (EGCG) activates PP2A in a cAMP/PKA dependent manner that results in dephosphorylation of MYPT1 at Thr696 [15] and activation of MP also leading to stimulation of eNOS activity [16]. Other positive regulators of the endothelial barrier are the extracellular purines (e.g., ATP, ATPγS, ADP, adenosine) which enhance barrier integrity, at least in part, via activation of MP by PKA dependent phosphorylation of MYPT1 [17-18].

In the following studies, we have investigated the roles of the above signaling mechanisms in the regulation of eNOS and endothelial barrier function with special emphasis on how inhibition and activation of PP2A and the MP holoenzyme may be involved in these events. We assess the influence of these phosphatases on the regulation of the phosphorylation level of eNOS which is coupled with altered NO production and barrier function. We also seek to define and compare the molecular mechanisms that mediate adenosine (Ado)- and ATPγS-induced purinergic receptor activation and barrier strengthening in human lung microvascular endothelial cells (HLMVECs).

LITERATURE REVIEW

The vascular endothelium

The vascular endothelium is composed of a single layer of closely connected squamous endothelial cells (ECs) that line the interior space of the whole circulatory system including the heart. The total area of the vascular endothelial surface in human has been estimated to be about 350 m^2 [19]. One of the major functions of the endothelium is to provide a selective barrier between the blood and surrounding tissues, thus limiting the exit of cells, fluids, and high molecular weight substances from the blood vessels to the organs [20]. This feature of endothelial cells is termed permeability [20]. The semipermeable properties of the endothelium not only enable nutrient and metabolic byproduct exchange but also allow for immune cells to exit to the surrounding tissues primarily at the level of capillaries and postcapillary venules[21]. However, the importance of the ECs was underappreciated for a long time. Until the 1950's the prevailing view on the function of the endothelium was that it was "little more than a sheet of nucleated cellophane", with no other specific functions than providing selective permeability to water and electrolytes [22]. The invention of the electron microscope gave a new impetus to the field, at least from a morphological perspective and over time it has become generally acknowledged that there are several kinds of endothelial cell types with certain structural and functional differences.

Structural characteristics of different endothelial cell types

Typically endothelial cells are long (nearly 30 μm) and thin cells that are approximately 3 μm wide at the nucleus and 0.2 μm at the periphery of the cells [22]. The shape of ECs varies across the vasculature. In a comparative study, Kibria *et al.* investigated whether the size and shape of endothelial cells from rat blood vessels of the pulmonary trunk differ from those of the pulmonary veins, the aorta and the inferior vena cava [23]. Aortic ECs were long and narrow (55×10 μm), ECs of the pulmonary artery were shorter and wider (30×14 μm), while pulmonary vein ECs were large and round shaped (48×10 μm), however, ECs of the inferior vena cava were long and narrow (50×14 μm) similar to aortic ECs. In a study of the microcirculation in rats, arteriole ECs were long and spindle-shaped, capillary ECs had irregular shapes, and postcapillary venule ECs were large, elliptical, or irregularly shaped [24].

Structural differences found in capillary endothelium led to subclassification of endothelial cells into continuous non-fenestrated, continuous fenestrated and discontinuous (Fig. 1.) [25]. The continuous endothelia are the predominant type in the walls of arterioles, capillaries, and venules in skeletal, smooth and cardiac muscles, skin, heart, lung, brain as well as in large arteries and veins. Continuous fenestrated endothelia are found in the capillaries of endocrine and exocrine glands, in the gastric mucosa, as well as in the glomerular and peritubular capillaries of the kidney. Fenestrae are transcellular pores that extend through the cell, usually with a thin, 5-6 nm non-membranous diaphragm [26]. Fenestrated endothelial cells occur in locations with increased filtration or increased transendothelial transport and are characterized by numerous transcellular "gaps" with 50-80 nm width. The frequency of fenestrae can be influenced by cytokines, ischemia/reperfusion, as well as by growth factors. Discontinuous endothelia are found in sinusoidal vascular beds of the liver, spleen, and even in bone marrow. Liver sinusoidal ECs possess larger fenestrations (100-200 nm) that lack a diaphragm and contain gaps within individual cells [27].

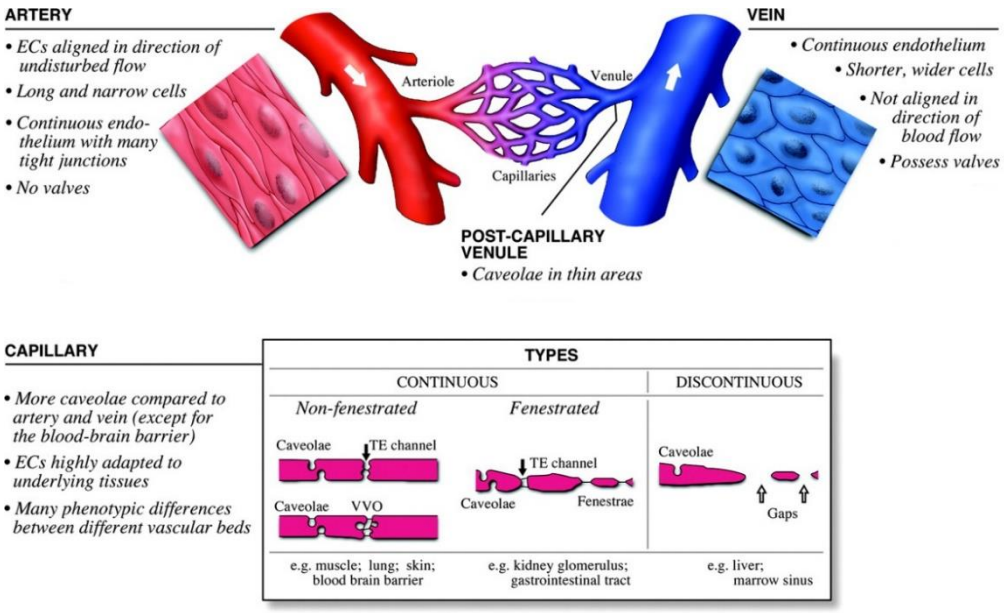

Figure 1. Classification of endothelial cells in arteries, veins and capillaries. Phenotypic differences between the major types of endothelium are presented. In continuous non-fenestrated endothelium, water and small solutes (with less than <3 nm radius) pass between ECs, while larger solutes use the transendothelial channels or caveolae mediated transcytosis. Continuous fenestrated endothelium demonstrates greater permeability to water and small solutes, compared to non-fenestrated ECs. Discontinuous endothelium is characterized by gaps and poorly organized basement membrane [modified from W. Aird, 2007].

Functional differences between endothelial cells

Endothelial cells regulate many functions of blood vessels, including permeability [28], leukocyte trafficking and hemostasis [25, 29], vascular tone [30], angiogenesis and vasculogenesis [31] and blood coagulation [32].

ECs from different vascular beds are similar, however differences in the permeability or responsiveness of ECs isolated from different regions of blood vessels have been observed [33-35], which can be detected in intact vessels as well [36-37]. Several techniques exist to determine the vascular permeability of isolated organs or cellular monolayers. A widely accepted technique used to measure the integrity of an endothelial monolayer is through measurements of transendothelial electrical resistance (TER). In a comparative study Blum *et al.* showed that TER values of microvascular endothelial cells are approximately ten times higher than that of ECs from large vessels [38], indicating the presence of tighter connections between microvascular ECs. Using an isogravimetric method, filtration coefficient (Kf) can be determined, that is an indicative of changes in the weight of isolated organs, resulting from changes in hydrostatic pressure [39]. Basal vessel wall Kf measurements of isolated lungs of various species indicated that total Kf is on average 19% arterial, 37% venous, and 42% microvascular, indicating that under basal conditions the arteries are less permeable to liquid infiltration than the venules or capillaries [1]. These data indicate that microvascular endothelial cells express higher levels of tightly regulated intercellular adhesion molecules that are responsible for regulating the flux of water and macromolecules. Intracellular signals regulating the endothelial barrier may also vary depending on where they reside in the circulation.

The endothelial barrier

Cell-cell and cell-extracellular matrix interactions

The barrier function of the endothelium derives from the integrity of EC monolayer, which is determined by interendothelial junctional complexes (IEJs), the reorganization of cytoskeletal proteins, and connections to the extracellular matrix [40-42]. Based on their structural and functional characteristics, three type of IEJs have been identified: gap junctions (GJs), adherens junctions (AJs) and tight junctions (TJs) (Fig. 2.) [43].

GJs link the cytoplasm of two adjacent cells and regulate the exchange of ions, small signaling molecules (e.g., cAMP, cGMP), and small metabolites (glucose) within the continuous monolayer of ECs [44]. Gap junctions are found primarily in larger vessels. The main structural proteins of GJs are transmembrane proteins of the connexin family. Six connexins assemble in the plasma membrane to form hexameric assemblies called connexon, which aligns in head-to-head direction with another connexon of the neighboring cell, thus forming a channel between the two cytoplasmic compartments [45]. In ECs, gap junctions play an important role in the regulation of blood coagulation [46], EC migration, and tube formation [47], and regulate the endothelial monolayer permeability in response to bacterial lipopolysaccharide (LPS) [48].

AJs are the major determinant of the endothelial barrier and are the most ubiquitous type of intercellular junction found in all endothelial cells [41]. AJs are impermeable to macromolecules and other large proteins like albumin (69 kDa) [49]. The main structural protein of endothelial AJs is vascular endothelial (VE)-cadherin that mediates homophilic binding and adhesion between adjacent endothelial cells in a Ca^{2+}-dependent manner [50]. The cytoplasmic region of VE-cadherin is linked to the actin cytoskeleton through adapter proteins (α-, β-, and γ-catenins), that play an important role in the organization of AJs and consequently in the regulation of endothelial permeability [1]. VE-cadherin is stabilized by its association with p120-catenin, which serves as a scaffolding protein that also binds to protein kinases (Src-kinase, receptor tyrosine kinases) and phosphatases, and thus is a crucial component of the signaling pathways that regulate AJs [51].

TJs are zipper-like structures that represent approximately 20% of total junctional complexes in endothelial cells [1]. They are less common in the peripheral microvasculature compared to AJs but important components of more specialized tissue (e.g., the blood-brain-barrier) [52]. Endothelial TJs are composed of integral transmembrane protein (occludin, claudins (3/5) and Junctional Adhesion Molecule-A; JAM-A) and intracellular membrane proteins like zona occludens (ZO-1, ZO-2) that connect JAM-A to the actin cytoskeleton [53]. TJs provide a more stringent barrier that prevents the passage of much smaller molecules (<1 kDa), even restricting the flow of small inorganic ions (e.g., Na^{+}) [54]. Although the role of TJs in the regulation of endothelial permeability is not fully understood [1], published studies have shown that treatment of ECs with the inflammatory cytokine TNF-α resulted in the dislocation of ZO-1 from the cell border and the disassembly of cadherins in parallel with the loss of barrier function [55].

Focal adhesions (FAs) are adherent structures located at the basal or basolateral side of endothelial cells that provide connections to the surrounding extracellular matrix (ECM) in the vascular wall. FAs are composed of integrins, a type of transmembrane receptor that connects the actin cytoskeleton to the ECM via cytoplasmic linker proteins (e.g., talin, vinculin, α-actinin or paxillin) [56]. *In vitro* studies have demonstrated that disruption of the integrin-matrix interaction results in cell detachment from fibronectin-coated cell culture dishes [57], indicating that integrins are important in the stable attachment of endothelial monolayers. Vascular endothelial growth factor (VEGF) treatment of ECs induces the recruitment of focal adhesion kinase (FAK) to integrins, facilitating the assembly of focal adhesion [58] and increasing microvascular permeability [59].

Cytoskeletal elements involved in mediation of endothelial permeability

There are three main types of cytoskeletal polymers: microtubules, intermediate filaments and microfilaments (or actin-filaments) [60]. Since the role of intermediate filaments in endothelial barrier function is not yet clear, only the role of the other two types of cytoskeletal elements will be discussed.

The major cytoskeletal protein in all cells are the actin filaments composed of (F)-actin polymers [61]. The stability of actin filaments is dependent upon the concentration of globular (G)-actin within the cell. Maintenance of the intracellular concentration of G-actin above a critical concentration (0.1 μM) favors actin polymerization and the formation of actin filaments [62]. Under normal physiological conditions, actin filaments are randomly distributed throughout the cell (short filaments and diffuse actin monomers) and at the peripheral boundary of cells (cortical actin) [62]. Exposure of endothelial cells to barrier disruptive agents such as thrombin leads to stress fiber formation [63]. In contrast, treatment of endothelial cells with barrier-protective agents like sphingosine-1-phosphate, leads to the reorganization of actin filaments that localize at the cell periphery (cortical-actin formation) and strengthen cell-cell contacts [64].

Microtubules are stiff tubular structures that are formed of heterodimeric α and β tubulin subunits. In endothelial cells, microtubules are cross-linked to actin filaments and can affect endothelial permeability through changes in the actin filaments [65]. Dynamic rearrangements of microtubules impact the organization of other cytoskeletal components and stabilization of microtubules has been shown to protect the endothelium against actin stress fiber formation and

hyperpermeability [55]. Exposure of endothelial cells to inflammatory cytokines like TNF-α leads to the destabilization and disassembly of microtubules, and consequently barrier disruption [55]. Nocodazole treatment activates guanine nucleotide exchange factors (GEFs) and signaling through the Rho family of GTPases inactivates MP leading to actin stress fiber formation [66]. In contrast, elevation of cAMP levels by cAMP-elevating agents leads to stabilization of microtubules in endothelial cells through the activation of PKA [67].

Regulation of the endothelial barrier function by reversible phosphorylation/ dephosphorylation

Reversible protein phosphorylation/dephosphorylation

Reversible protein phosphorylation, catalyzed by protein kinases and protein phosphatases, is one of the most common types of posttranslational modification that affects approximately one-third of the proteins in eukaryotic organisms [68]. Protein phosphorylation regulates signaling pathways controlling cellular metabolism, transcription, cell-cycle progression, differentiation, cytoskeleton arrangement and cell movement, apoptosis, intercellular communication, and neuronal and immunological functions [69]. Protein phosphorylation is accomplished by protein kinases that transfer the terminal γ-phosphate group of ATP to serine (Ser), threonine (Thr) or tyrosine (Tyr) residue of protein substrates [70]. Protein phosphatases provide reversibility of these phosphorylation processes by hydrolyzing the phospho-ester groups from the above residues [71]. The human genome encodes 518 protein kinases that can be classified into Ser/Thr-, Tyr-, or dual specific protein kinases [72-73]. More than 420 genes encode Ser/Thr specific kinases which are responsible for 98.2% of all phosphorylation events within the cells [74]. However, the number of protein phosphatases is less than one-third of the kinases. Intriguingly, the protein phosphatase family is comprised of only ~150 members, of which 107 are Tyr phosphatases and less than 40 are Ser/Thr phosphatases [75-76]. Despite the relatively small number of Ser/Thr protein phosphatase catalytic subunits, greater diversity in regulating physiological responses is achieved through their association with numerous regulatory subunits, forming holoenzymes with distinct activity and substrate specificity [71]. In the first part of our experiments we have focused on the involvement of Ser/Thr-specific protein phosphatases in the regulation of eNOS and EC barrier function, and

therefore next the primary characteristics of these phosphatases with special attention to PP1 and PP2A will be summarized.

Classification of Ser/Thr phosphatases

Based on their substrate specificity and sensitivity to thermostable inhibitory proteins (inhibitor-1 and inhibitor-2) as well as to heparin, the Ser/Thr phosphatases (PSPs) were initially classified into two subclasses: protein phosphatase-type 1 (PP1) and type 2 (PP2) [77]. According to a more recent classification, the PSPs comprise three major families: phosphoprotein phosphatases (PPPs), metal-dependent protein phosphatases (PPMs) and the aspartate-based phosphatases (Fig. 2.) [71]. PPPs can be further classified into seven subclasses: protein phosphatase 1 (PP1), -2A (PP2A) and -2B (PP2B, also termed calcineurin) that contain Fe^{2+}/Zn^{2+} ions in their active sites, and the novel protein phosphatases such as PP4, PP5, PP6, PP7. The PPM family includes PP2C and pyruvate dehydrogenase phosphatase. A common feature of the PPM family is the catalytic requirement for additional metal ions (Mn^{2+}/ Mg^{2+}) ions [71, 78]. The third group, the aspartate-based phosphatases, has only two members, the TFIIF-associating component of RNA polymerase II CTD phosphatase (FCP) and small CTD phosphatase (SCP) and both share a distinguishing

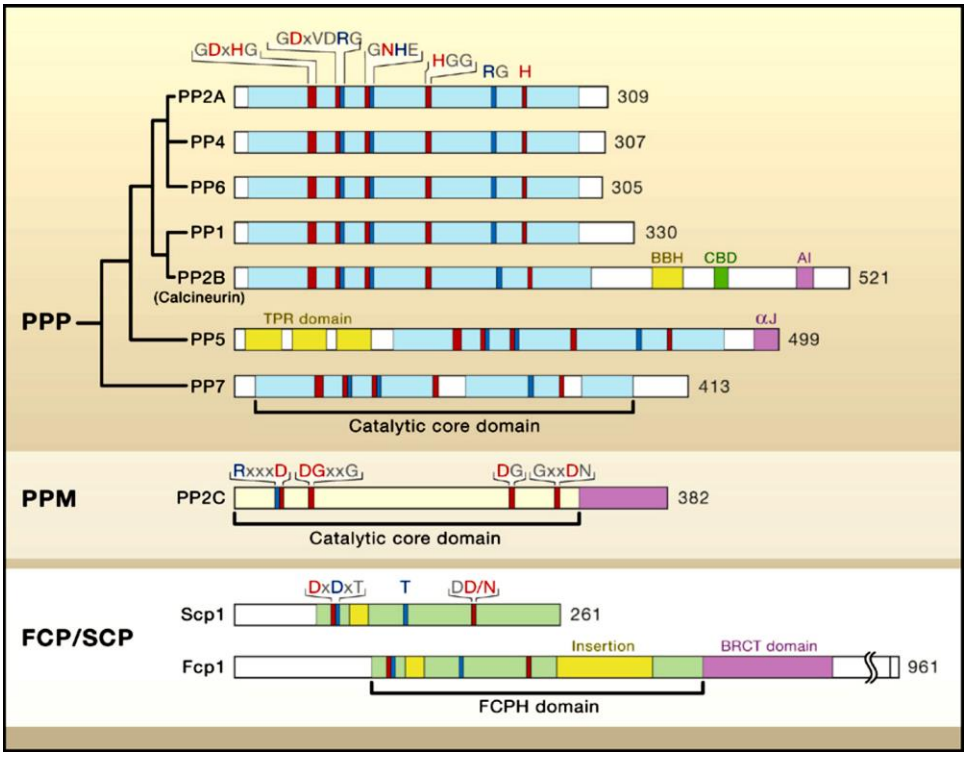

Figure 2. Classification of Ser/Thr phosphatases (Shi et al., 2009).

DxDxT/V motif in their active site [71, 79]. The catalytic subunits of phosphatases are considered less specific compared to protein kinases. PP1, PP2A and PP2B of the PPP family, together with PP2C of the PPM family, account for the vast majority (more than 90%) of the protein serine/threonine phosphatase activity *in vivo* and selectivity is achieved through regulatory subunits.

Protein phosphatase 1

PP1 catalytic subunit (PP1c) is widely expressed in all eukaryotic cells. PP1c has been shown to be involved in the regulation of actin and actomyosin rearrangement, cell cycle and apoptosis, protein synthesis, glycogen metabolism and the regulation of receptors and ion channels [80]. PP1 holoenzymes consist of a 35–38 kDa highly conserved catalytic subunit (PP1c) which in mammals are encoded by three genes and have five splice variants that are: PP1cα1, PP1cα2, PP1cγ1, PP1cγ2, and PP1cβ (also termed as PP1cδ), furthermore various regulatory subunits that provide substrate specificity (Fig. 3.) [80-81]. PP1cα, PP1cβ, and PP1cγ1 are ubiquitously expressed, while PP1cγ2 is expressed exclusively in the testis [74].

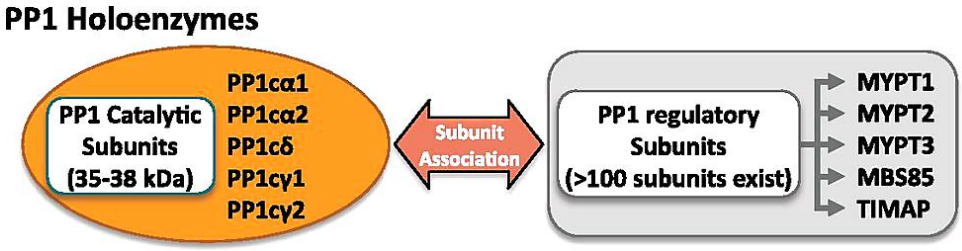

Figure 3. Schematic representation of PP1 holoenzymes.
Modified figure, Butler et al., 2013.

The structure of PP1c shows compact folding with a central β-sandwich excluding the N- and C-terminals. The active site is located at the bifurcation center of a Y-shaped substrate binding groove where three histidine, two aspartates, and one asparagine coordinate the Fe^{2+} and Zn^{2+} ions that contribute to the dephosphorylation process. They also play an important role in the inhibitory mechanism of cell-permeable toxins. The arms of this surface depression are known as C-terminal, hydrophobic and acidic grooves [80].

Although PP1c is catalytically active on its own, its substrate specificity is very low [82], which highlights the importance of the associated regulatory subunits. To date, PP1c has been reported to form functional complexes with over 200 targeting proteins [74] that can regulate the catalytic activity of PP1c directly or indirectly, provide substrate specificity and influence its

cellular localization. A common feature of the regulatory subunits is that most of them interact with PP1 via a consensus sequence (K/R)x_1(V/I/)x_2(F/W), (where x_1 can be absent, and both x_1, x_2 can be any amino acid except Phe, Ile, Met, Tyr, phospho-Ser, and Asp or Pro. This sequence is most commonly known as RVxF (or KVKF) motif [74]. In addition to the PP1c binding motif, the targeting subunits also possess substrate binding site(s).

Based on their function, the regulatory proteins can be classified into three distinct groups, which includes the inhibitors, substrate-specifiers (targeting subunits) and substrates. The endogenously expressed PP1-specific inhibitory proteins are the thermo-stable inhibitor-1 (I1), inhibitor-2 (I2), phospho-CPI-17 and the dopamine and cAMP-regulated phosphoprotein of 32 kDa (DARPP-32), they all block the catalytic activity of PP1 [74]. Among the targeting subunits, the MYPT-family has been well characterized in smooth muscle cells [10], but regulatory roles in non-muscle cells are also emerging [83-84]. A-kinase anchoring protein of 220 kDa (AKAP220) also possess a PP1c binding motif [75]. Well-characterized PP1c substrates are the Aurora kinase or the Ser/Thr specific protein kinase Nek2 [80]. The activity of PP1c can be regulated by phosphorylation. CDK-2 has been reported to phosphorylate a C-terminal Thr-320 residue in a cell-cycle dependent manner, thus inhibiting the phosphatase activity of PP1c [85-86].

Protein phosphatase 2A

Similar to PP1c, PP2A plays an important role in the regulation of a variety of cellular processes like cell-cycle progression [87], cell signaling [88] apoptosis [89] and tumor suppression [15]. PP2A is found predominantly in heterotrimeric forms (>90%), but heterodimers also exist. The holoenzyme is comprised of a 36 kDa catalytic subunit (PP2Ac), a 65 kDa scaffolding subunit A, and a variable regulatory B subunit (Fig. 4.) [90]. The catalytic (C) and scaffolding subunits (A) each have two isoforms (α and β), which are always associated, and together they form the core enzyme (AC). [91]. The more dissociable regulatory B subunits can be classified into 4 structurally unrelated groups each encoded by 3-5 related genes of the B subunit family and these include the B or PR55 (α, β, γ, and δ), the B' or PR56/61 (α, β, γ, δ and ε), B'' or PR48/59/72/130 and B''' or PR93/110/SG2NA/striatin [92]. Unlike PP1c, PP2A binding motifs on PP2A subunits or substrates have not yet been identified [90].

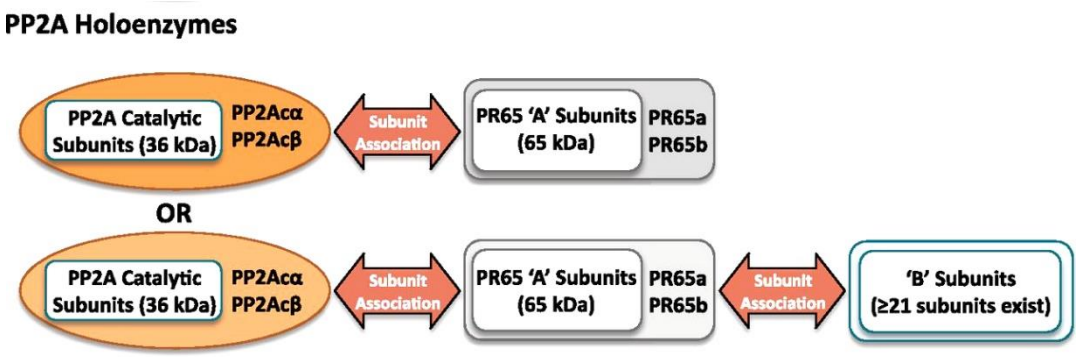

Figure 4. Schematic representation of PP2A holoenzymes.

Modified figure, Butler et al., 2013.

The multiplicity of regulatory subunits and isoforms suggests the existence of functional differences between PP2A holoenzymes, and also indicates that subunit combinations have an important role in modulating not only substrate specificity but also the catalytic activity of PP2A [93]. The activity of PP2A holoenzymes can be further regulated by posttranslational modifications. The phosphorylation of Tyr-307 residue within PP2Ac by $p60^{v\text{-}src}$ kinase or other receptor- or non-receptor tyrosine kinases can effectively decrease the activity of the enzyme [94]. Furthermore, it also has been shown that phosphorylation of the B'δ subunit on Ser-566 by PKA can increase PP2A activity [95]. Another posttranslational modification is the reversible methylation of PP2A at Leu309 by leucine carboxyl methyltransferase 1, which facilitates the binding affinity of the PP2A core enzyme to distinct regulatory subunits [96]. However, the impact of methylation on PP2A activity is not yet established [97].

Several toxins have been discovered to inhibit the activity of protein phosphatases, and most of these are naturally occurring membrane permeable non-selective phosphatase inhibitors. Both PP1c and PP2Ac activity can be inhibited by okadaic acid (OA), fostriecin, cantharidin and nodularin, microcystin-LR (MC-LR), calyculin-A (CLA) and tautomycin (TM), in a concentration-dependent manner. Okadaic acid is a polyether isolated from the marine sponge, *Halicondria okadai* [98]. OA has higher selectivity for PP2A (IC_{50} values: PP1 15-50 nM; PP2A 0.1-0.3 nM). MC-LR is a monocyclic heptapeptide isolated from freshwater cyanobacteria (*Microcystis aeruginosa*) with a similar potency for both PP1 and PP2A (IC_{50} values: PP1 0.3-1 nM; PP2A 0.1-1 nM) [99]. MC-LR binding results in irreversible inhibition of the phosphatase, because the toxin covalently couples to a cysteine residue at the hydrophobic loop adjacent to the

active center of PP1c and PP2Ac enzymes, thus completely and permanently blocking the access of the substrate to the active sites [100]. CLA was isolated from the marine sponge, *Discodermia calyx* [101] and was first identified as a strong anti-tumor metabolite (IC_{50} values: PP1 0.4 nM; PP2A 0.25 nM). TM was first isolated from *Streptomyces spiroverticillatus* and exhibits partial preference for inhibition of PP1 (IC_{50} values: PP1 0.23-22 nM; PP2A 0.94-32 nM).

CLA and TM inhibit both PP1 and PP2A *in vitro*, however, their inhibitory effects in cellular systems remain controversial. In our experiments we have used CLA at a concentration (10 nM) that results in partial, but selective inhibition of PP2A [102], and TM (1 μM) that results in predominant inhibition of PP1c [102-104].

Myosin phosphatase

Structure of myosin phosphatase

MP was first isolated from chicken gizzard [10] as a trimeric holoenzyme consisting of a ~38 kDa PP1cδ catalytic subunit, a 110-130 kDa myosin phosphatase targeting subunit 1 (MYPT1; also termed as myosin binding subunit, M110 or M130/133), and a small 20-21 kDa subunit (M20) (Fig. 5.) [105]. The function of M20 is poorly understood, however, in a study on permeabilized renal arteries and cardiac myocytes, the M20 subunit increased Ca^{2+} sensitivity in muscle contraction [106]. The main properties of MP can be attributed to a complex of PP1cδ and MYPT1 without M20 as a functional subunit [107]. Additionally, the M20 expression has not been detected in skeletal muscle or brain [108]. MYPT1 has a crucial role in determining the substrate specificity of MP via targeting the PP1 catalytic subunit to the diphospho-myosin light chain (ppMLC20) [109-110]. However, the multiple subcellular targets of MYPT1 suggests a much broader role of MP in cellular processes than only dephosphorylation of ppMLC20 [111].

Human MYPT1 is a product of a single gene (PPP1R12A) located at chromosome 12q15-q21 [112]. It is expressed in many cell types, but at higher concentration in phasic smooth muscle [107]. Several MYPT1 isoforms with distinct molecular masses (110-133 kDa) are generated by alternative splicing and can be distinguished by the absence or presence of a central insert (between amino acid 512-552) and a C-terminal leucine zipper motif (L) [111, 113]. The PP1c binding KVKF motif is located at the N-terminal region of MYPT1 isoforms, between amino acids 35-38 [75]. This motif interacts with six amino acid residues of PP1c that forms a hydrophobic groove (Ile^{169}, Leu^{243}, Phe^{257}, Leu^{289}, Cys^{291}, and Phe^{293}) and anchors PP1cδ to MYPT1 without affecting its

catalytic activity [111]. The PP1c binding motif is flanked by two domains: an N-terminal arm that precedes the KVKF motif (amino acids 1-34) and the ankyrin repeat domains (8 repeats from amino acids 39-296) [114]. Although only the KVKF motif has high affinity to PP1c, other secondary interaction sites also exist that may stabilize MYPT1-PP1cδ binding. These include residues 1–22 of the N-terminal arm, the amino acid region between 167–295 of the ankyrin repeats, and a site within the sequence from residue 304 to 511 [115]. Two nuclear localization signals have also been identified in MYPT1, one at the N-terminal (amino acids 25-33) and another at the C-terminal amino acids (843-852) region [116].

Regulation of myosin phosphatase

The regulation of MP in smooth muscle and in endothelial cells is similar. The activity of MP can be regulated (activated or inhibited) by reversible MYPT1 phosphorylation via Ser/Thr kinases, the binding of inhibitory proteins, and the dissociation of the holoenzyme [111]. Among the aforementioned regulatory processes, the first two have been intensively investigated.

Two major phosphorylation sites of MYPT1 are the Thr[696] and Thr[853] residues (Fig. 6.) [81], which have a prominent role in the regulation of cell contractility. Both can be phosphorylated by ROCK leading to inhibition of MP [117], thus a unique mechanism of phosphatase inhibition (autoinhibition) is exemplified by regulatory phosphorylation of MYPT1. The amino acid sequences flanking the Thr[696] residue of MYPT1 exhibits a high degree of similarity to that

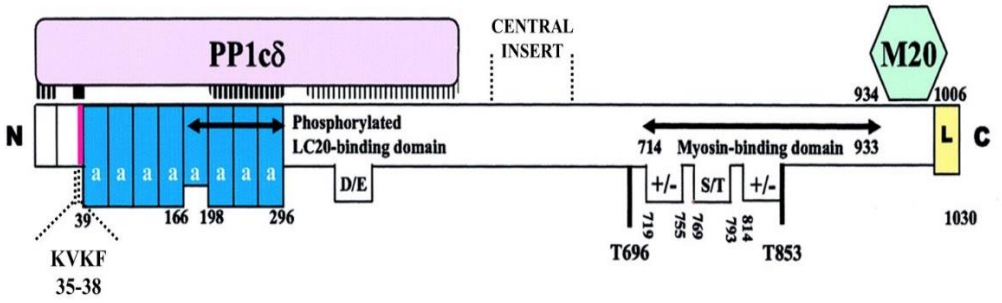

Figure 5. Schematic representation of human myosin phosphatase holoenzyme. Regions of MYPT1 are indicated as follows: *KVKF* PP1c-binding motif; *a*, ankyrin repeat; *D/E*, acidic region; +/–, ionic region; *S/T*, Ser- and Thr-rich region; *L*, leucine zipper. Residue numbers are given, and some phosphorylation sites are indicated (*bold lines*). For the holoenzyme, interactions of varying strengths between MYPT1 and PP1c are indicated (lines with varying thickness). Suggested binding sites for phosphorylated light chain and myosin are indicated by *arrows* [modified figure, Hartshorne et al., 2004].

observed in the myosin light chain amino acid sequence that flanks Ser^{19} (pMLC20-S^{19}). Consequently, the phosphorylated form of MYPT1 binds to the active site of PP1cδ catalytic subunit and suppresses its phosphatase activity [118]. Other kinases that have been implicated in phosphorylating MYPT1 at the Thr^{696} residue include integrin-linked kinase (ILK) [119], myotonic dystrophy protein kinase (MDPK) [120], zipper-interacting protein kinase (ZIPK) [121], Raf-1 kinase [122], and p-21 activated kinase (PAK) [123]. Although the physiological role of Thr^{696} phosphorylation is not yet well understood, it reflects the convergence of different signaling pathways on MP [111]. Phosphorylation of MYPT1 at Thr^{853} by ROCK has been shown to decrease the affinity of MP toward its phospho-myosin substrate [124]. However, a confocal microscopic study of Shin et al. demonstrated that although the phosphorylation of MYPT1 by ROCK induced translocation of MP holoenzyme to the plasma membrane, it did not elicit dissociation of the holoenzyme [125], thus dissociation of MP upon phosphorylation at Thr^{696} and Thr^{853} is unlikely [126].

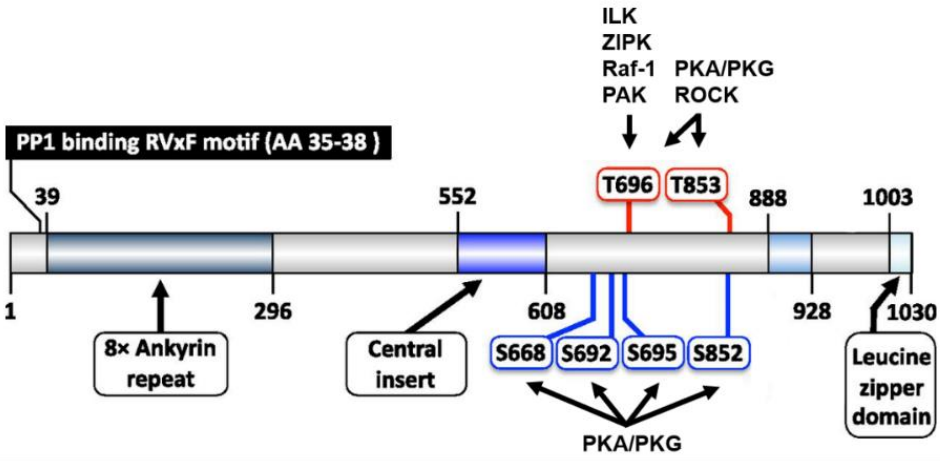

Figure 6. Major phosphorylation sites of human MYPT1 involved in the regulation of cell contractility and barrier function. Modified figure, Butler et al., 2013**.**

On the other hand, phosphorylation of MYPT1 at specific serine residues prevents the inhibitory phosphorylation of MYPT1 by ROCK, thus preserving MP in its active holoenzyme form. These two major residues are the Ser^{695} and Ser^{852}, which can be phosphorylated in a cyclic nucleotide (cAMP/cGMP) dependent manner by protein kinase A (PKA) [12] and protein kinase G (PKG) [127]. However, dual-phosphorylation of these sites by PKA/PKG, at Ser^{695}/Thr^{696} and/or Ser^{852}/ Thr^{853} has also been reported with no significant effect on MP activity [128]. Phosphorylation of Thr^{696} and Thr^{853} by ROCK precludes the phosphorylation of the preceding Ser residues, thus

phosphorylation of the Thr residues by PKA/PKG can only be observed when the preceding Ser residues are already phosphorylated [129].

MYPT1 contains several other phosphorylation sites as well, namely Ser^{445}, Ser^{472}, and Ser^{910}, that have important roles in regulating cell adhesion [130] and the mitosis-specific phosphorylation of Ser^{432} by cdc2 kinase increases MP holoenzyme activity towards phosphorylated myosin [131].

It is important to note that MP holoenzyme activity can also be regulated by interacting proteins that can inhibit or activate the holoenzyme. The most important endogenous inhibitor of MP holoenzyme is the small (17 kDa) protein phosphatase 1 regulatory subunit 14A also known as CPI-17, that was first described in porcine aortic homogenates [132]. The amino acids 35-140 in CPI-17 are responsible for recognition of MYPT1 [133]. Unlike inhibitor-1 and inhibitor-2, CPI-17 inhibits both the PP1cδ catalytic subunit and the MP holoenzyme in a phosphorylation-dependent manner. Phosphorylation of CPI-17 at Thr^{38} by multiple kinases such as PKC (α and δ) or by ROCK, ZIPK, ILK, and PAK (which also phosphorylates MYPT1) enhances its inhibitory potency [134-135]. However, Tyr^{41} has a prominent role in the prevention of CPI-17 dephosphorylation at Thr^{38}, as Ala substitution at Tyr^{41} eliminated phosphorylation-dependent inhibition, and enabled phospho-Thr^{38} dephosphorylation by MP itself [133].

Other MP holoenzyme inhibitory proteins show sequence similarities to CPI-17. These homologs are the protein phosphatase holoenzyme inhibitor-1, and -2 (PHI-1 and PHI-2), kinase C-enhanced PP1 inhibitor (KEPI), and gastrointestinal- and brain-specific PP1 inhibitor (GBPI). The inhibitory domain of the CPI-17 family members are conserved, thus they all display structural similarities, however, the PP1c binding KVKF motif at the N-terminal domain of PHI-1, KEPI, and GBPI also can be identified [136].

The impact of pCPI-17 versus MYPT1 in the regulation of MP holoenzyme activity is still not exactly clear, however, tissue-specific differences can be identified (CPI-17 is higher in phasic smooth muscles) [111, 137]. CPI-17 is expressed in endothelial cells where it has been shown to be involved in actin cytoskeleton reorganization in response to inflammatory stimuli [138]. At the same time, a number of studies have emerged suggesting that MYPT1 phosphorylation at Ser/Thr residues is a primary determinant of MP activity and this is also reflected in MLC20 phosphorylation levels that mirror changes in endothelial barrier function [66-67, 139-140].

Regulation of actomyosin contractile machinery

Similar to smooth muscle cells, the phosphorylation of the 20 kDa myosin-II regulatory light chain (MLC20) in ECs is essential for actomyosin contraction, which is a key step in the regulation of permeability, cell adhesion, migration, and cytokinesis. Similar to muscle myosin II, the ubiquitously expressed non-muscle myosin II (NM-II) consists of two 230 kDa heavy chains, two 20 kDa regulatory light chains (MLC20) and two 17 kDa essential light chain peptides, that stabilize the structure of the heavy chains [141]. Phosphorylation of MLC20 evokes the reversible binding of the filamentous homodimer NM-II to the actin cytoskeleton and cross-linking the microfilaments. The elevated Mg^{2+}-ATPase activity of NM-II, promotes the sliding of microfilaments against each other, resulting in increased cytoskeletal tension [43, 141-142]. As previously described, the microfilaments are connected to the AJs, TJs, and focal adhesion molecules, thus an increase in contractile forces is usually leading to elevated endothelial permeability [143].

The regulation of EC permeability involves the reversible phosphorylation of MLC20 at Ser^{19} and subsequently at Thr^{18} by the Ca^{2+}/calmodulin dependent MLCK [144], and dephosphorylation by MP [110]. ECs express a higher molecular weight MLCK (~214 kDa) than the smooth muscle isoform which shares the same primary structural elements (catalytic domain and Ca^{2+}/calmodulin binding motif), but it also includes an N-terminal 922 amino acid fragment that is important in mediating protein-protein interactions with multiple kinases, suggesting that the regulation of MLCK is more complex in ECs than in smooth muscles. Phosphorylation of MLCK by PKA decreases its affinity to Ca^{2+}/CaM [9, 145]. However, MLCK activity can also be increased via the phosphorylation mediated by a number of different kinases (e.g., CaMKII, PKC, $p60^{Src}$) [146].

Proinflammatory autacoids (e.g., histamine, bradykinin) increase the intracellular Ca^{2+} level [147] in EC and induce MLCK activation resulting in MLC20 phosphorylation and EC hyperpermeability. Furthermore, tumor necrosis factor-α (TNF-α) has been shown to slowly induce barrier disruption in cultured bovine pulmonary artery ECs (BPAEC). While TNF-α also induces MLCK activation and robust MLC20 phosphorylation that is sensitive to kinase inhibitors, suppression of this mechanism fails to attenuate the loss of endothelial barrier function suggesting the involvement of other mechanisms in TNFα induced EC hyperpermeability [148].

Cellular contraction can be regulated not only by MLCK dependent pathways but also via mechanisms independent of MLCK, such as protein kinase C (PKC)-dependent signaling mechanisms. Phorbol-12-myristate-13 acetate (PMA), a known PKC activator, induces an increase in BPAEC permeability without a significant effect on MLC20 phosphorylation or stress fiber formation. PKC instead stimulates the phosphorylation of caldesmon, an actin-, and myosin-binding protein [149]. Agonist-induced changes in EC permeability frequently involve the activation of the small GTPase RhoA, and the subsequent activation of ROCK induced signaling pathways. ROCK elicits bidirectional activation of the contractile apparatus [64] by phosphorylating MYPT1 at its inhibitory Thr^{696} and Thr^{853} phosphorylation sites resulting in inactivation of MP [150], but also phosphorylating MLC20 at both Thr^{18} and Ser^{19} sites in ECs [8].

In contrast, extracellular purines (e.g., Ado, ATP, and ATPγS a very slowly hydrolysable ATP analog) have been shown to be barrier protective in macrovascular ECs [17, 151]. Activation of PKA/PKG pathways by these agonists induces the phosphorylation of MYPT1 at Ser^{695} and Ser^{852} preventing the phosphorylation and inactivation of MP by ROCK [12], thus leading to MLC20 dephosphorylation and cellular relaxation. However, the specific molecular signaling needs to be further elucidated.

Barrier preservation mediated by cAMP can also involve an exchange factor that is directly activated by cAMP termed EPAC1 [152]. It has been reported that both, PKA and EPAC1 can activate Ras-related C3 botulinum toxin substrate 1 (Rac1), a small GTPase [152-153], which is commonly implicated in EC barrier strengthening due to its ability to facilitate actin cytoskeletal rearrangement [154] and regulate MP activity [155]. In smooth muscle cells, EPAC1 can also modulate MP activity via a Rap1-RhoA-ROCK1 mediated pathway [156], however, the detailed signaling mechanisms responsible for its ability to strengthen the EC barrier are not precisely known.

Increasing cAMP level is best known as the classical pathway of PKA activation, however, it has also been demonstrated that PKA activation may occur independent of cAMP, and instead is mediated via the coupling of specific trimeric G-proteins with scaffolding proteins known as PKA-anchoring proteins (AKAPs), where the PKA catalytic subunit can be released from its regulatory subunit, thus leading to PKA activation [157]. Recent studies have also demonstrated that specific AKAPs, e.g., AKAP9 and 12 may contribute to cAMP-independent EC barrier regulation [158-159].

Endothelial nitric oxide synthase

Nitric oxide (NO), is a highly diffusible and reactive free radical gas [160] with a relatively short half-life in biological fluids (~ 5 seconds). NO is synthesized by a family of enzymes collectively referred to as NO synthases (NOS). These are 3 isoforms of NOS, the neuronal- (nNOS or NOSI), inducible- (iNOS or NOS II), and the endothelial (eNOS or NOSIII) nitric oxide synthase which were originally designated based on their function and more recently according to the order of their first purification and identification of cDNA sequence [161-162]. The nNOS was first identified in brain and is constitutively expressed in central and peripheral neuronal cells [163]. However, the nNOS expression has been shown outside the brain via immunohistochemistry in peripheral cell types including epithelial cells of various organs, in the macula densa cells of the kidney, in pancreatic islet cells, and in the vascular smooth muscle of certain types of blood vessels [162]. The second isoform, iNOS was found in immune cells stimulated by bacterial toxins and cytokines which "induce" its expression [164]. The primary cell type that expresses iNOS is the macrophage, but under certain circumstances, iNOS can be expressed in neuronal cells and even in vascular smooth muscle cells [165]. In contrast, eNOS is a constitutively expressed enzyme that is predominantly expressed in endothelial cells [166]. Expression of eNOS has also been reported in cardiomyocytes, platelets, and kidney epithelial cells but the level of expression is much lower than that found in endothelial cells [162, 167].

Structure and regulation of eNOS catalytic activity

The human eNOS gene was first cloned and characterized in 1992 by a couple of groups [168-169]. It is located on chromosome 7 and encodes 1203 amino acids that comprise a protein of 133 kDa molecular mass [168]. eNOS is a multi-domain enzyme comprised of an N-terminal oxygenase, and a C-terminal reductase domain (Fig. 7.) [167]. The oxygenase domain (amino acids 1-491) contains binding sites for fatty acids (myristic and palmitic), heme/ oxygen, Zn, (6*R*-)5,6,7,8-tetrahydrobiopterin (BH4), and the substrate, L-arginine (L-Arg) [170]. The reductase domain (which spans amino acids 518-1203) contains binding sites for nicotinamide adenine dinucleotide phosphate (NADPH), two flavin mononucleotide (FMN), and a flavin adenine dinucleotide (FAD)

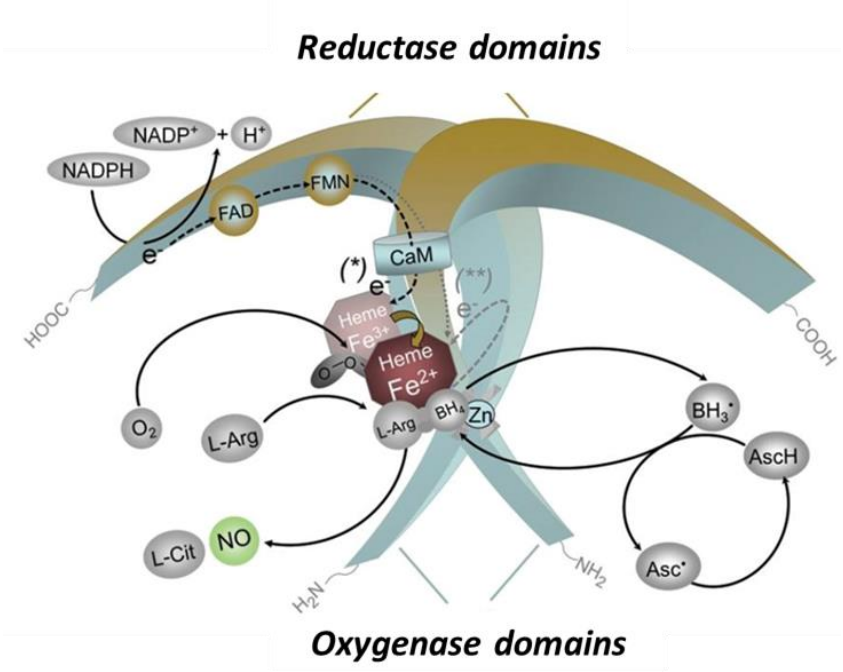

Figure 7. Structure and catalytic mechanism of eNOS. Modified figure, Förstermann and Sessa, 2012.

[2]. The oxygenase domain (binds oxygen and L-arginine) and reductase domain (binds NADPH and shuttles electrons) are connected with a linker sequence that contains the CaM binding site (amino acids 493-512) (Fig. 7.) [171]. Dimerization of eNOS monomers in head to tail orientation is required for NO production [172]. The primary mode of eNOS enzyme activation is through the elevated Ca^{2+} level which is required for Ca^{2+}/CaM binding to each monomer [2]. Ca^{2+}/CaM subsequently displaces an adjacent autoinhibitory loop (a 45 amino acids insert in the FMN binding domain) that then enables the flow of electron from NADPH through the flavins to the heme [173]. Upon activation, electrons flow from the reductase domain of one monomer to the oxygenase domain of the other monomer [172] to enable reduction of heme-bound oxygen that subsequently reacts with the guanidino nitrogen of L-arginine to liberate NO and L-citrulline as the byproduct (Fig. 7B) [167]. This reaction can be inhibited by L-arginine analogs containing a modification of the guanidino nitrogen (e.g., *N*ω-nitro-L-arginine-methyl ester (L-NAME) and N^G-nitro-L-arginine (L-NOARG)) [174]. For each mole of NO that is generated, 1 mole of L-arginine, 1.5 moles of NADPH, and 2 moles of O_2 are consumed [160]. It is important to note that a second autoinhibitory domain in the reductase domain has also been identified (amino acids 1165-1178 of the human isoform). Interestingly several phosphorylation sites involved in the post-translational regulation of eNOS activation lie within these two domains [175-176]. In all NOS

isoforms, N-terminal cysteine residues (Cys 94 and Cys99) of the monomers coordinate a zinc ion in a tetrahedral conformation (ZnS_4) at the dimer interface which has a structural function rather than catalytic role [177]. The amino acid sequence of eNOS is highly conserved across species, but there are differences, i.e., the bovine eNOS contains an N-terminal insertion of +2 amino acids, and the mouse has a -1 deletion.

The availability of the L-Arg substrate and the cofactor BH_4 have been shown to be important determinants of eNOS activity. A lack of L-Arg or BH_4 (and particularly its oxidation to BH2) can promote uncoupling of the eNOS enzyme which results in a loss of NO synthesized and leads to the liberation of reduced O_2 in the form of superoxide [178]. Numerous reports have shown that pathological conditions can result in eNOS monomers with altered catalytic activity. However, the consensus is that monomers are unable to transfer electrons to the other monomer which results in an irreversible loss of activity [179]. Uncoupling and monomerization are different for iNOS and nNOS.

Regulation of endothelial nitric oxide synthase

Because of the relatively short biological half-life of NO, it cannot be stored within cells, and thus NO is typically synthesized on demand. The activity of eNOS enzymes and NO-dependent signaling is meticulously controlled temporally and spatially and involves the integration of multiple interconnected mechanisms that operate at the transcriptional, posttranscriptional and posttranslational levels [160].

The expression of eNOS can be detected in all endothelial cells, and it is regarded as a constitutively expressed enzyme. However, its expression can be increased and decreased in response to several physical and chemical stimuli such as hypoxia, fluid shear stress, and growth factors both *in vitro* and *in vivo* [160, 180]. The signaling pathways involved in the regulation of eNOS mRNA transcription are complex, but important roles have been attributed to the transcription factors nuclear factor kappa-light-chain-enhancer of activated B cells (NF-κB) and Krüppel-like Factor 2, hypoxia-inducible factor-1, and -2 and also to select microRNAs and other epigenetic mechanisms [181].

eNOS expression can be regulated at the posttranscriptional level as well [160]. The mRNA encoding eNOS is very stable, with a half-life of 48h under normal physiological conditions [182]. However, proinflammatory cytokines such as TNFα can destabilize eNOS mRNA in endothelial

cells in a time and concentration-dependent manner, thus negatively affecting NO production [183]. It has also been demonstrated that in human umbilical vein endothelial cells (HUVECs) relatively low concentrations of TNFα can potently decrease eNOS mRNA levels (to 5% of control) and shorten eNOS mRNA half-life from 48 h to 3 h [182], possibly via a translation elongation factor 1-α 1 dependent pathway (eEF1A1) [184].Interestingly, TNFα also has been reported to be involved in the suppression of eNOS promoter activity which possibly involves ROCK and the NF-κB cascade [185], and acute inhibition of eNOS catalytic activity [186-187].

eNOS activity can be robustly influenced by several posttranscriptional mechanisms which include protein phosphorylation/dephosphorylation, fatty acid modification and subcellular localization and protein-protein interactions [2].

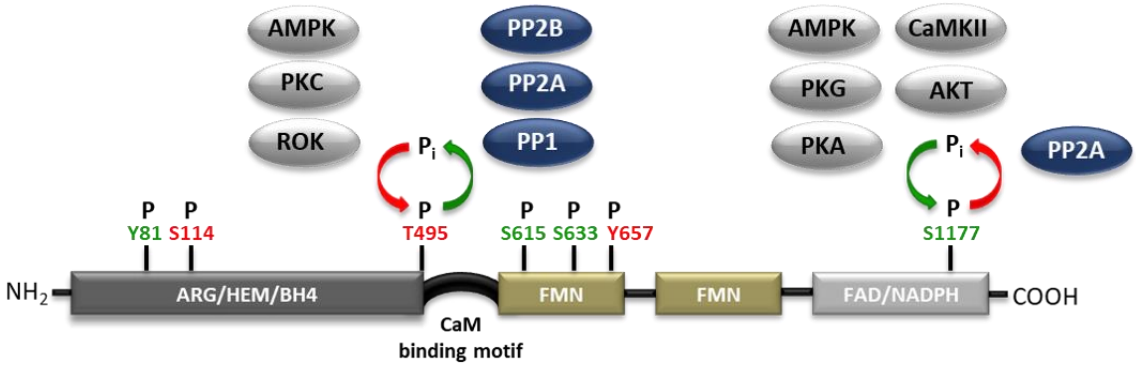

Figure 8. The regulation of eNOS by phosphorylation. eNOS phosphorylation sites that associate with increased (green) or decreased (red) eNOS activity are shown. The functionally most important phosphorylation sites are Ser1177 and Thr495, thus the kinases and phosphatases involved in the regulation of these sites are indicated on the figure. The kinases responsible for phosphorylation of these sites (gray ovals) depend on the primary stimulus. The phosphatase involved in dephosphorylation of Thr495 (indicated in blue ovals) appear to be PP1, PP2A, and calcineurin (PP2B), while Ser1177 is dephosphorylated by PP2A. Numbering corresponds to human eNOS sequence. Modified figure based on Mount et al., 2007 [188].

Multiple kinases and phosphatases have been implicated in the regulation of eNOS activity through the phosphorylation of Ser, Thr and Tyr residues (Fig. 8.) [188-189]. Seven major phosphorylation sites have been described in human eNOS, and these include Ser114, Ser615, Ser633, Ser1177, Thr495, Tyr81 and Tyr657 (corresponding to Ser116, Ser617, Ser635, Ser1179, Thr497, Tyr83 and Tyr659 in the bovine sequence due to the two extra amino acids), but most is known about the phosphorylation of Ser615, Ser633 and Ser1177 and Thr495 in the regulation of eNOS activity which have special importance [2, 180].

Ser1177 was the first identified eNOS phosphorylation site located in the second autoinhibitory region of reductase domain close to the end of the C-terminus [190]. Phosphorylation of this residue results in a conformational change in the structure of the enzyme that facilitates electron flow between the reductase and oxygenase domains and increases eNOS activity independent of the increase in Ca^{2+} and increase in the sensitivity of eNOS to Ca^{2+}/CaM [191-192]. In cultured endothelial cells Ser1177 is not phosphorylated, but it undergoes rapid phosphorylation by protein kinase B (also known as Akt) [190] in response to multiple stimuli, including shear stress, VEGF, or bradykinin-induced stimulation [188]. Bradykinin and Ca^{2+} ionophore (e.g., ionomycin) can also induce eNOS S1177 phosphorylation via the calcium-calmodulin-dependent kinase II (CaMKII). Fluid shear stress has also been shown to elevate Ser1177 phosphorylation levels via increased activity of PKA [193]. Other kinases including PKG, adenosine-monophosphate activated kinase (AMPK) have also been reported to phosphorylate eNOS on Ser1177 [2, 188]. Dephosphorylation of eNOS at Ser1177 is mediated by PP2A, but its regulation remains poorly understood [4].

In contrast, the phosphorylation of eNOS at Thr495 in the CaM-binding domain negatively regulates the catalytic activity of eNOS interfering with CaM binding to the enzyme [192]. Stimulation of bovine aortic endothelial cells with the PKC activator PMA, increases eNOS phosphorylation at Thr495 and reduces NO production [194]. However, PKC signaling has been demonstrated to promote not only the phosphorylation of Thr495 residue but also the dephosphorylation of Ser1177 in a coordinated manner [4]. Treatment of cultured HUVEC by thrombin also induces the phosphorylation of eNOS at Thr495 via a ROCK dependent manner [187]. AMPK has also been reported to be involved in the phosphorylation of eNOS at Thr495 [195], but to date, there is no evidence supporting the existence of this pathway *in vivo*. On the other hand, multiple phosphatases have been shown to be involved in the dephosphorylation of Thr495. PP1 can dephosphorylate eNOS at Thr495 [192], however, the activity of calcineurin (PP2B) may also be involved as cyclosporine-A treatment of BPAE cells leads to an increase in the phosphorylation level of eNOS-Thr495 [6]. PP2A has also been presumed to dephosphorylate eNOS at Thr495 [196]. But despite its ability to dephosphorylate eNOS at Thr495, based on recent experimental data PP2A appears to be a negative regulator of eNOS activity, and this may be due to its ability to actively dephosphorylate Ser1177 [160]. Both PP1 and PP2A exist in endothelial cells in multiple

holoenzyme forms, however, very limited information exists in how PP1 and PP2A coordinate the dephosphorylation of eNOS at the above phosphorylation sites.

Phosphorylation of eNOS at Ser615 and Ser633 has also has been shown to promote increased eNOS activity [197]. Both phosphorylation sites are located within the first inhibitory loop of eNOS and can be phosphorylated by PKA. Ser615 was also shown to be phosphorylated by Akt [197]. Phosphorylation of Ser615 promotes the binding of Ca^{2+}/CaM to the enzyme, however, it did not, on its own, alter the overall enzyme activity. In contrast, mimicking the phosphorylation of Ser635 by the introduction of a negative charge at this residue (through mutation to aspartic acid, D) not only increased the eNOS sensitivity toward Ca^{2+}/CaM but also stimulated eNOS activity [198]. A demonstration of the importance of the two autoinhibitory domains and their regulation by site-specific phosphorylation was obtained through deletion mutants in which both autoinhibitory loops have been removed. The resulting enzyme retained a high degree of activity but was calcium-insensitive [175]. The first identified eNOS phosphorylation site which can be activated by shear stress is Ser116 [199]. The function of this phosphorylation site remains somewhat controversial. Increased shear stress stimulates the phosphorylation of this site, which was initially proposed to increase eNOS activity [199]. In contrast, others have shown that dephosphorylation of this site by PP2B upon VEGF stimulation, increases NO production [200]. The activity of eNOS can also be regulated by phosphorylation of Tyr residues. Phosphorylation of Tyr81 can be mediated by Src-kinase which increases eNOS activity [201]. In contrast, the Tyr phosphorylation of eNOS at Tyr659 by proline-rich tyrosine kinase 2 (P2YK) has been recently reported which impairs eNOS activity [202].

The subcellular localization of eNOS can also significantly impact eNOS activity. In unstimulated cells eNOS is localized mainly to the Golgi complex and to the plasma membrane within special membrane compartments referred to as caveolae or “small caves” [203]. Caveolae are flask-shaped 50-100 nm membrane invaginations that are further characterized by high levels of cholesterol and sphingolipids and the presence of the transmembrane scaffolding protein caveolin-1 (Cav-1) [204]. Caveolae have been described as “preassembled signaling complexes”, that coordinate intracellular signaling of G-protein-coupled receptors, heterotrimeric G proteins, receptor tyrosine kinases, Ras–mitogen-activated protein kinase (MAPK), Src-kinas, PKC, PKA as well as eNOS [205]. The caveolar localization of eNOS is achieved through the irreversible myristoylation of the N-terminal glycine 2 residue [206] that is a prerequisite for the subsequent

palmitoylation of cysteines 15 and 26 residues and the translocation of eNOS to the plasma membrane [175, 207]. Myristoylation deficient eNOS (in which glycine has been replaced with alanine) cannot undergo subsequent palmitoylation, remains cytosolic and produces less NO compared to acylated, membrane-associated eNOS [175]. Palmitoylation is a reversible posttranslational modification that is carried out by palmitoyl transferases [208], and the reverse reaction is catalyzed by acyl-protein thioesterase 1 (APT1) [209]. *In vitro* studies have revealed that unpalmitoylated eNOS (Cys15 and 26 residues mutated to Ser) is redistributed compared to WT eNOS and its capacity to make NO was diminished [203]. It has been demonstrated that eNOS is most active at the plasma membrane where it is highly phosphorylated and more sensitive to transmembrane Ca^{2+} flux, and produces more NO compared to Golgi localized eNOS [210]. Although, Golgi-localized eNOS is less phosphorylated under basal conditions, and less sensitive to changes in the intracellular Ca^{2+} concentration, it is highly sensitive to Akt-dependent phosphorylation of Ser1177 which activates the enzyme [211]. Interestingly, agents inducing endothelial hyperpermeability, such as VEGF, PAF or bradykinin promote eNOS translocation to the cytosol. In contrast, vasodilating agents such as acetylcholine induce the movement of eNOS to the Golgi complex, but does not promote hyperpermeability [212].

In addition to CaM and APT1, the activity of eNOS can be influenced by many other protein-interacting partners. In EC, eNOS localized to caveolae interacting with caveolin-1 which is a negative regulator of eNOS activity and NO production. This inhibition occurs through the scaffolding domain of Cav-1 which binds to a caveolin-binding motif on eNOS (amino acids 348-356) which then obscures the Ca^{2+}/CaM binding site [213]. Another important interacting partner that positively affects eNOS activity is the molecular chaperone, heat-shock protein 90 (Hsp90) [214]. Hsp90 interacts with eNOS under basal conditions, and this interaction can be further increased by agonists like VEGF, bradykinin or fluid shear stress [214]. Hsp90 has multiple actions on eNOS activity. First, Hsp90 likely affects the binding of heme via its binding to the oxygenase domain of bovine eNOS between amino acids 310–323 [215-216]. Second, Hsp90 acts as a scaffolding protein that coordinates the regulation of diverse signaling proteins and facilitates signaling initiated by growth-factors, G-protein coupled signaling pathways, kinases, and phosphatases [173, 214]. The localization and activity of eNOS can also be regulated by proteins called nitric oxide synthase interacting protein (NOSIP) and nitric oxide synthase traffic inducer (NOSTRIN) which promote

the translocation of eNOS from the plasma membrane to the Golgi complex and reduce the NO synthesis [217-218].

Physiological role of endothelial nitric oxide synthase and NO

Endothelial NOS and eNOS-derived NO are important regulators of numerous cardiovascular functions. Because nitric oxide (NO) is a highly lipophilic gas, it readily diffuses from the site of synthesis in the endothelium to traverse across cell membranes into the cytoplasm of the underlying vascular smooth muscle cells, and in the luminal direction to interact with blood cells [160].

In blood vessels, NO exerts its effects via at least two distinct mechanisms that can be direct or indirect. One of the most important biological actions of NO is the activation of the soluble guanylyl cyclase (sGC) and the subsequent generation of cGMP [219-220]. In unstimulated cells sGC catalyzes the conversion of GTP to the second messenger cGMP at a low basal rate. Exposure of sGC to very low concentrations of NO (10–100 nM) results in binding of NO to the high-affinity heme group of sGC which triggers a conformational change in dimeric sGC that results in enzyme activation (up to 500-fold) [160]. The primary downstream target of cGMP in vascular smooth muscle is protein kinase G (PKG), which in turn activates MP [221], and consequently promotes vasorelaxation [127]. Thus, it is not surprising that eNOS knock out mice exhibit a complete absence of vasorelaxant capacity (in conduit blood vessels) to established agonists such as acetylcholine and elevated blood pressure in both the systemic and pulmonary circulations (45).

In addition to its vasodilatory effects, NO has also been shown to inhibit the proliferation of vascular smooth muscle cells in a cGMP dependent manner [222]. Also, the luminal delivery of NO can stimulate cGMP synthesis in platelets which reduces calcium mobilization and negatively regulates platelet membrane glycoprotein IIb/IIIa, which are essential for platelet aggregation and adhesion to the blood vessel walls [223]. NO can also inhibit leukocyte adhesion to the vessel wall by suppressing CD11/CD18 expression on leukocytes [224]. Furthermore, several studies have been shown that exogenous NO donors decrease adhesion molecule expression in ECs as well [225-227]. Because platelet aggregation and leucocyte adhesion are early events in the development of atherosclerosis, NO is thought to have a protective role against atherogenesis, and this is supported by studies with knockout mice [167]. Furthermore, endothelial-derived NO plays an important role

in angiogenesis where it contributes to the downstream signaling of angiogenic factors like VEGF and has a critical role in the formation of collateral vessels, and in post-ischemia angiogenesis [228].

NO has multiple actions on endothelial barrier function. It has been demonstrated that inflammatory agonists and agents that promote hyperpermeability such as VEGF increase NO levels [229-230] which contribute to the leakiness of the endothelial barrier via the opening of IEJs [231], and through modification of actin polymerization that alters the shape of ECs [232]. This mechanism is mediated by the NO-cGMP-PKG signaling cascade in coronary [230] and other microvessels [233]. In contrast to VEGF, under basal conditions NO can have barrier protective effects in cultured endothelial cells and in several organs, such as the skin, kidney, or intestine, heart, lung, diaphragm and skeletal muscles [3, 234]. Several studies have shown that inhibition of NO synthesis either by L-NAME or genetic deletion of eNOS promotes the transendothelial leakage at the level of arterioles, capillaries, and postcapillary venules [3, 235-236]. Open IEJs following L-NAME treatment or in eNOS knock out animals has also been reported [3]. However, unlike the effects of hyperpermeability inducing mediators (e.g., histamine, platelet activating factor) that operate in a short period of time (i.e., an increase in endothelial permeability in minutes), the effect of L-NAME is more chronic indicating that different molecular mechanisms are responsible for the endothelial hyperpermeability [3]. The exact molecular mechanisms responsible for the barrier protective effects of NO are not yet well understood, but the basal level of NO likely serves to stabilize IEJs, a mechanism that involves activation of PKA [237]. In other studies, EGCG has been shown to stimulate PKA-dependent activation of eNOS and increases in NO that results in vasodilation in macro vessels [16]. In contrast to VEGF, EGCG elicits barrier protective effects on cultured endothelial cells [238].

The other important mechanism underlying the actions of NO is the reversible S-nitrosylation of target proteins. S-nitrosylation is a covalent modification of cysteine residues in selected proteins that yields S-nitrosothiols (SNO) [239]. In contrast to the high-affinity activation of sGC (nM range), the S-nitrosylation of target proteins requires significantly higher amounts of NO (μM) [240]. Reversibility of SNO modified proteins is mediated by the enzymes, S-nitrosoglutathione reductase [241] and thioredoxin 1 [242]. To date, several proteins have been shown to be dynamically regulated by S-nitrosylation including eNOS itself at Cys94 and Cys99 residues, which has been shown to negatively regulate NO production [239, 243]. However, the specificity by which cysteine S-nitrosylation modifies some proteins but not others remain incompletely understood [244].

AIMS

The molecular mechanisms regulating endothelial function have been intensively investigated over the past several decades and despite significant advances in our knowledge, the mechanisms involved in the preservation of endothelial barrier integrity are not yet fully understood. As discussed in the literature review, endothelium-derived NO plays a vital role in the regulation of numerous functions of blood vessels which includes changes in endothelial permeability. Dysregulation of eNOS phosphorylation and reduced expression of eNOS decreases NO bioavailability and is associated with increased severity of cardiovascular disease. Therefore, a better understanding of eNOS regulation and new approaches to improve eNOS function are important goals. The phosphorylation of eNOS on Thr495 has been shown to influence negatively the activity of eNOS and enzyme fidelity. Several kinases have been identified that mediate Thr495 phosphorylation, but the phosphatase regulatory subunits and signaling mechanisms mediating eNOS Thr495 dephosphorylation have not been described. ROCK phosphorylates eNOS at Thr495 and the amino acid sequences flanking this site show similarity to the phosphorylation sites of other ROCK substrates, which are often dephosphorylated by myosin phosphatase (MP), suggesting a possible involvement of this phosphatase in $eNOS^{pT495}$ dephosphorylation. Thus, based on our preliminary data and the published literature our first aim was:

1. To investigate whether the MP holoenzyme is involved in the dephosphorylation of eNOS at Thr495 and to determine the underlying interactions and signaling mechanisms involved in eNOS inhibition or activation as well as in influencing the barrier function of endothelial cells.

On the other hand, Ado and ATPγS are important regulators of endothelial homeostasis that strengthen barrier function via cAMP-dependent and independent mechanisms, resulting in increased MP activity and consequently decreased MLC20 phosphorylation. The effect of Ado and ATPγS on microvascular endothelial function remains poorly undersood. Thus, our second aim was:

2. To define and compare the molecular mechanisms linking Ado- and ATPγS-induced purinergic receptor activation and barrier strengthening in HLMVECs.

MATERIALS AND METHODS

Materials

The chemicals and vendors were as follows. Fetal bovine serum (FBS), fetal calf serum, bovine serum albumin (BSA), antibiotic-antimycotic solution, sodium pyruvate, L-glutamine, Minimum Essential Medium (MEM) and Dulbecco's modified Eagle's medium (DMEM) (Gibco Gaithersburg, MD, USA). Endothelial basal medium-2 (EBM-2) and EGM-2™-MV BulletKit™ (Clonetics San Diego, CA, USA). M199 media, HEPES buffered saline, amphotericin B, penicillin-streptomycin and trypsin-EDTA solution, anti-FLAG M2 antibody-coupled EZviewTM Red affinity gel, anti-FLAG antibodies, EZviewTM Red anti-c-Myc affinity gel, anti-c-myc antibody, anti-P2Y13, horseradish-peroxidase (HRP) conjugated anti-mouse IgG and HRP-conjugated anti-rabbit IgG, microcystin-LR, phorbol 12-myristate-13-acetate (PMA), acetylcholine cloride, phosphatase inhibitor cocktail, adenosine, Duolink® in situ red proximity ligation assay kit, Mowiol and Fluorimetric nitric oxide synthase detection kit (Sigma-Aldrich, St Louis, MO, USA). Complete mini protease inhibitor Cocktail Tablets (Roche Diagnostics, Mannheim, Germany). Dynabeads® Protein G, and Trizol reagent were from Life Technologies, Grand Island, NY, USA. jetPEI transfection reagent (Polyplus Transfections, Illkirche, France). X-tremeGENE HP DNA transfection reagent was from Roche, Indianapolis, IN. 4–20% Mini-PROTEAN® TGX™ Gel, Precision Plus ProteinTM Dual Color Standard and 0.45 µM pore size nitrocellulose membrane, 0.2 µM pore size polyvinylidene difluoride (PVDF) membrane, and Trans-Blot® Turbo™ Transfer System, iScript™ cDNA synthesis kit and Syber Green were purchased from Bio-Rad, Hercules, CA, USA. Enhanced chemiluminescence (ECL) reagent (Pierce, Rockford, IL, USA). Protein-A Sepharose and glutathione-Sepharose beads (Amersham Bioscience, Arlington Heights, IL, USA). Polyclonal antibodies for dual MYPT1 phosphorylation (MYPT1$^{pSer696/pThr697}$) were generated and affinity-purified as described previously by Sutherland *et al.* [245]. Anti-MYPT1^{pT696}, anti-PP1c, anti-eNOS^{pT495}, anti-PKAcα, anti-MLC20$^{ppT18/S19}$, anti-EPAC1, and anti-GST antibody (Cell Signaling, Beverly, MA, USA). Anti-67LR, anti-PP2A-B56δ, anti-P2Y2, anti-P2Y12, anti-AKAP12, and anti-glutathione antibody (Abcam, Cambridge, MA, USA). Anti-P2Y1 and anti-P2Y11 antibodies were from Alomone Labs, Jerusalem, Israel. Anti-AKAP2, and anti-AKAP9 antibody were from Bethyl Laboratories Inc., Montgomery, TX, USA. ProLong Gold Antifade mountant with DAPI, Alexa-488 anti-rabbit IgG and Alexa-546

anti-mouse IgG (Molecular Probes, Eugene, OR, USA). Non-specific (scrambled), pan PP1c specific, EPAC1, P2Y4 and P2Y13 siRNAs, anti-HA antibody, anti-G_{i2}, anti-AKAP3, anti-P2Y4-antibody, and normal rabbit serum were purchased from Santa Cruz Biotechology Inc., Santa Cruz, CA, USA. MYPT1, AKAP2, P2Y14 and PKAcα, and siPKAcα specific siRNA duplexes (Dharmacon Research, Lafayette, CO, USA). P2Y1, P2Y11 and P2Y12 receptor specific siRNAs were obtained from Ambion, Austin, TX. DharmaFect 2 transfection reagent, and siPORT™ Amine Transfection Agent (Thermo Fisher Scientific, Waltham, MA, USA). Tautomycin and anti-β-tubulin antibody (Millipore, Solna, Sweden). Calyculin A (Calbiochem, Darmstadt, Germany). pcDNA3.1c-myc-eNOS (kind gift of Prof. Dr. Stefanie Dimmeler, University of Frankfurt, Germany); pM11-FLAG-MYPT1, pcDNA3.1-FLAG-MYPT1, and pReceiver-M45-AKAP2-C-3xHA+IRES-eGFP (GeneCopoeia, Rockville, MD, USA), Anti-eNOS antibody (BD Transductional Laboratories, San Jose, CA, USA). Anti-PP1cδ and ROCK (Upstate, Lake Placid, NY, USA). CM5 sensor chips and anti-GST capture kit (GE Healthcare, Uppsala, Sweden). HyBlot® ES autoradiography film (Denville Scientific Inc., Holliston, MA, USA). ATPγS was purchased from Tocris, Mineapolis, MN. cAMP assay EIA kit was from Cayman chemicals, Ann Arbor, MI. PKA activity assay kit was from Enzo Life Science, Farmingdale, NY, USA. Infliximab was obtained from Centocor Ortho Biotech Inc., Horsham, PA, USA). ^{32}P-MLC20 was purified as previously described [246].

Cell cultures

Umbilical cords were collected from the local clinic (Department of Obstretrics and Gynecology, University of Debrecen) during normal deliveries with informed consent given and the procedure was performed by the approval of the Ethics Committee of the University of Debrecen (Ref. number: 2909-2008) conform the Declaration of Helsinki. Human umbilical vein endothelial cells (HUVEC) were isolated as previously described [247]. Cells were maintained in M199 media supplemented with 20% (v/v) FBS, 10 mM HEPES, 2 mM L-glutamine, 0.25 μg/ml amphotericin B, 100 U/ml penicillin, 100 μg/ml streptomycin. Cells were cultured from the same batch and used at passages 4–7 for all experiments.

Bovine pulmonary artery endothelial cells (BPAEC) (cell culture line-CCL 209) were obtained frozen at passage 8 (American Type Tissue Culture Collection Rockville, MD, USA), and were used between passages 17–23. Cells were cultured in MEM supplemented with 10% (v/v) heat

inactivated FBS, 1 mM sodium pyruvate, 0.1 mM non-essential amino acids solution, 2 mM glutamine, 1% (v/v) antibiotic-antimycotic solution.

Human pulmonary artery endothelial cells (HPAEC) were purchased from Clonetics (San Diego, CA, USA) were cultured in EBM-2 supplemented with 10% (v/v) FBS, 0.2 ml of hydrocortisone, 2 ml of human FGF-B, 0.5 ml of VEGF, 0.5 ml of long-arm insulin-like growth factor-1, 0.5 ml of ascorbic acid, 0.5 ml of human epidermal growth factor (EGF), 0.5 ml of GA-1000, and 0.5 ml of heparin solutions. Cells were cultured from the same batch and used at passages 4–7 for all experiments as previously described [13].

Human Embryonic Kidney cell line (HEK293) (American Type Tissue Culture Collection Rockville, MD, USA), tsA201 (Health Protection Agency Culture Collection, Salisbury, UK) and eNOS knock-in HEK293 cells (a kind gift of Dr. David Fulton, Augusta University, Augusta, GA, USA) were cultured in DMEM supplemented with 10% (v/v) FBS, 2 mM L-glutamine, and 1% (v/v) antibiotic-antimycotic solution.

Primary human lung microvascular endothelial cells (HLMVECs) were purchased from Lonza and were utilized at passages 4–9 (Walkersville, MD). Cells were cultured in EBM-2 supplemented with 5 % (v/v) FBS, 0.2 ml of hydrocortisone, 2 ml of human FGF-B, 0.5 ml of VEGF, 0.5 ml of long-arm insulin-like growth factor-1, 0.5 ml of ascorbic acid, 0.5 ml of human epidermal growth factor (EGF), 0.5 ml of GA-1000 and 0.5 ml of heparin solutions.

Cells were maintained at 37 ºC, 5% CO_2 in a humidified atmosphere.

Immunoblotting

Preparation of the samples was as follows. For immunoprecipitation and pull-down assays the cells were lysed in 0.1% (v/v) Triton X-100, 150 mM NaCl, 50 mM Tris–HCl (pH 7.4), 20 mM EDTA and 0.5% (v/v) protease, and phosphatase inhibitor mix containing lysis buffer. After supplementation with SDS sample buffer in a final concentration of 62.5 mM Tris-HCl (pH 6.8), 2% SDS, 10% (v/v) glycerol 50 mM dithiothreitol (DTT), 0.01% (w/v) bromophenol blue, the samples were boiled for 10 minutes at 100 °C in and applied for Western blotting. Protein samples were separated by either 4-20% or 10% SDS-PAGE and transferred to a 0.45 µM pore size nitrocellulose-, or 0.2 µM PVDF membrane (ppMLC20 and pMYPT1$^{Ser696/Thr697}$ blots) at 100V for 1.5 h. The membranes were blocked with 5% (w/v) non-fat dry milk powder solution in phosphate buffered saline (PBS) consisting of 137 mM NaCl, 2.7 mM KCl, 10 mM Na_2HPO_4 and 1.8 mM

KH_2PO_4, PBS plus 0.1% (v/v) Tween20 (PBST), alternatively in Tris-buffered saline (TBS) consisting of 50 mM Tris–HCl (pH 7.4), 150 mM NaCl, or in TBS plus 0.1% (v/v) Tween 20 (TBST) when phospho-specific antibodies were used. During Western blotting the membranes were incubated for 3 hours at room temperature, or overnight at 4 °C with the following antibodies at the indicated dilutions in PBST or TBST: mouse monoclonal anti-eNOS (1:2000), rabbit polyclonal anti-MYPT1 (1:1000), rabbit polyclonal-anti-GST (1:1000), rabbit polyclonal anti-MYPT1^{pT696} (1:1000), rabbit polyclonal anti-eNOS^{pT495} (1:1000), rabbit polyclonal anti-MLC20$^{ppT18/S19}$, mouse monoclonal anti-β-tubulin (1:2000), rabbit polyclonal anti-PP1cδ (1:1000), rabbit polyclonal anti-PKAcα (1:1000), mouse monoclonal anti-67LR (1:1000), rabbit polyclonal anti-PP2A-B56δ (1:1000), rabbit polyclonal anti-P2Y1 (1:500), rabbit polyclonal anti-P2Y2 (1:500), rabbit polyclonal anti-P2Y4 (1:500), rabbit polyclonal anti-P2Y12 (1:1000), rabbit polyclonal anti-P2Y11 antibody (1:1000), rabbit polyclonal anti-MYPT1$^{ppSer696/Thr697}$ (1:1000), rabbit polyclonal anti-AKAP2 (1:2000), goat polyclonal anti-AKAP3 (1:500), rabbit polyclonal anti-AKAP9, mouse monoclonal anti-AKAP12 (1:1000), mouse monoclonal anti-EPAC1, and mouse monoclonal anti-G_{i2} antibody (1:1000). After incubation with the primary antibodies, the membranes were washed three times with PBST or TBST and incubated with HRP-conjugated goat polyclonal anti-rabbit- or rabbit polyclonal anti-mouse antibody (1:4000). Immunoreactive proteins were developed with ECL based detection system. The signals were detected either with FluorChem AIC system (Alpha Innotec, San Jose, CA, USA) or on autoradiography films. Representative images of the Western blots were cropped from the whole blot images by Adobe Photoshop CS5 software (Adobe Systems Inc., San Jose, CA, USA). For densitometric analysis ImageJ software (Research Services Branch, National Institute of Health (Bethesda, MD, USA) was used.

Transfection and gene silencing protocolsls

In order to overexpress MYPT1 and/or eNOS, tsA201 cells cultured in six well plates were transfected with 2 μg pcDNA3.1c-myc-eNOS plasmid alone, 1 μg pM11-FLAG-MYPT1 alone or co-transfected with both 2 μg pcDNA3.1-myc-eNOS and 1 μg pM11-FLAG-MYPT1 expression vectors, using jetPEI transfection reagent as follows. Human embryonic kidney-derived tsA201 cells were plated in 6-well plates and transfected at 70–80% confluency with DNA/jetPEI complex. In 100 μl serum free medium, maximum 3 μg DNA and 12 μl jetPEI was mixed then the

diluted transfection reagent was added to the DNA. The mixture was incubated at room temperature for 30 min and added to the cells on 6 well plates with 1.8 ml complete medium. After 48 h incubation the medium was collected for nitrite/NO measurement and the cells were lysed in 100 µl lysis buffer (1% (v/v) Triton X-100, 150 mM NaCl, 50 mM Tris–HCl (pH 7.4), 0.1% (w/v) SDS, 1% (w/v) Na-deoxycholate, 20 mM EDTA and 0.5% (v/v) protease inhibitor mix), then boiled with SDS sample buffer and applied for immunoblot analysis. In parallel experiments, the media was replaced with fresh media for treatment with agonist and then collected for nitrite measurement. Overexpression of eNOS and MYPT1 was assessed in whole cell lysate by immunoblot analysis.

HEK293 cells were transfected in 10 cm cell culture dishes with AKAP2 coding pReceiver-M45-AKAP2-C-3xHA+IRES-eGFP and MYPT1 coding pcDNA3.1-FLAG-MYPT1 expression vectors using X-tremeGENE™ HP DNA transfection reagent according to the manufacturer's instructions. In 600 µl serum free medium, 6 µg DNA was added and the mixture was gently suspended, then 18 µl X-tremeGENE™ HP DNA transfection reagent was added to the mixture and incubated for 25 minutes at room temperature. Then, the transfection mixture was added to the cells in complete media containing 10% FBS and incubated for 48 hours at 37 °C. Overexpression of AKAP2 and MYPT1 was assessed in whole cell lysate by immunoblot analysis.

For gene silencing experiments BPAE cells seeded on 6 well plates were transfected with non-specific (scrambled) or pan PP1c, or MYPT1 specific siRNA duplexes in 20 nM final concentration using DharmaFect 2 transfection reagent. Transfection reagent and different siRNAs were diluted in serum-free media in separate tubes. After 5 minutes of incubation at room temperature, diluted transfection reagent was added to the diluted siRNA, followed by incubation at room temperature for 20 minutes. When the transfection complex was formed, the transfection mixture was added to BPAECs in serum-free media. After 6 hours of incubation FBS was supplemented to the cell cultures in 20% final concentration, followed by 48 h further incubation. The transfected cells were washed once with ice-cold PBS, lysed in 100 µl lysis buffer and used for Western blotting.

HLMVEC cells seeded on 6 well plates were transfected with non-specific, EPAC1, AKAP2, PKAcα or P2Y receptor specific siRNAs in 50 nM final concentration using siPORT™ Amine transfection reagent according to the manufacturer's instructions. Non-specific siRNA was used as negative control. Briefly, siPORT™ *Amine* transfection reagent and different siRNAs were

diluted in Opti-MEM in separate tubes. After 5 minutes of incubation at room temperature diluted transfection reagent was added to the diluted siRNA, followed by incubation at room temperature for 20 minutes. When the transfection complex was formed, the mixture was added to HLMVECs in serum free media. After 6 hours of incubation the serum free media was changed to complete EBM-2 supplemented with the components of EGM™-MV BulletKit™ and the cells were incubated for 72 hours at 37 °C. Then, the transfected cells were used for further TER measurements and Western blotting.

Nitric-oxide measurement

NO-content of the cell culture medium was determined by Sievers NO Analyzer NOA 280i (Sievers Instruments Inc., Boulder, CO) according to the manufacturer's instructions. After 30 minutes or 48 hours of incubation the NO formed in the cells diffused to the medium and was converted to nitrite in the presence of oxygen. The protein content of cell culture medium was precipitated with 200 mM $ZnSO_4$. One hundred microliters of each sample were applied to the reaction chamber, where nitrite was converted to NO by sodium iodide and was liberated by purging. The NO liberated was converted by ozone to NO_2 and chemiluminescence of NO_2 equivalent to NO formation was determined.

Nitric-oxide measurement with DAF-2 DA

The BPAE cells were seeded on 13 mm diameter coverslips which were placed in 24 well plates before seeding. The cells were then cultured until 60-80 % of confluence. The culturing media was then replaced with the reaction buffer, which includes 1 μM β-NADH, arginine substrate, 25 μM 4,5-diaminofluorescein diacetate (DAF-2 DA) provided by the manufacturer and the cells were incubated for 2 hours at 37 ºC. Then PMA or EGCG was added to the corresponding wells for 1 hour. In parallel, non-treated coverslips (control) were also incubated with reaction buffer. Afterward, the cells were washed with PBS and fixed in 4% (v/v) paraformaldehyde (PFA) solution for 10 minutes at room temperature. After washing three times with PBS, the samples were mounted with 4.3 (w/v) Mowiol and prepared for confocal microscopy. The DAF-2 was excited at 488 nm, and the detection range was 500-580 nm [248]. The intensity of single-cell fluorescence from 8-bit tiff images was determined using Image-J (NIH). The dye formation was calculated using the equation:

$Dye\ formation = \frac{F_{cell} - F_{bkg}}{F_{bkg}}$, which was based on the dye uptake equation described previously by Nagy *et al.* [249].

Pull-down assays

GST-MYPT1 pull-down experiments were carried out by coupling of GST (in control experiments) or GST-MYPT1 to glutathione-Sepharose beads as described by Lontay *et al.* [83], then the HUVEC lysate was applied to the resin and incubated for 3 hours at 4 °C. The resin was washed three times with washing buffer (1 M NaCl, 20 mM Tris-HCl, pH 7.4, 0.1% Triton X-100), then boiled for 10 minutes with SDS sample buffer and subjected to immunoblot analysis with the anti-eNOS antibody. Pull-down of overexpressed c-myc-eNOS or FLAG-MYPT1 from tsA201 cell lysate were carried out using anti-c-myc and anti-FLAG M2 antibody-coupled EZview™ Red affinity gel and analysed with anti-MYPT1 and anti-eNOS or with anti-c-myc and anti-FLAG antibodies.

In vitro phosphorylation/dephosphorylation assays

C-myc-eNOS was overexpressed in tsA201 cells and the cells were lysed in lysis buffer containing 1% (v/v) Triton X-100, 150 mM NaCl, 50 mM Tris–HCl (pH 7.4), 0.1% (w/v) SDS, 1% (w/v) Na-deoxycholate, 20 mM EDTA and 0.5% (v/v) protease inhibitor mix, centrifuged (10 000 *g*, 10 min) and the supernatant was bound to EZview™ Red anti-c-myc affinity gel. The gel was washed three times with a solution containing 1% (v/v) Triton X-100, 300 mM NaCl, 50 mM Tris–HCl (pH 7.4), 0.1% (w/v) SDS, 1% (w/v) Na-deoxycholate, 20 mM EDTA and 0.5% (v/v) protease inhibitor mix. Next, the affinity gel matrix was resuspended in ROCK assay buffer (30 mM Tris–HCl (pH 7.5), 85 mM KCl, 5 mM $MgCl_2$, 1 mM EGTA, 1 mM DTT and 1μM MC-LR. Twenty percent of the gel was removed and boiled in hot SDS sample buffer (ROCK, 0 min). Phosphorylation of c-myc-eNOS was started by addition of 0.2 mM ATP in the presence of 5 mU/mL ROCK, and the mixture was incubated for 60 min, followed by 6 washing steps with 20 mM Tris-HCl (pH 7.5) to remove MC-LR, ATP, and Mg^{2+}. The gel was resuspended again in 100 μl 20 mM Tris-HCl (pH 7.5) buffer and another 20% of the initial gel amount was removed and boiled in SDS sample buffer (ROCK 60 min). The ROCK-phosphorylated sample was divided into three equal aliquots and was incubated for 15 min with 15 nM purified FLAG-MYPT1, 5 nM purified native rabbit skeletal muscle PP1c or 5 nM PP1c plus 15 nM FLAG-MYPT1. The reactions were stopped by

adding hot SDS sample buffer, then the samples were boiled for 5 minutes and subjected to Western blotting.

Assay of protein phosphatase activity

The assay of phosphatase activity of BPAECs was carried out as previously described for THP-1 cells (106). Prior to treatments, BPAECs were incubated in serum-free medium for 16 h, then cells were untreated (control), or treated with 10 nM CLA for 30 min, or with 20 μM EGCG for 1 hour. Cells were collected by centrifugation (600 *g*, 5 min) and washed with PBS followed by washing with TBS containing 0.1 mM EDTA. Cells were resuspended in 100 μl ice-cold TBS containing 0.1 mM EDTA supplemented with 0.5% (v/v) protease inhibitor cocktail and 50 mM 2-mercaptoethanol. Cells were lysed by sonication on ice, then clarified by centrifugation (13 000 g, 10 min). The phosphatase activity of the supernatants was determined at 30 °C in 20 mM Tris–HCl (pH 7.4) and 0.1% 2-mercaptoethanol with 1 μM ^{32}P-MLC20 in the absence or presence of 2 μM His-inhibitor-2 (I2). The reaction was initiated by addition of the substrate. After a 10 min incubation, the reaction was terminated by the addition of 200 μl 10% TCA and 200 μl 6 mg/ml BSA. The precipitated proteins were collected by centrifugation, and the released $^{32}P_i$ was determined from the supernatant (370 μl) in a scintillation counter.

Immunofluorescence and confocal microscopy

BPAECs and HPAECs were plated on gelatin-coated glass coverslips and were grown for 24 hours. After fixation with 4% (v/v) PFA for 10 minutes, the cells were permeabilized with 0.1% Triton X-100, 4% BSA (w/v) and 0.01% (w/v) NaN_3 in PBS (pH 7.5) for 1 hour followed by three washing steps with 4% (w/v) BSA in PBS to block the nonspecific binding sites and once with antibody diluting solution (0.1% Triton X-100, 0.1% BSA (w/v) and 0.01% (w/v) NaN_3 in PBS (pH 7.5). After blocking the cells were incubated overnight at 4 °C with mouse monoclonal anti-eNOS in 1:250, or with rabbit polyclonal anti-MYPT1$^{1\text{-}296}$ antibody at 1:100 dilution. Next, the cells were washed gently (three times) with PBS and incubated with goat polyclonal Alexa-488 (1:250) or goat polyclonal Alexa-546 (1:250) conjugated secondary antibodies for 1 hour at room temperature. Finally, the cells were washed three times with PBS and covered in Prolong Gold Antifade mounting medium. The localization of the specifically labeled eNOS and MYPT1 was visualized using a confocal microscope (Olympus Fluoview 1000, Hamburg, Germany) equipped

with 60X UPLSAPO (NA 1.35) oil immersion objective, or with Leica X8 confocal microscope (Leica Microsystems CMS GmbH, Mannheim, Germany). The optical thickness of the co-localization images was 1 μm.

Duolink proximity ligation assay

BPAECs cultured in 24 well plates on glass coverslips were fixed with 4% PFA solution for 10 minutes, permeabilized with 0.1% Triton X-100 for 10 minutes and blocked with 5% BSA in PBS. The proximity ligation assay (PLA) was carried out according to the manufacturer's instructions. Briefly, to visualize the interaction between eNOS and MYPT1 the samples were stained with mouse anti-eNOS (1:400) and rabbit anti-MYPT1$^{1-296}$ (1:500) antibodies overnight, at 4 °C prior to incubation with PLA probes for 1 hour at 37 °C. Then, ligase was added to hybridize the probes and after the rolling-circle amplification the labeled probes were hybridized to the rolling-circle amplification product. After washing three times with PBS, the samples were mounted with 4.3 % (w/v) Mowiol and prepared for confocal microscopy.

Surface plasmon resonance measurement

Interaction of GST-MYPT1 with c-myc-eNOS was analyzed by surface plasmon resonance-based binding experiments using a Biacore 3000 instrument (GE Healthcare, Uppsala, Sweden) as described previously [13]. Anti-GST was immobilized on CM5 sensor chip by amine-coupling according to the instructions of the manufacturers. On one surface recombinant GST while on the two other surfaces full-length GST-MYPT1 were immobilized in running buffer containing 10 mM HEPES (pH 7.4), 0.15 M NaCl, 3 mM EDTA, and 0.005% Surfactant P20. C-myc-eNOS at 0.5 μM or 1 μM in running buffer was injected over the surfaces, and the amount of the captured analyte was determined from the changes of the resonance signal expressed as response units (RU). The surface (with immobilized recombinant GST) was treated identically to the GST-MYPT1 surfaces to determine unspecific binding which was subtracted from the data obtained with the GST-MYPT1 surfaces.

Transendothelial permeability measurement

Transendothelial electrical resistance (TER) of BPAECs and HLMVECs were measured using electric cell-substrate impedance sensing (ECIS) instrument, Model 1600R (Applied BioPhysics,

Troy, NY, USA). Approximately equal numbers ($3.5x10^4$/well) of BPAECs or ($2.5\text{-}3x10^4$ cell/well) HLMVECs were seeded on electrode arrays (8W10E), and the experiments were performed when the resistance values of the wells achieved ≥1000 Ω of baseline steady-state resistance. One hour before treating BPAECs media was changed to serum-free MEM and changes in the resistance values were monitored after treatments with PMA, CLA TM or EGCG. When HLMVECs were analyzed, six hours before treatment cell culture media was changed to complete EBM-2 and changes in the initial resistance were recorded when the basal resistance was stable using the same ECIS instrument. HLMVECs were treated with Ado or ATPγS agonists, and data recordings were stopped when the resistance values were returned to basal level. Collected data were normalized to the initial resistance values and plotted as normalized resistance.

cAMP measurement

HLMVECs cultured in 6 well plates were treated at 90% confluency with 100 μM Ado or ATPγS for 30 minutes. After washing with 1 ml PBS, HLMVECs were incubated in 250 μl, 0.1 M HCl at room temperature for 20 minutes, then scraped, and the mixture was further processed by pipetting up and down until the suspension became homogeneous. The cell lysate was centrifuged at 1000 g for 10 minutes, then cAMP was measured from the supernatant by using a cyclic AMP EIA kit (Cayman Chemical) according to the manufacturer's instructions.

Quantitative real-time PCR (qPCR)

Total RNA was isolated using Trizol reagent according to the manufacturer's instructions. cDNA synthesis was conducted using iScript cDNA Synthesis Kit and 1 μg RNA template. 7.5x diluted cDNA was used for quantitative PCR (qPCR) reactions. qPCR was performed using a Qiagen Rotor-Gene Q system (QIAGEN, Hilden, Germany) and iQ™ SYBR Green supermix (forward and reverse primers are listed in Table I.). Data were analyzed using internal tools.

Name	Forward	Reverse
Adenosine A1 receptor	5'-TTCCCTGGAACTTTGGGCAC-3'	5'-GCCTGGAAAGCTGAGATGGA-3'
Adenosine A2A receptor	5'-CTGTCAGGTGAAGCCTCGTG-3'	5'-CGCTCTCCAAGGGCTTTTTC-3'
Adenosine A2B receptor	5'-CTGTGTCCCGCTCAGGTAT-3'	5'-GGGTTCTGTGCAGTTGTTGG-3'
Adenosine A3 receptor	5'-TCGCTGTGGACCGATACTTG-3'	5'-GCCAAACATGGGGGTCAATC-3'

Purinergic receptor P2Y1	5'-TCGTCTTCCACATGAAGCCC-3'	5'-TCCCCGAAGATCCAGTCTGT-3'
Purinergic receptor P2Y2	5'-CCTGAGAGGAGAAGCGCAG-3'	5'-GAACTCTGCGGGAAACAGGA-3'
Purinergic receptor P2Y4	5'-GCAGTTGTCTTTGTGCTGGG-3'	5'-GCAGCGACAGCACATACAAG-3'
Purinergic receptor P2Y6	5'-TGGGTAGAGGATGAGTCAGCA-3'	5'-GCAGAAGTCTGGAGAGGCAG-3'
Purinergic receptor P2Y11	5'-AGGAAACGTGGGTGGAAAGG-3'	5'-TCCTCAGCCTGTGTCTGCTA-3'
Purinergic receptor P2Y12	5'-GGAGCTGCAGAACAGAACACT-3'	5'-GCAACCTGCAGAGTGGCAT-3'
Purinergic receptor P2Y13	5'-TGTTGTCGTGGCTGTCTTCTT-3'	5'-AGTTGCTGCCAAAAAGAGAGTTG-3'
Purinergic receptor P2Y14	5'-TCCCTTTTCACAGCTGGTTTCA-3'	5'-ATGCTTGCATAAGTTGGACCTG-3'

Table I. List of primers used to study the mRNA level of P2Y receptors.

PKA activity measurement

HLMVECs were incubated in the absence or presence of 50 μM Ado or ATPγS for 30 minutes, then HLMVECs were washed three times with 1 ml ice cold PBS on ice and lysed in 20 mM MOPS, 50 mM β-glycerolphosphate, 50 mM sodium fluoride, 1 mM sodium orthovanadate, 5 mM EGTA, 2 mM EDTA, 1% NP-40, 1 mM AEBSF and 1% (v/v) protease inhibitor cocktail containing lysis buffer. PKA activities were measured using a commercial kit (Enzo Life Sciences) according to the manufacturer's instructions. Briefly, 96 well assay plates pre-coated with PKA specific substrate were incubated with the extracted proteins (1 μg/well) in the presence of ATP and PKA activity was revealed with a phospho-specific substrate antibody.

RESULTS

Identification of the interaction between the regulatory subunit of MP (MYPT1) and eNOS

Most of the regulatory subunits in PP1 holoenzymes have a targeting role implying that they also interact with substrates and help PP1c to fulfill its catalytic activity during the dephosphorylation process. Exploring of MYPT1-binding protein partners led to the identification of several putative substrates and other interactive proteins important in the regulation of the MP holoenzyme [250].

To prove that eNOS is a possible substrate of MP, first we assessed if eNOS and MYPT1 interact in ECs or in tsA201 cells where these two proteins were co-expressed. Thus first, we performed pull-down experiments of eNOS from HUVEC lysate by GST-MYPT1 by capturing recombinant GST-MYPT1 and the associated endothelial proteins on glutathione-Sepharose matrix (Fig. 9A). Subsequently, eNOS was identified in the eluate on Western blots using an anti-eNOS antibody, suggesting its co-precipitation with GST-MYPT1, whereas no eNOS was detected in control GST-pull-down fraction. Immunoprecipitations from the lysates of tsA201 cells co-expressing both FLAG-MYPT1 and c-myc-eNOS proteins were analyzed with anti-MYPT1$^{1\text{-}296}$ and anti-eNOS (Fig. 9B and C), and these data confirmed reciprocal co-immunoprecipitation of c-myc-eNOS and FLAG-MYPT1 with each other.

To further demonstrate the interaction of MYPT1 and eNOS, c-myc-eNOS was purified from the lysate of myc-eNOS overexpressing tsA201 cells using anti-c-myc affinity matrix. This purified eNOS was applied as an analyte to surface plasmon resonance based binding assays (performed by Dr. Bálint Bécsi) to assess its interaction with GST-MYPT1 (Fig. 9D) immobilized on the anti-GST coupled sensor chip [250]. The sensorgrams indicated stable interaction of MYPT1 with eNOS that was reversible as dissociation occurred when the eNOS solution was exchanged for running buffer.

Interactions of eNOS and MYPT1 were visualized *in situ* in ECs of different origin using confocal microscopy. Co-localization of eNOS and MYPT1 was apparent at the perinuclear regions in human pulmonary artery EC (HPAEC) (Fig. 9E). Co-localization of MYPT1 and eNOS was also identified in bovine pulmonary artery EC (BPAEC) (Fig. 9F) at similar locations to that of HPAECs and confirmed by proximity ligation assay (PLA), too (Fig. 9G). The PLA assay was carried out by Dr. Dénes Nagy. Thus, the above data suggest that eNOS and MYPT1 interact in

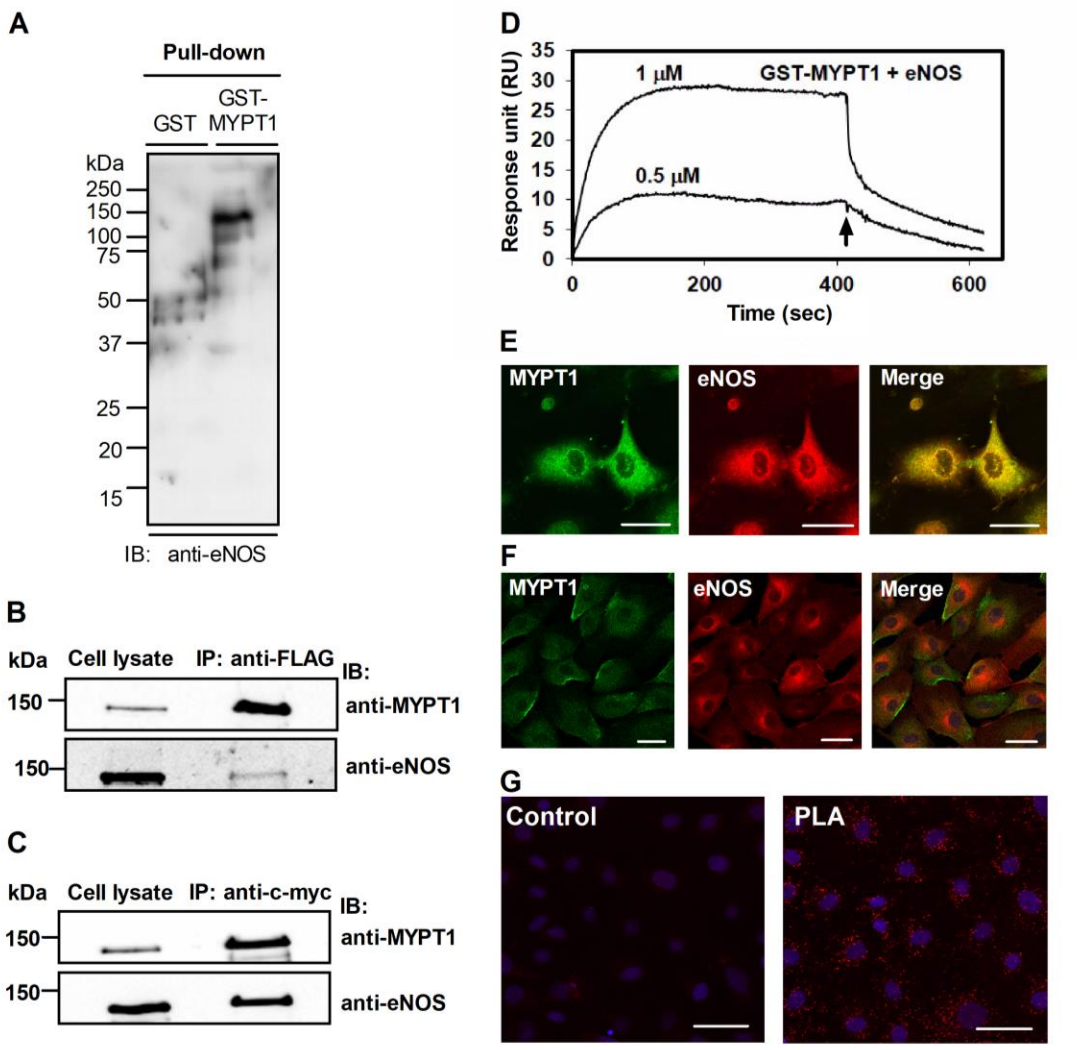

Figure 9. Interaction of eNOS with MYPT1. (**A**) Identification of eNOS in GST (control) or GST-MYPT1 pull-down fractions of HUVEC lysate using glutathione-Sepharose to isolate the interacting proteins. (**B, C**) Co-immunoprecipitation of overexpressed FLAG-MYPT1 and c-myc-eNOS in tsA201 cell lysates using anti-FLAG (**B**) or anti-c-myc-agarose (**C**) beads to isolate the protein complexes. Cropped images of representative Western blots are shown in (**A**), (**B**) and (**C**). (**D**) Binding of eNOS to full-length GST-MYPT1 immobilized to anti-GST coupled CM5 sensor chips. Purified c-myc-eNOS at 0.5 or 1 μM concentrations was injected over the GST (control) and GST-MYPT1 surfaces in running buffer at 0 time, and the association phase of the interaction was monitored for 7 min. The dissociation phase in running buffer without c-myc-eNOS was started (at 7 min as indicated by an arrow) and recorded for 3.5 min. The surface (with immobilized recombinant GST) was treated identically to the GST-MYPT1 surfaces to determine unspecific binding which was subtracted from the data obtained with the GST-MYPT1 surfaces. Representative sensorgram of two independent experiments is shown. (**E**) Co-localization of MYPT1 (green) and eNOS (red) in human pulmonary artery endothelial cells (HPAEC). Images were captured by confocal microscopy. Merged images of eNOS and MYPT1 are also shown. Scale bar, 10 μm. (**F**) Co-localization of MYPT1 (green) and eNOS (red) in BPAECs. Images were captured by confocal microscopy and merged images are shown. Scale bar, 50 μm. (**G**) MYPT1 and eNOS interactions were assessed by PLA assay as described in Materials and Methods. For the control, only the secondary antibodies were added. Red fluorescence indicates interacting MYPT1-eNOS complexes. Scale bar, 50 μm.

ECs implying that MP may be a possible PP1 holoenzyme candidate involved in the dephosphorylation of eNOS.

Assessment of the effects of eNOS phosphorylation level on NO production

The tsA201 cells do not express eNOS, however, they are assumed to include the kinase/phosphatase machinery able to phosphorylate/dephosphorylate eNOS and MYPT1 [250]. Thus, tsA201 cells transfected with c-myc-eNOS construct appeared to be a suitable model system to assess phosphorylation/dephosphorylation of eNOS upon PKC activation and phosphatase inhibition by calyculin-A (CLA), a cell-permeable toxin inhibitor of PP1 and PP2A. Fig. 10A shows that in c-myc-eNOS expressing cells there is a basal level of eNOS phosphorylation at Ser1177 ($eNOS^{pSer1177}$), while $eNOS^{pThr495}$ is very low (Fig. 10A, upper panel). In agreement with the low level of the inhibitory phosphorylation ($eNOS^{pThr495}$) and the occurrence of activator phosphorylation ($eNOS^{pSer1177}$) eNOS expressing tsA201 cells produced a significant amount of NO as judged by NO measurements (Fig. 10B). Activation of PKC by treatment of tsA201 cells with PMA alone, or in combination with CLA, increased the level of $eNOS^{pThr495}$ by ~4- or ~7-fold, respectively. On the other hand, the level of $eNOS^{pSer1177}$ was slightly enhanced only. PMA or PMA plus CLA treatments suppressed dramatically the NO production of eNOS expressing tsA201 cells as shown in Fig. 10B. These data confirm previous suggestions that phosphorylation of eNOS at Thr495 is a significant determinant in the regulation of eNOS activity [192]. The nitric oxide measurement (Fig. 10B.) from the provided samples was performed by Dr. Csaba Hegedűs.

Assessment of the effects of MYPT1 and eNOS co-expression on NO production

To test whether MYPT1 overexpression may influence eNOS activity we overexpressed both, FLAG-MYPT1 and c-myc-eNOS in tsA201 cells. As seen in Fig. 11A NO production was not induced via FLAG-MYPT1 expression alone. When only c-myc-eNOS expressed, NO synthesis was observed, which was significantly higher when FLAG-MYPT1 was co-expressed with c-myc-eNOS in tsA201 cells. These data might also implicate MYPT1 in the regulation of eNOS activity and NO production.

To further confirm the above data, we also carried out experiments with eNOS knock-in HEK293 cells (HEK293-eNOS) in which FLAG-MYPT1 was overexpressed, then NO production was measured in the absence or presence of L-NAME, a NOS inhibitor (Fig. 11B). In accord with

the previous experiment, the NO production in HEK293-eNOS cells was higher compared to HEK293 cells, which do not express eNOS. It was also apparent that FLAG-MYPT1 overexpression increased eNOS activity significantly, but surprisingly neither the expression of

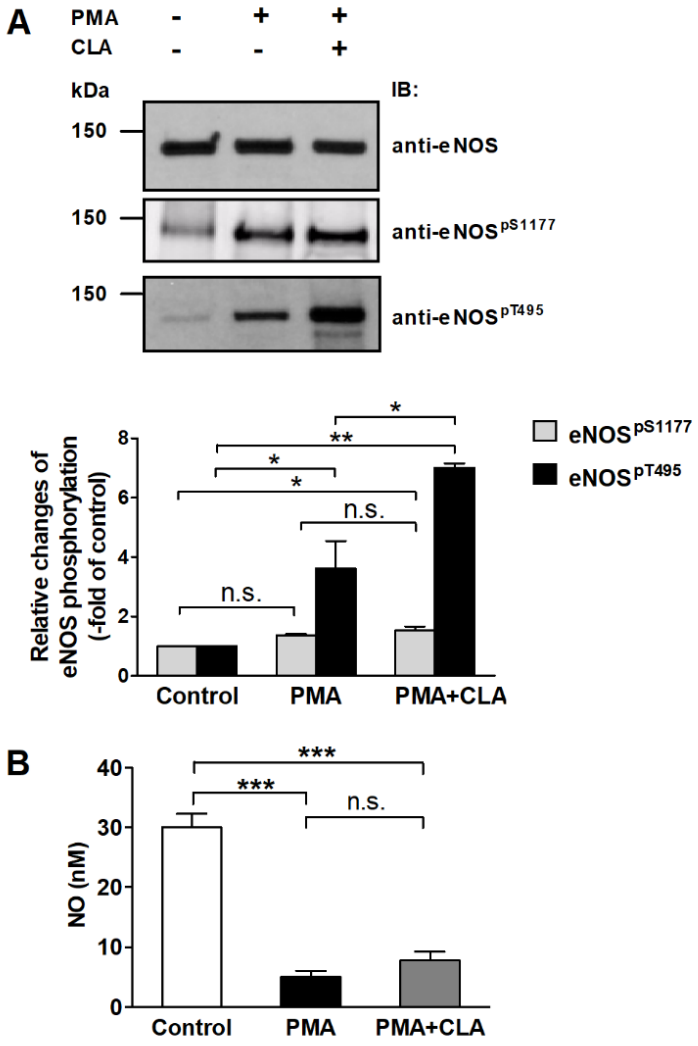

Figure 10. Phosphorylation of eNOS in eNOS overexpressing tsA201 cells upon challenges with PMA, or PMA plus CLA. ***(A)*** Phosphorylation of eNOS at Ser1177 or at Thr495 was analyzed using by anti-eNOS^{pSer1177} or anti-eNOS^{pThr495} in untreated control, and in 100 nM PMA (for 30 minutes) or 10 nM CLA plus 100 nM PMA (for 30 minutes) treated cells. Anti-eNOS was applied to determine eNOS as a loading control. Representative Western blots (upper panel) and densitometric analysis of the blots (lower panel) of three independent experiments are shown. (**B**) Effect of 100 nM PMA (for 30 minutes) or 10 nM CLA plus 100 nM PMA (for 30 minutes) treatments on NO production in the culture medium of eNOS overexpressing tsA201 cells. Following treatment with the effectors, the supernatants of cell cultures were collected, and NO was determined as described in Materials and Methods. Data represent means ± SEM (n = 3), n.s.: not significant, *p < 0.05, **p < 0.01, ***p < 0.001, One-way ANOVA, Newman-Keuls post-hoc testing.

eNOS nor the phosphorylation level of eNOS^{pThr495} was changed under our experimental conditions (Fig. 11B, upper panel). L-NAME suppressed increased eNOS activity to control level in both the non-transfected and FLAG-MYPT1 transfected HEK293-eNOS cells (Fig. 11B, lower panel). The nitric oxide measurement (Fig. 11B.) was performed by Zsuzsanna Bordán.

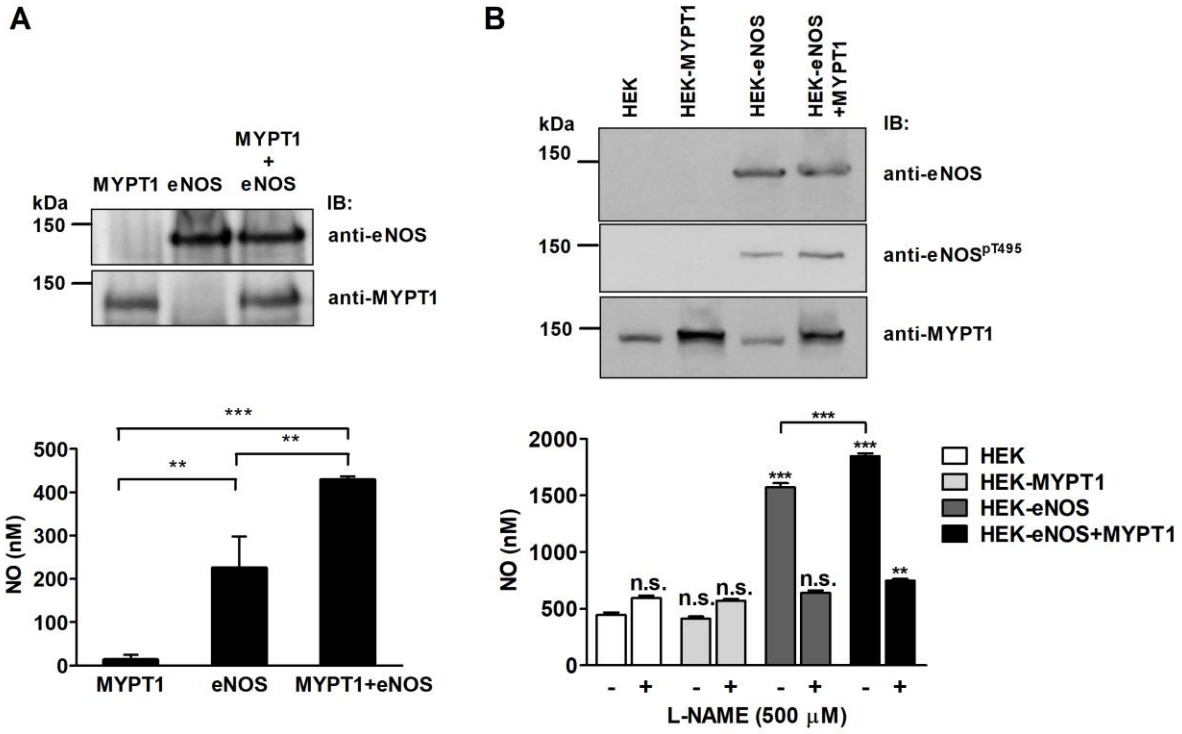

Figure 11. Effect of MYPT1 and eNOS co-expression on NO production. (**A**) The effect of co-expression of MYPT1 and eNOS in tsA201 cells on eNOS activity and NO production. Approximately equal number of tsA201 cells were plated in 6 well plates, and 24 hours later the cells were transfected with pM11-FLAG-MYPT1 and/or pcDNA3.1c-myc-eNOS. 48 hours after transfection NO was determined in the culture medium. (**B**) L-NAME inhibits eNOS activity and NO production in HEK293-eNOS cells in the absence or the presence of FLAG-MYPT1 overexpression. **Upper panel**: identification of eNOS, eNOS^{pThr495}, and MYPT1 by Western blotting in non-transfected (HEK and HEK-eNOS) and FLAG-MYPT1 transfected (HEK-MYPT1, and HEK-eNOS-MYPT1) cells. **Lower panel**: Approximately equal number of HEK, HEK-MYPT1, HEK-eNOS and HEK-eNOS+MYPPT1 cells were plated in 24 well plates and incubated in the absence or the presence of 500 μM L-NAME for 24 hours, then NO was determined in the culture medium. Data represent means ± SEM (n=3), n.s.: not significant, **p < 0.01, ***p < 0.001, One-way ANOVA, Newman-Keuls post-hoc testing.

MP dephosphorylates eNOS at Thr495

It has been already shown that PP1 can dephosphorylate of eNOS at Thr495 (human isoform) [192]. Although, it is unclear whether MYPT1, the regulatory subunit of MP can facilitate the dephosphorylation of eNOS at this phosphorylated residue. Thus, c-myc-eNOS was overexpressed

in tsA201 cells and isolated on anti-c-myc-Sepharose, then the matrix-bound eNOS was phosphorylated by ROCK at Thr495 (Fig. 12.) in the presence of microcystin-LR (PP1 and PP2A inhibitor). After washing the anti-c-myc-Sepharose-bound phosphorylated eNOS to remove ATP, Mg^{2+}, and microcystin-LR, the mixture was divided into four equal aliquots, and beside control (incubated with assay buffer only) they were subjected to addition of FLAG-MYPT1, PP1c and PP1c plus FLAG-MYPT1. It is shown that FLAG-MYPT1 was without effect, while PP1c alone dephosphorylated $eNOS^{pThr495}$ to a relatively low extent, which was significantly increased when both PP1c and FLAG-MYPT1 were present (Fig. 12.). These results suggest that MP holoenzyme (i.e., the PP1c-MYPT1 complex) is an $eNOS^{pThr495}$ phosphatase, and since MYPT1 enhances the phosphatase activity of PP1c on $eNOS^{pThr495}$ it fulfills a targeting and activating role in this dephosphorylation process.

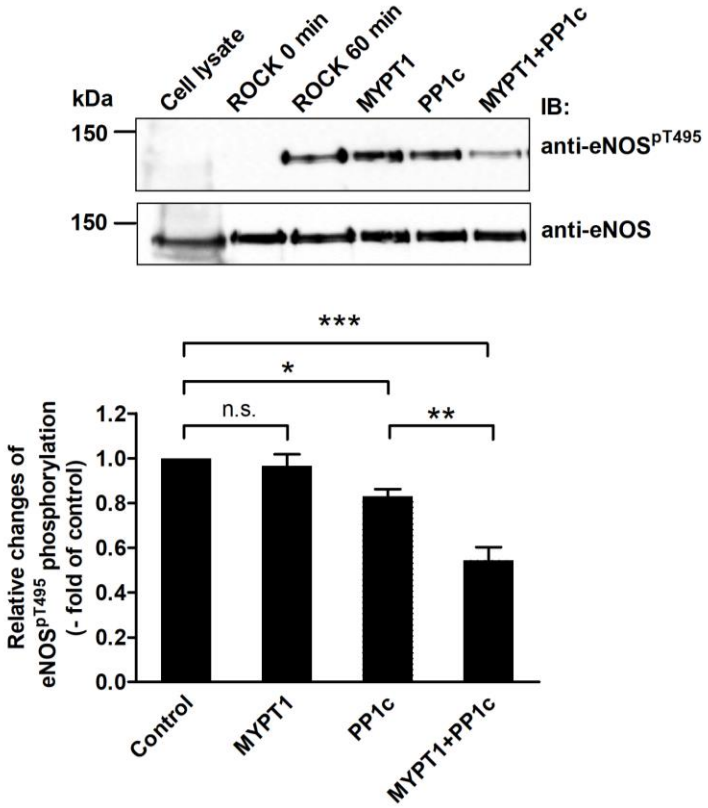

Figure 12. Myosin phosphatase dephosphorylates eNOS at the inhibitory phosphorylation site, pThr495. c-myc-eNOS was isolated from the lysate of c-myc-eNOS expressing tsA201 cells on anti-c-myc-agarose beads and was phosphorylated by ROCK for 60 minutes as described in Materials and Methods. Then, the resin was separated into four equal parts. Phosphorylated c-myc-eNOS was subjected to dephosphorylation for 15 min by FLAG-MYPT1 alone, PP1c alone, or by a mixture of PP1c and FLAG-MYPT1. The relative level of $eNOS^{pT495}$ was considered as control (100%) after phosphorylation by ROCK but before addition of the phosphatase components. Cropped images of representative Western blots (**upper panel**), and densitometric analysis (**lower panel**) of blots from three independent experiments are shown (means ± SEM (n=3), *$p < 0.05$, **$p < 0.01$, One-way ANOVA, Newman-Keuls post-hoc testing).

In order to further confirm the role of PP1c and MYPT1 in the dephosphorylation of eNOS^{pThr495} depletion experiments of these proteins were carried out in BPAECs and in parallel, the level of eNOS^{pThr495} was determined. PP1c was depleted with siRNA specific for all isoform (PP1cα, PP1cβ/δ, PP1cγ1), however, decrease in the level of PP1cδ was assessed as this isoform was identified to associate with MYPT1 specifically in cells [251]. It is apparent on Fig. 13. (upper panel) that silencing either PP1cδ, MYPT1 or both, led to decreased expression of these proteins which was accompanied by an increase in the level of eNOS^{pThr495} (Fig. 13.) implicating both subunits of MP holoenzyme in the dephosphorylation of this phosphorylated residue.

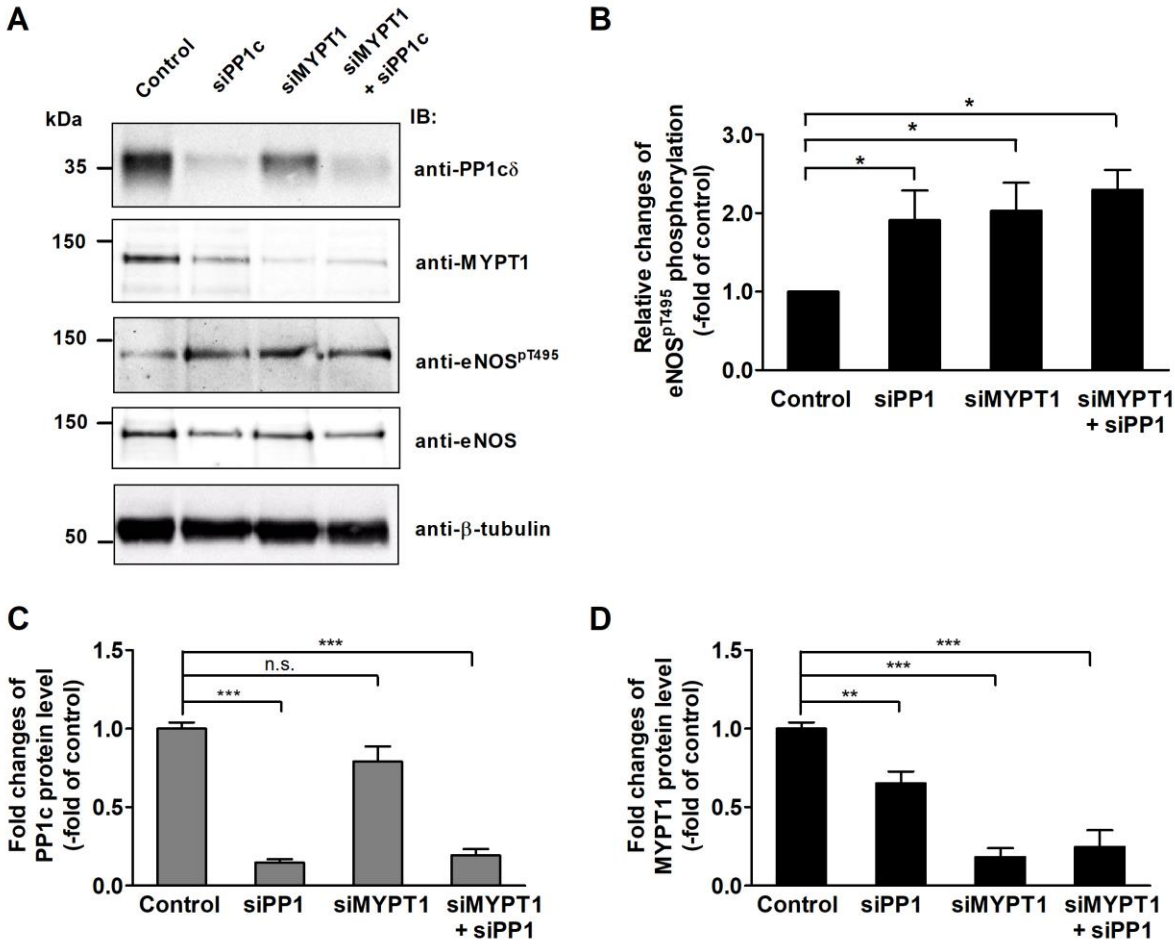

Figure 13. Effect of silencing of PP1c, MYPT1, or both PP1c and MYPT1 by siRNAs on the level of eNOS^{pThr495}. BPAECs were transfected with nonspecific siRNA (control), or with siRNA-PP1, siRNA-MYPT1 and with a mixture of siRNA-PP1 and siRNA-MYPT1. The changes of PP1cδ and MYPT1 protein levels, as well as the level of eNOS^{pThr495}, were determined by Western blotting. (**A**) Cropped images of representative Western blots are shown. The bar graph represents the change in the level of (**B**) eNOS^{pThr495}, (**C**) PP1c, (**D**) and MYPT1 compared to the control. Densitometric analysis of blots from at least four independent experiments (**left panel**) are shown (means ± SEM, * $p < 0.05$, One-way ANOVA, Newman-Keuls post-hoc testing).

The effects of phosphatase inhibitors on the inhibitory phosphorylation of MYPT1 and eNOS

We challenged BPAECs with 10 nM calyculin-A (CLA) or 1 μM tautomycin (TM) to inhibit PP2A and PP1, respectively. CLA and TM inhibit both PP2A and PP1 in *in vitro* phosphatase assays, and there are also controversies concerning their selectivity in cellular systems [102-103]. However, as indicated in the introduction, our recent results [104] confirmed that CLA (up to 50 nM) caused partial, but predominant inhibition of PP2A, while TM (up to 1 μM) primarily suppressed PP1 in THP-1 cells. Fig. 14A illustrates that treatment of BPAECs with CLA alone resulted in a dramatic increase in the phosphorylation of MYPT1 at Thr696 (MYPT1^{pThr696}) while TM and PMA did not increase the level of MYPT1^{pThr696} significantly. Fig. 14B illustrates that enhanced level of MYPT1^{pThr696} paralleled with the increase of the inhibitory phosphorylation of eNOS^{pThr495}. In contrast, TM increased the level of eNOS^{pThr495} slightly, but not significantly.

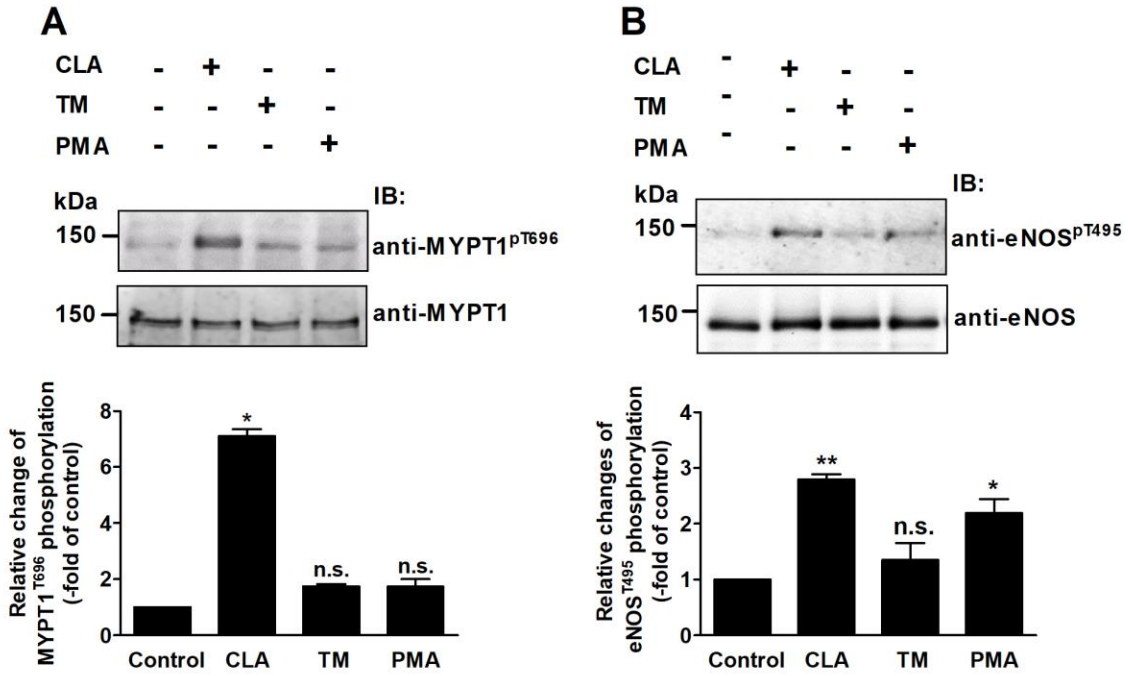

Figure 14. The effect of PKC activation and phosphatase inhibition on the level of MYPT1^{pThr696} and eNOS^{pThr495}. BPAECs cells were treated with 10 nM CLA, 1 μM TM or 100 nM PMA for 30 min and the level of MYPT1^{pThr696} (**A**) and eNOS^{pThr495} (**B**) was monitored by Western blotting (**upper panel**) and quantified by densitometry (**bar graphs, lower panel**). Cropped images of representative Western blots are shown. Densitometric analyses of blots from 3-4 independent experiments were carried out (means ± SEM, n.s.: not significant, *p<0.05, **p<0.01, *** p<0.001, compared to control. One-way ANOVA, Newman-Keuls post-hoc testing).

Activation of PKC by PMA also increased the level of eNOS^{pThr495} in accordance with results shown earlier for eNOS expressing tsA201 cells (see Fig. 10A). As PP2A is assumed to dephosphorylate MYPT1^{pThr696}, the above data support the scenario that PP2A specific inhibition increased the level of MYPT1^{pThr696} resulting in inhibition of MP and suppression of eNOS activity consequently resulting in an increase of eNOS^{pThr495}.

Determination of type-specificity of CLA

To specifically inhibit PP1 and to identify the type-specific inhibition by CLA (Fig. 15.), we determined the distribution of the activity of PP1 and PP2A in the lysates of untreated or CLA treated BPAECs using type-specific phosphatase inhibitor-2 (I2). It is seen that ~65% of the total phosphatase activity was due to PP1 while PP2A (the activity measured in the presence of I2) represented ~35%. CLA decreased the phosphatase activity of the lysate by ~25%, and a large portion (~20%) of this inhibitory impact was exerted on the I2 suppressed (i.e., PP2A) activity indicating predominant inhibition of PP2A by CLA in accord with the previous findings of Dedinszki *et al.* in THP-1 cells [104]. The phosphatase activity assay was carried out by Zoltán Kónya.

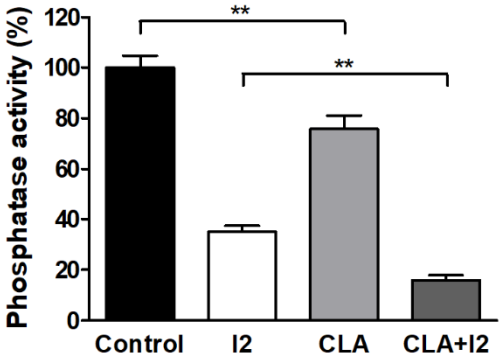

Figure 15. Distribution of PP1 and PP2A activity in BPAECs. BPAECs cells were treated with 10 nM CLA and the phosphatase activity in the lysates of untreated (control) or CLA treated cells was determined in the absence or the presence of 2 μM inhibitor-2 using ^{32}P-MLC20 as substrate. Data represent means ± SEM, **p<0.01 (n=3), One-way ANOVA, Newman-Keuls post-hoc testing.

Investigation of eNOS^{pThr495} dephosphorylation upon EGCG induced PP2A mediated MP activation

The above data are consistent with a dephosphorylation sequence of PP2A→MYPT1^{pThr696}-PP1c→eNOS^{pThr495}, but this putative mechanism requires further experimental confirmation.

Therefore, activation of PP2A in BPAECs and subsequent dephosphorylation of both MYPT1^{pThr696} and eNOS^{pThr495} were probed. It was previously shown that in melanoma cells EGCG binds to the 67LR [252] and increases PP2A activity [15] in a PKA dependent manner. This activation of PP2A was shown earlier to be specific for the PP2A trimer holoenzyme including the Bδ subunit and was due to phosphorylation of Bδ by PKA [95]. We confirmed that both PP2A-Bδ and 67LR are present in BPAECs (Fig. 16.), therefore we attempted to activate PP2A with EGCG. (the Western blot experiment (Fig. 16) was performed by Dr. Bálint Bécsi). Since the endogenous level of eNOS^{pThr495} was quite low, we treated BPAECs with PMA to achieve a higher level of eNOS^{pThr495}, and to detect more reliably the eNOS^{pThr495} dephosphorylation. Treatment of BPAECs with EGCG in a concentration range from 1 µM to 20 µM resulted in substantial decrease in the levels of both MYPT1^{pThr696} (Fig. 17A, B) and eNOS^{pThr495} (Fig. 17A, C), suggesting that PP2A is involved in their dephosphorylation. Presumably, PP2A induces activation of MP via dephosphorylation of MYPT1^{pThr696} resulting in subsequent dephosphorylation and activation of eNOS as well. Moreover, EGCG also induced substantial dephosphorylation of 20 kDa light chain of myosin II (MLC20) as assessed by an antibody specific for dual phosphorylated MLC20 at Thr18/Ser19 (ppMLC20) as shown in Fig. 17A and D (bar graph).

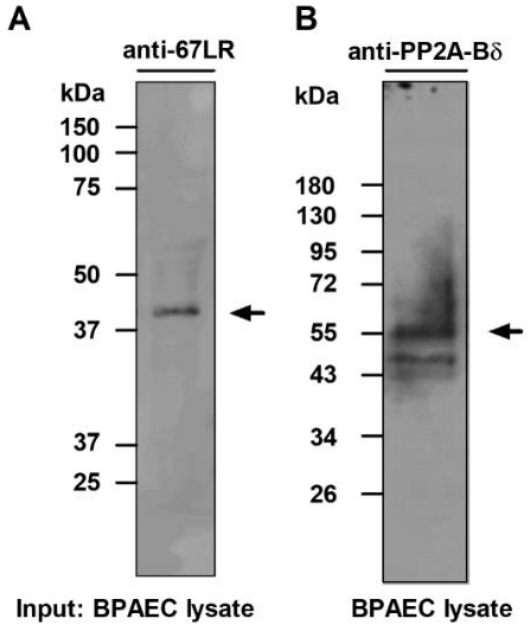

Figure 16. Identification of 67-kDa laminin receptor and the B56δ subunit of PP2A (PP2A-Bδ) in BPAE cells. The antibodies gave cross-reactions according to the same pattern described by the suppliers.

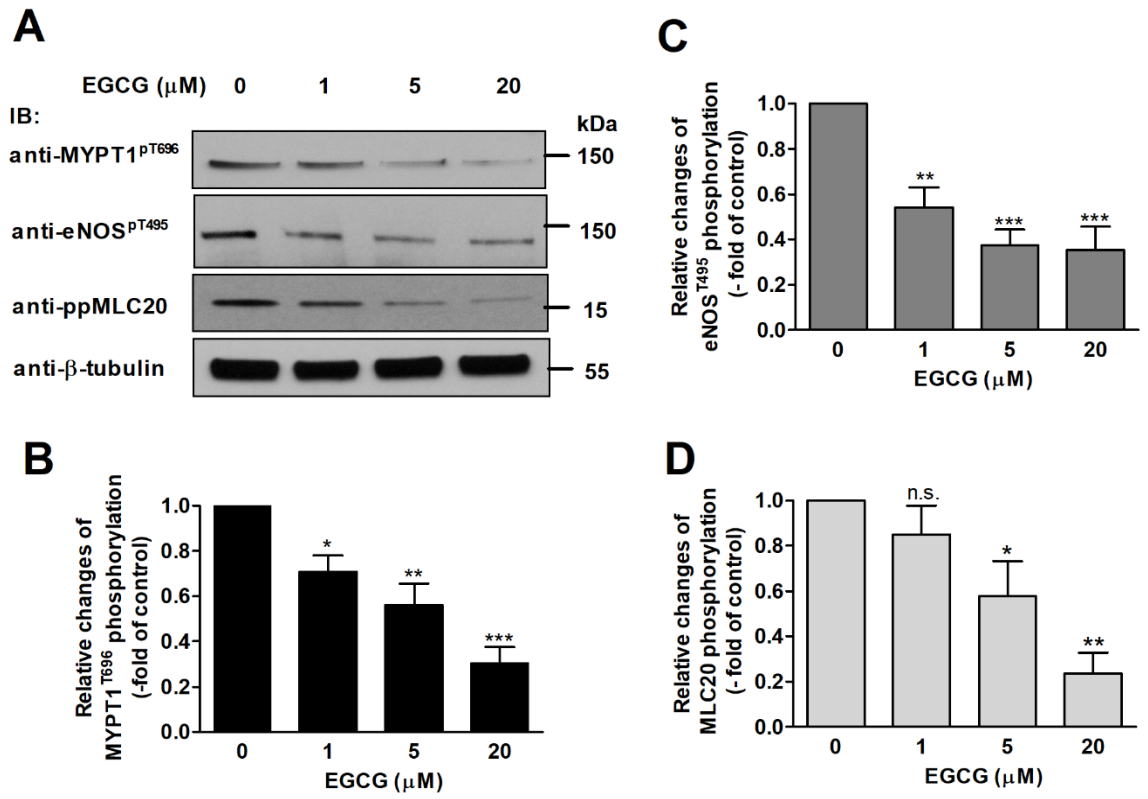

Figure 17. The effect of EGCG treatment on the level of MYPT1^{pThr696}, eNOS^{pThr495} and ppMLC20. (**A**) BPAECs were pre-treated with 100 nM PMA for 30 minutes, then challenged with EGCG in the indicated concentrations for 1 hour. Changes in the level of MYPT1^{pThr696}, eNOS^{pThr457} and ppMLC20 were assessed by Western blotting with phospho-specific antibodies upon the different challenges with EGCG. Cropped images of representative Western blots are shown. Bar graphs represent the changes in the level of MYPT1^{pThr696} (**B**), eNOS^{pThr495} (**C**) and ppMLC20 (**D**) determined by densitometric analysis of blots from 3-4 independent experiments (means ± SE, n.s.: not significant, *p<0.05, **p<0.01, *** p<0.001 compared to control, i.e. without EGCG, One-way ANOVA, Newman-Keuls post-hoc testing).

In accordance with the above assumptions, Fig. 18. demonstrates that EGCG treatment of BPAECs significantly increased the phosphatase activity (the phosphatase activity assay was performed by Zoltán Kónya). It is also important to note that EGCG has been shown to increase the phosphorylation level at Ser1177 of eNOS, a phospho-site which is known to stimulate eNOS activity [16, 253-254].

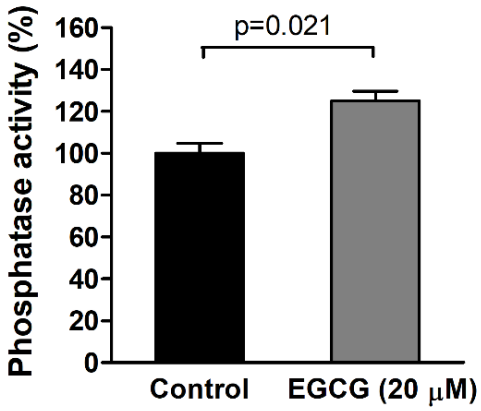

Figure 18. The effect of EGCG treatment on total phosphatase activity. BPAECs cells were treated with 20 μM EGCG and the phosphatase activity in the lysates of untreated (control) or EGCG treated cells was determined using ^{32}P-MLC20 as substrate. Data represent means ± SEM (n=3), two-tailed Student's *t*-test.

Next, we searched for further evidence of the PKA dependence of EGCG induced dephosphorylation processes. We silenced the catalytic subunit α of PKA (PKAcα) in BPAECs and assessed the level of MYPT1^{pThr696}, eNOS^{pThr495} and ppMLC20 in the cells. Fig. 19. illustrates the changes in the level of MYPT1^{pThr696}, eNOS^{pThr495} and ppMLC20 in BPAECs transfected with scrambled or PKAcα specific siRNAs and then challenged with different concentration of EGCG. It is apparent that transfection of BPAECs with scrambled siRNA resulted in similar patterns of dephosphorylation of MYPT1^{pThr696}, eNOS^{pThr495} and ppMLC20 upon EGCG treatments as observed in Fig. 17. In BPAECs transfected with PKAcα specific siRNAs a slight decrease in the basal phosphorylation of MYPT1^{pThr696}, eNOS^{pThr495} and ppMLC20 were observed, however, no significant dephosphorylation of these proteins were detected upon challenges by EGCG. These data confirmed that EGCG induced phosphatase activation in BPAECs is also accomplished in a PKA dependent manner.

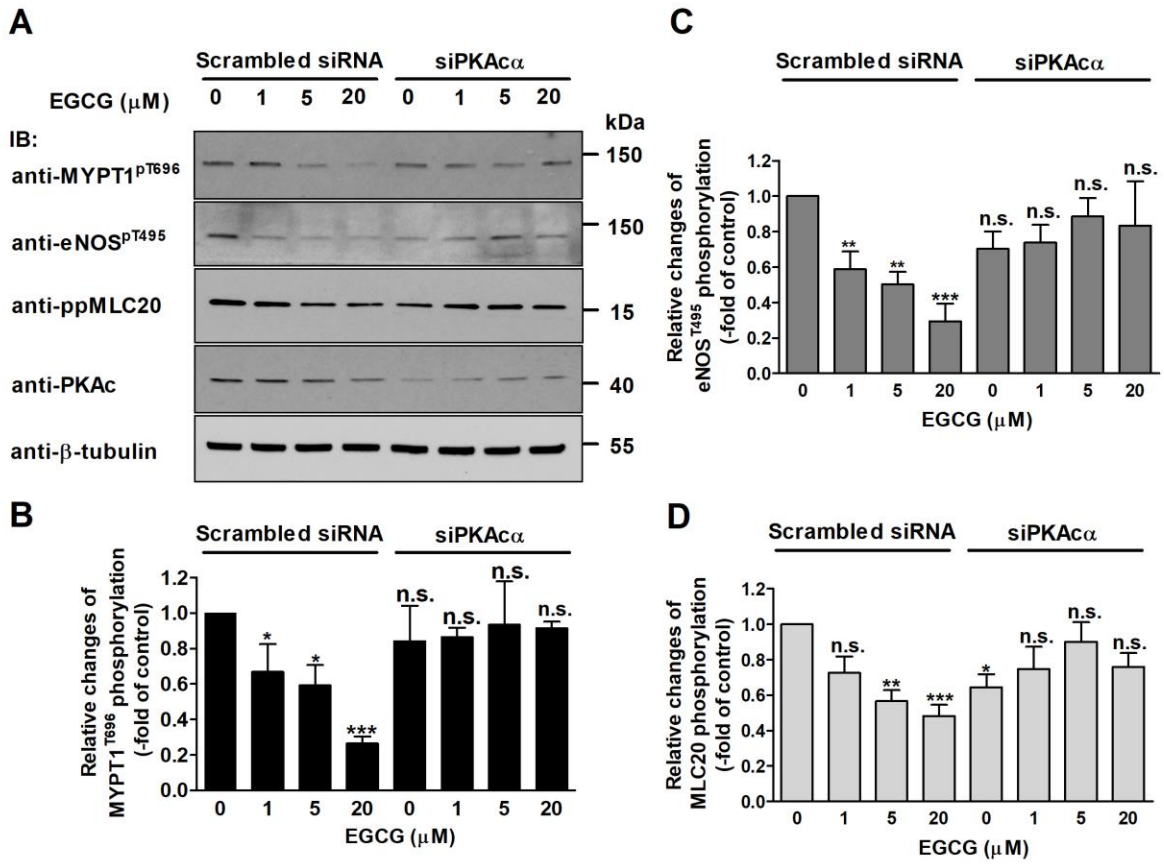

Figure 19. The effect of PKA silencing on EGCG treatment and the level of MYPT1^{pThr696}, eNOS^{pThr495}, and ppMLC20*. **(A)** BPAECs were transfected with scrambled or PKA catalytic subunit (PKAc) specific siRNA then treated with PMA and EGCG and the changes in the level of MYPT1^{pThr696}, eNOS^{pThr495} and ppMLC20 were assessed as described by Western blotting with phospho-specific antibodies upon EGCG treatment. Cropped images of representative Western blots are shown. Bar graphs represent the changes in the level of MYPT1^{pThr696} (**B**), eNOS^{pThr495} (**C**) and ppMLC20 (**D**) determined by densitometric analysis of blots from three independent experiments (means ± SE, n.s.: not significant, *p<0.05, **p<0.01, *** p<0.001 compared to control, i.e. without EGCG, One-way ANOVA, Newman-Keuls post-hoc testing).

The effects of PKC activation and phosphatase inhibition/activation on NO production and transendothelial electrical resistance of BPAECs

The effect of PKC activation, as well as phosphatase inhibition/activation was also assayed on physiological responses of BPAECs such as NO production and barrier function. For NO measurement NO specific 4,5-diaminofluorescein diacetate (DAF-2 DA) fluorescence of cells was captured (Fig. 20A). The DAF-2 DA NO measurements (Fig. 20.) were carried out by Dr. Dénes Nagy. BPAECs loaded with the reaction mixture including DAF-2 DA were subjected to different treatments, then fluorescent intensities of cells were determined (Fig. 20B). It is seen that PMA

moderately, but significantly decreased NO synthesis. In contrast, EGCG spectacularly enhanced NO production, and it also attenuated PMA suppressed NO synthesis. These changes in NO synthesis well correlate with the influence of these effectors on the phosphorylation level of $eNOS^{pThr495}$ (see Figs. 10, 14 and 17.).

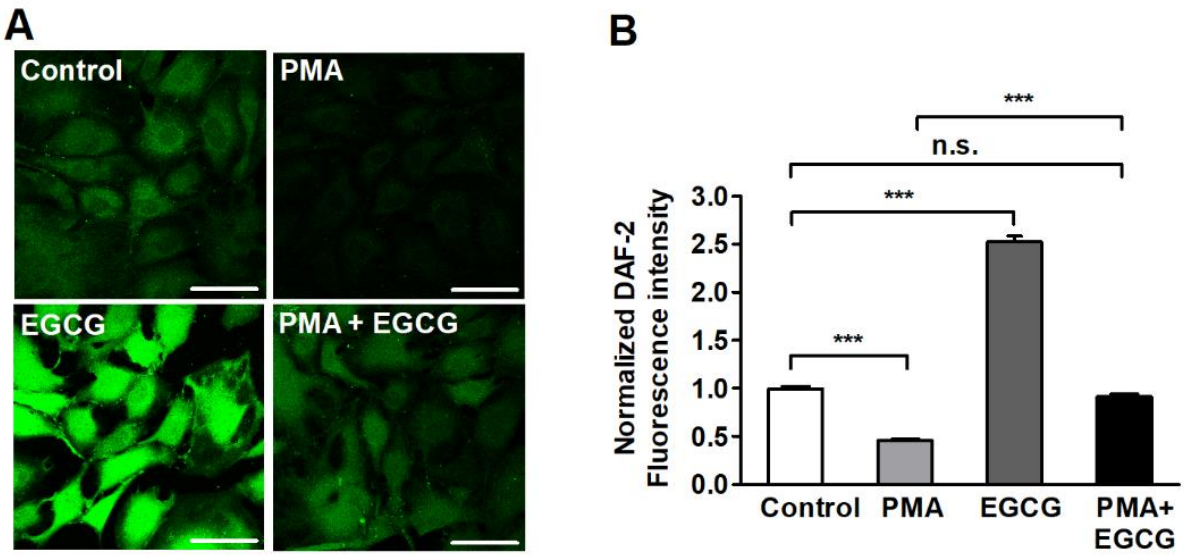

Figure 20. Effect of PKC and phosphatase activation on NO production of BPAECs. (**A**) BPAECs were grown on coverslips in serum-free medium and loaded with the reaction mixture including DAF-2 DA for 60 min. Next, coverslips were incubated with the PKC activator PMA (100 nM), EGCG (20 μM) and the combination of PMA and EGCG in parallel with the non-treated coverslips (control) for 60 min. Scale bar, 50 μm. (**B**) Single cell fluorescence activity determined by ImageJ after different treatments indicated in (**A**). Results of single cell values (120-153 individual cells) of two independent experiments are shown in means ± SEM. (n.s.: not significant, *** $p<0.001$, One-way ANOVA, Newman-Keuls post-hoc testing).

In another set of experiments, we investigated how PMA, CLA, TM, EGCG and the combination of PMA and EGCG affect TER of BPAECs. PMA and TM suppressed TER moderately, and the decreasing tendency in TER appeared to be partially reversible in case of PMA, but irreversible with TM during the assay period (Fig. 21A). CLA also induced a fast and dramatic decrease in TER in an irreversible manner. In accord with the earlier findings of Kolozsvari et al. [250] this "acute" effect of the phosphatase inhibitors on TER was presumably due to the inhibition of MP resulting in sustained phosphorylation of MLC20 which highly contributes to decreasing TER. In contrast, EGCG enhanced TER of BPAECs and attenuated PMA induced suppression of TER either when it was added together or 30 min after PMA (Fig. 21B). These data suggest that PKC activation or phosphatase inhibition suppress TER compromising barrier

function of BPAECs. On the other hand, phosphatase activation by EGCG appears to improve barrier function and helps to restore, at least in part, the effect of barrier suppressing agents.

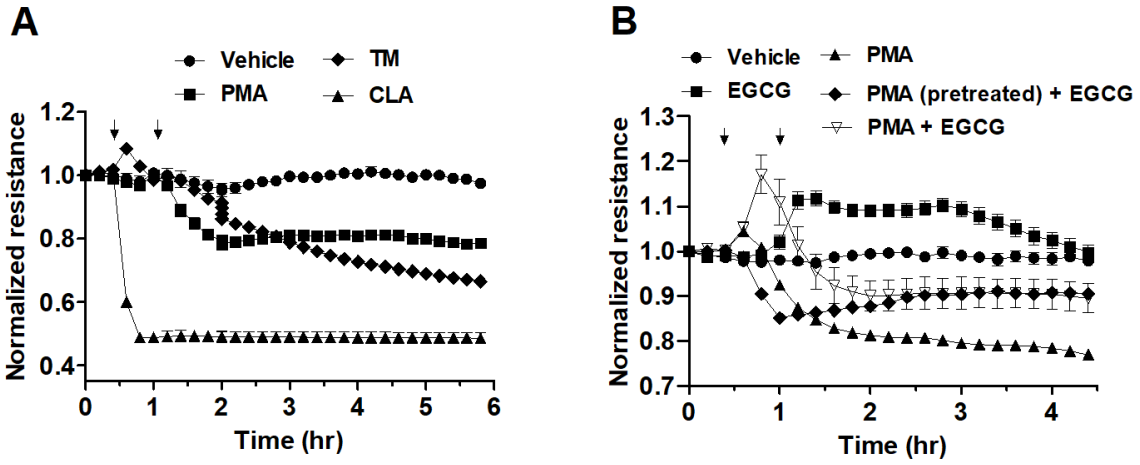

Figure 21. Effect of PKC activation and phosphatase inhibition/activation on the transendothelial electrical resistance of BPAECs. *(***A**) BPAECs grown in serum-free medium in ECIS arrays were untreated (control), or treated with PMA (100 nM), 10 nM CLA or with 1 μM tautomycin (TM) for 30 minutes. (**B**) BPAECs cells grown on ECIS arrays were treated with vehicle, 20 μM EGCG, 100 nM PMA or with 100 nM PMA and 20 μM EGCG, added together or EGCG was added 30 minutes after PMA. Time points of treatment with effectors are indicated by arrows. Normalized TER values were expressed as mean ± SEM of 3-4 individual experiments.

Investigation of the barrier function of HLMVECs upon Adenosine and ATPγS administration

It has long been known that extracellular purines function as intercellular signaling molecules [255-257] that may positively affect the barrier function of macrovascular endothelial cells, however, their effects on microvascular endothelium are less explored. Thus, in the next part of our studies we examined the effects of Ado and ATPγS which is a very slowly hydrolysable ATP analog, on HLMVEC barrier function. First, we challenged HLMVECs with increasing concentrations (25-200 μM) of Ado (Fig. 22A) or ATPγS (Fig. 22B) and TER was measured. Both Ado and ATPγS induced TER increase of HLMVECs in a dose-dependent manner, reflecting HLMVEC barrier strengthening with maximal effect at 100 μM. As such, we used 50 or 100 μM Ado or ATPγS in subsequent experiments.

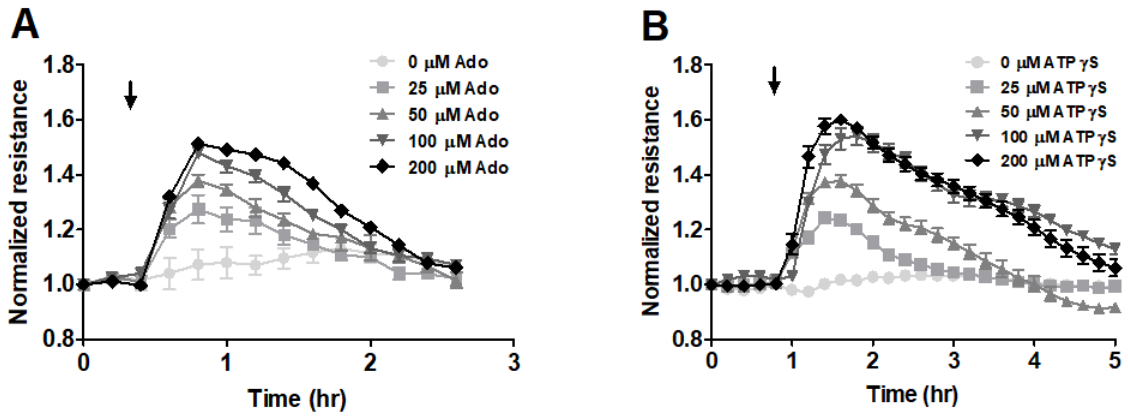

Figure 22. Ado and ATPγS enhance the EC barrier in HLMVEC. HLMVECs were treated with increasing concentrations (10-200 μM) of Ado (**A**) or ATPγS (**B**), and TER was recorded. Results are presented as mean ± SEM of three independent experiments. Arrows indicate the time points of Ado and ATPγS administration.

Mapping of the expression of purinergic receptors in HLMVECs

Adenosine initiate its effects via P1-, while ATPγS exert its effect by binding to cell surface P2 purinergic receptors [258]. The P1 adenosine receptors can be divided into four subclasses, namely A1, A2A, A2B and A3 [259]. The A1 and A3 receptors are coupled to G_i proteins that inhibit adenylyl cyclase, while A2A and A2B are G_s protein-coupled receptors, therefore can increase intracellular cyclic-AMP (cAMP) level [259]. P2 receptors are divided into two subclasses: the P2X (P2X1-7) receptors are extracellular ATP-gated, calcium-permeable, non-selective cation channels, that are unlikely to be involved in the endothelial barrier regulation [18]; while P2Y receptors (P2Y1, P2Y2, P2Y4, P2Y6, P2Y11-14) are G-protein coupled receptors. The expression pattern of purinergic receptors in ECs from different regions of the vasculature is various and not unambiguously described [260-261]. Therefore, we investigated the expression of G-protein coupled P1 and P2Y receptors in HLMVECs. Our quantitative RT-PCR analysis showed that among P1 adenosine receptors (the identification of P1 receptors were performed by Zsuzsanna Bordán.) HLMVECs expressed A2B receptors alone with a negligible expression of other adenosine receptor subtypes (Fig. 23A). This expression pattern differs significantly compared to HUVEC [261] and also vary that as observed in HPAEC [17] suggesting differences in P1 receptor signaling in ECs from different vascular beds. Analysis of P2Y receptors profile revealed that HLMVECs express mRNAs of all eight receptor types (Fig. 23B) with preferential expression of P2Y1, 4, 6, 13 and 14 mRNAs, while the expression level of other receptor subtypes was lower.

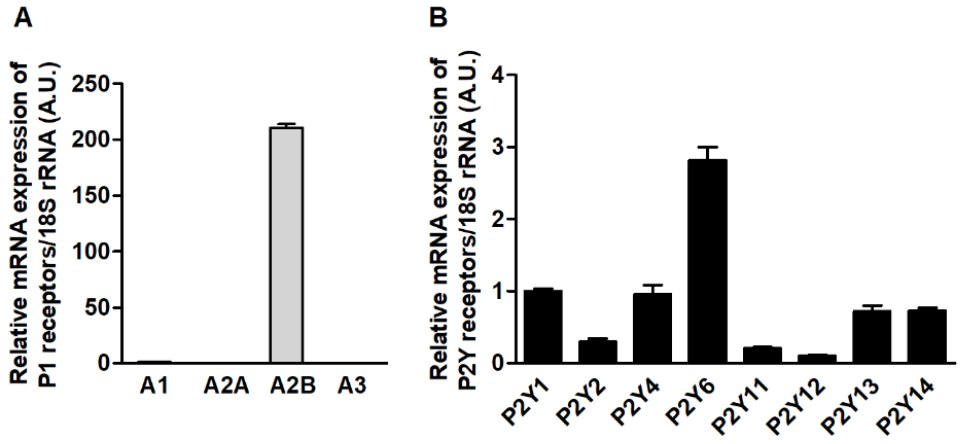

Figure 23. Relative expression of adenosine (P1) and P2Y receptor mRNAs in HLMVEC. Receptor mRNA expression was determined by quantitative RT-PCR. Bar graphs represent the normalized level of adenosine (P1) receptors (A1, A2A, A2B, and A3) (**A**) or P2Y receptors (**B**) by 18S rRNA and are presented as arbitrary unit (A.U.).

Identification of G-protein coupled P2Y receptors involved in ATPγS-induced HLMVEC barrier enhancement

Since five P2Y receptors (P2Y1, 2, 4, 11 and 12) may be activated by ATPγS, in the next set of experiments we individually depleted them to identify those ones which are involved in the ATPγS-induced increase in TER. HLMVECs were treated with siRNA specific to P2Y1, 2, 4, 11 and 12 for 72 hours, then TER was measured in the presence or absence of ATPγS. We have demonstrated that depletion of P2Y4 and P2Y12, but not other receptors resulted in significant decrease in TER, indicating that these receptors are involved in ATPγS-induced HLMVEC barrier enhancement (Fig. 24.). P2Y12 is solely G_i-coupled receptor [262], while P2Y4 is the best known to be coupled to G_q [262]. However, some recent literature data revealed G_i coupling for P2Y4 as well [263]. While none of the other G_q or G_s coupled P2Y receptors are involved in ATPγS-induced barrier enhancement (Fig. 24.), it is reasonable to assume that ATPγS-induced HLMVEC barrier enhancement is mediated through G_i signaling. Interestingly, in contrast to ATPγS, Ado induced HLMVEC barrier strengthening most likely involves G_s- and G_q-coupled A2B receptors (Fig. 23A), suggesting that mechanisms of Ado- and ATPγS-induced EC barrier strengthening are different in the microvasculature.

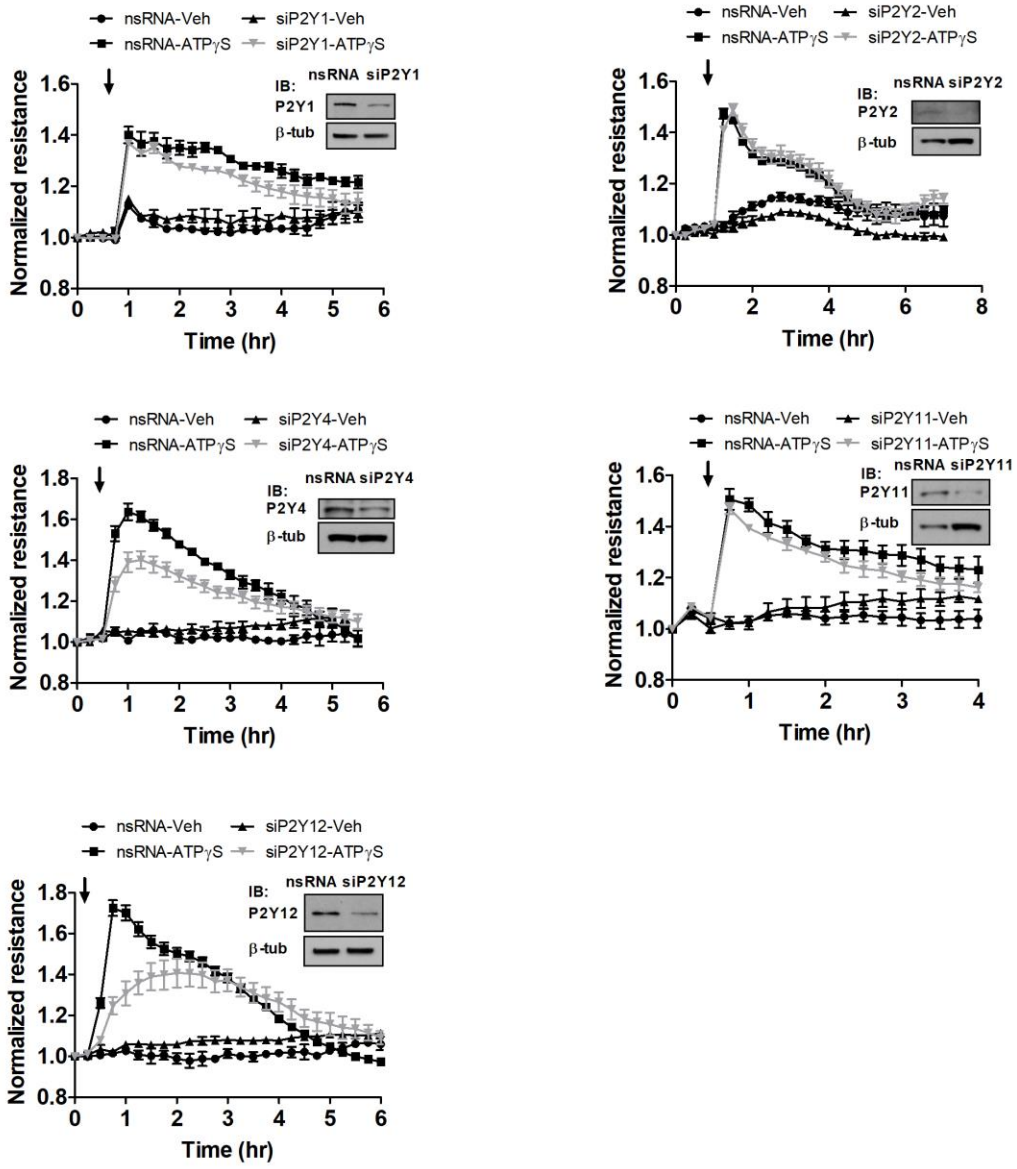

Figure 24. ATPγS improves endothelial barrier function via P2Y4 and P2Y12 receptors in HLMVEC. Endothelial cells were treated either with non-specific siRNA (nsRNA) or silencing RNA specific to different P2Y receptors for 72 hours, and TER was measured upon challenge with 50 μM ATPγS. Depletion of receptors was determined by Western blotting with specific antibody using β-tubulin as a loading control (insets). Arrows indicate the time points of ATPγS administration.

Adenosine and ATPγS increase PKA activity by different signaling mechanisms

It has been shown that PKA activation is a requirement for Ado- and ATP-induced barrier strengthening in HPAEC [17-18]. The primary activation pathway for PKA involves the binding of four cAMP molecules to the regulatory subunit leading to dissociation of the holoenzyme [264-265].

While the G_s-mediated cAMP-dependent activation of PKA by Ado is well described, cAMP-independent mechanisms of PKA activation are by comparison poorly understood.

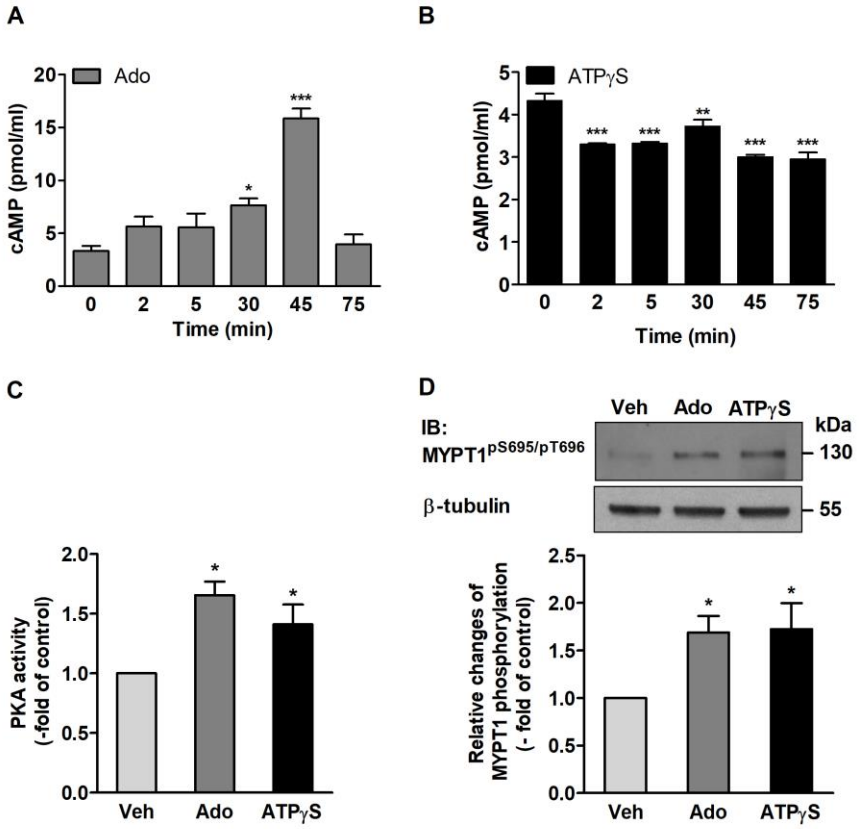

Figure 25. Effect of ATPγS and Ado on cAMP levels and PKA activity in HLMVEC. HLMVECs were treated with 100 μM Ado (**A**) or ATPγS (B) for 30 minutes, and the levels of cAMP were measured by competitive enzyme-linked immunosorbent assay (Cyclic AMP EIA Kit). Results are shown as mean of three individual experiments, with three parallels each time ± SEM (*$p < 0.05$, **$p < 0.01$, ***$p < 0.001$ versus control (0 time point), one-way ANOVA, Newman-Keuls post-hoc testing). (**C**) HLMVECs were treated with 100 μM Ado or ATPγS for 30 minutes, and PKA activity was measured by colorimetric protein kinase activity assay. Results are shown as mean of three individual experiments ± SEM.*$p < 0.05$, Veh vs. Ado or Veh vs. ATPγS, one-way ANOVA, Newman-Keuls post-hoc testing. (**D**). Changes in the level of $MYPT1^{pS695/T696}$ was assessed by Western blotting upon the vehicle, 50 μM Ado or ATPγS treatment (upper panel). Bar graphs represent the changes in the level of $MYPT1^{pS695/pThr696}$ determined by densitometric analysis of immunoblots from four independent experiments (mean ± SEM, *$p<0.05$, Veh vs. Ado or Veh. vs. ATPγS, one-way ANOVA, Newman-Keuls post-hoc testing).

Our data indicate (Fig. 25.) that Ado treatment induced immediate elevation of cAMP levels in HLMVEC (Fig. 25A), culminating at 30-45 minutes which paralleled with Ado-induced TER increase (see Fig. 22A). In contrast, ATPγS-induced HLMVEC barrier enhancement accompanied by modest, but significant cAMP decrease started as early as 2 min (Fig. 25B), supporting the involvement of G_i-mediated signaling in ATPγS-induced HLMVEC barrier enhancement. In a

parallel experiment, we examined the effect of Ado and ATPγS on PKA activity in HLMVEC homogenates (Fig. 25C). We found that both compounds induced significant activation of PKA after 30 min of treatment. Activation of PKA in EC homogenates is accompanied by increased MYPT1 dual phosphorylation at Ser695/Thr696, which are established PKA phosphorylation sites [128, 245] (Fig. 25D). These data strongly suggest that ATPγS activates PKA via an unconventional G_i-mediated pathway. Since PKA-mediated phosphorylation of MYPT1 is involved in the regulation of MP activity, at least *in vitro* [12], these data also suggest that the effects of PKA on ATPγS-induced HLMVEC barrier enhancement are MP-dependent. The cAMP level measurement upon Ado treatment (Fig 25. A.) and PKA activity assays were carried out by Dr. Sanjiv Kumar.

Investigation of the involvement of EPAC1 and PKA in Adenosine- and ATPγS-induced HLMVEC barrier enhancement

To directly evaluate the role of PKA activity in HLMVEC barrier strengthening induced by either Ado or ATPγS, we next examined the effects of PKAc depletion on the phosphorylation state of MLC20 in the presence or absence of these purinergic agonists (Fig. 26.). In control, non-specific siRNA transfected cells both Ado and ATPγS decreased the phosphorylation level of MLC20 at Thr18/Ser19 phosphorylation sites, as anticipated (Fig. 26A-C). However, depletion of PKAc abolished ATPγS-, but not Ado-induced MLC20 dephosphorylation (Fig. 26A), suggesting the involvement of another, perhaps more complex signaling pathway that is stimulated by Ado. Since the other cAMP effector, EPAC1 has been reported to be involved in SM relaxation and regulation of MLC20 dephosphorylation [156, 266], we investigated the involvement of EPAC1 in Ado-induced MLC20 dephosphorylation in HLMVEC. Predictably, EPAC1 depletion had no effect on cAMP-independent ATPγS-induced MLC20 dephosphorylation (Fig. 26B), but surprisingly, had no effect on Ado-induced cAMP-dependent MLC20 dephosphorylation either. Simultaneous depletion of PKAc and EPAC1 in double knock-down experiment (Fig. 26C) abolished Ado-induced MLC20 dephosphorylation indicating that both PKA and EPAC1 activities are simultaneously required to achieve MLC20 dephosphorylation in cAMP-dependent Ado model. To examine the role of PKA and EPAC1 in HLMVEC barrier strengthening induced by Ado and ATPγS we depleted both PKAc and EPAC1, then challenged HLMVECs with Ado or ATPγS and measured TER changes. We found that PKAc silencing significantly attenuated

ATPγS- but not Ado-induced effects on TER (Fig. 27A). However, depletion of EPAC1 had no effect on TER changes induced by either Ado or ATPγS (Fig. 27B). In accord with the effects on MLC20 phosphorylation, simultaneous depletion of PKAc and EPAC1 attenuated Ado-induced TER increase indicating that PKA effects on EC barrier properties are EPAC1-dependent (Fig. 27C). Simultaneous depletion of PKAc and EPAC1 decreased ATPγS-induced increase in TER in similar extent as depletion of PKAc alone (Fig. 27A), as anticipated, indicating that EPAC1 is not

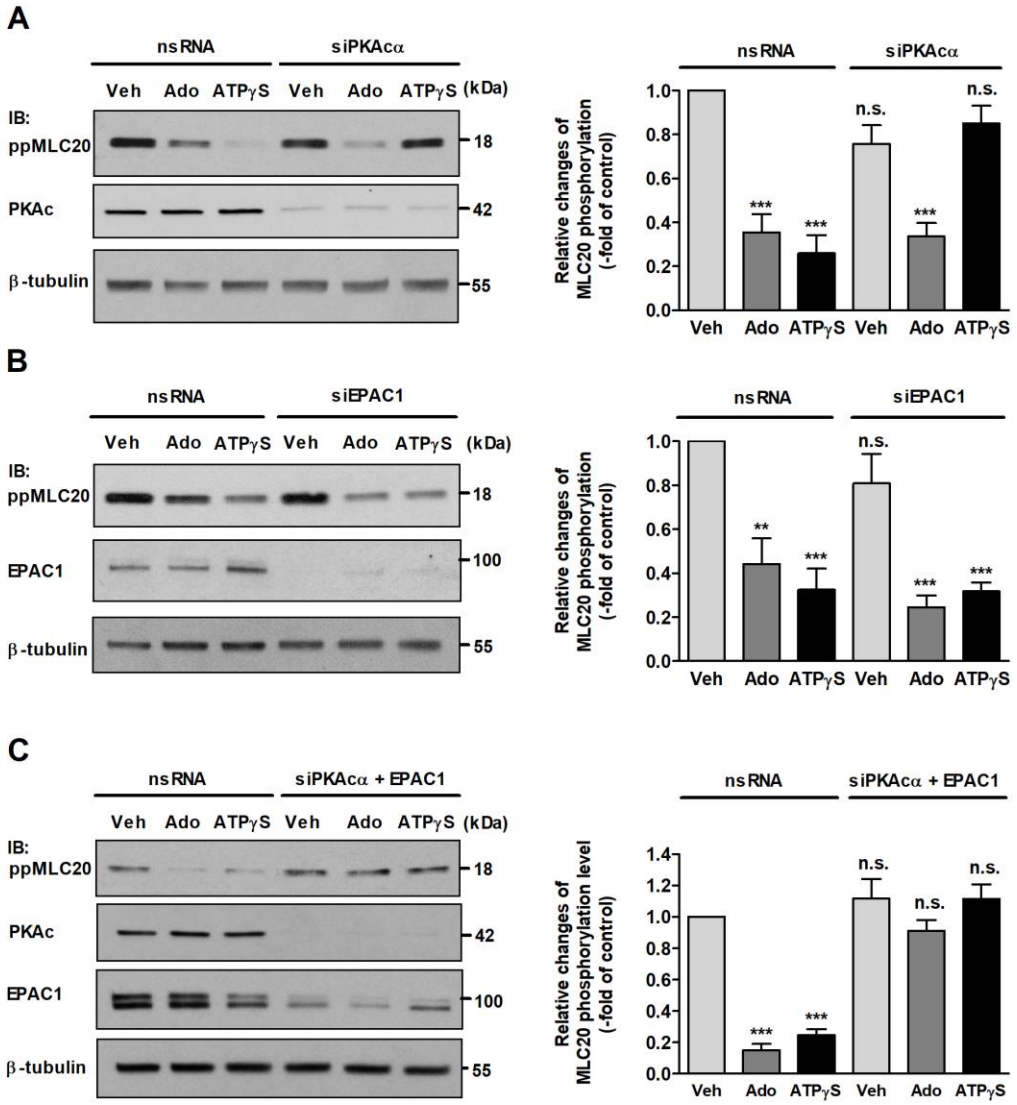

Figure 26. Effect of PKA and EPAC1 depletion on Ado and ATPγS induced MLC20 dephosphorylation. HLMVECs were transfected with non-specific siRNA (nsRNA), PKACα (**A**) or EPAC1 (**B**) specific silencing RNA or with both together (**C**). Three days after transfection the cells were treated with 50 μM ATPγS or Ado for 30 minutes and the level of ppMLC20, depletion of PKAc and EPAC1 was determined by Western blotting. The bar graphs represent the changes in the level of ppMLC20. Densitometric analysis of blots from 3-7 independent experiments (mean ± SEM, n.s.= not-significant, **p<0.01, ***p<0.001 versus non-specific siRNA treated vehicle control, one-way ANOVA, Newman-Keuls post-hoc testing).

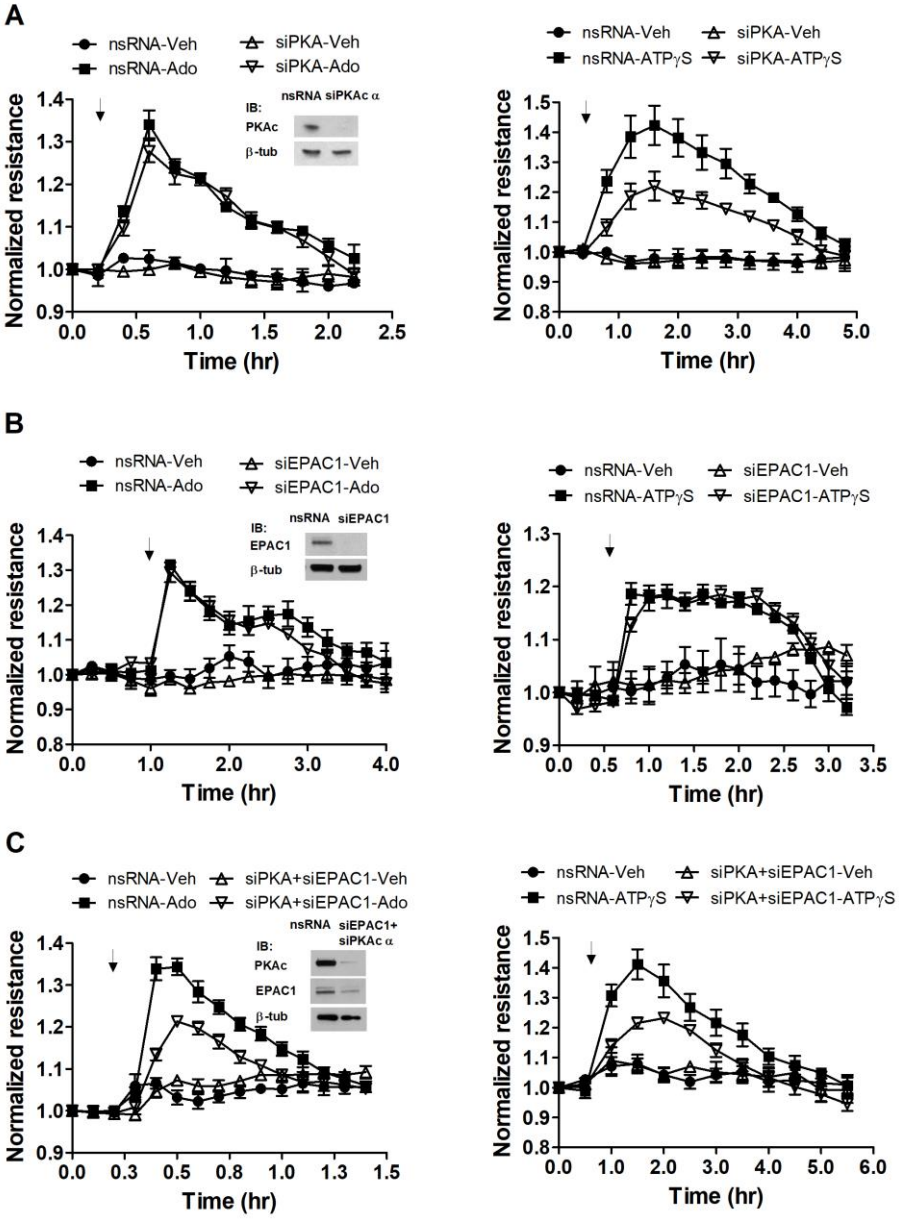

Figure 27. Effect of PKAc and EPAC1 depletion on Ado- and ATPγS-induced EC barrier enhancement. HLMVECs were transfected with non-specific siRNA (nsRNA), PKAcα specific (**A**), EPAC1 specific (**B**), or both EPAC1 and PKAcα specific silencing RNAs (**C**). Three days after transfection HLMVECs were treated with 50 μM Ado (left panel) or ATPγS (right panel) and changes in TER was recorded. Arrows indicate the time points of ATPγS and Ado administration. Data are presented as mean ± SEM. Depletion of PKA catalytic subunit or EPAC1 (**insets**) was confirmed by Western blotting.

involved in G_i-mediated ATPγS-induced EC barrier enhancement. These data suggest that while PKA alone is sufficient to exert a barrier-enhancing effect in ATPγS model, PKA-mediated Ado-induced EC barrier strengthening requires simultaneous EPAC1 activation. Conversely, EPAC1-mediated effects of Ado on EC barrier are PKA-dependent.

AKAP2-MP axis is involved in ATPγS-, but not Adenosine-induced barrier-enhancing effect in HLMVEC

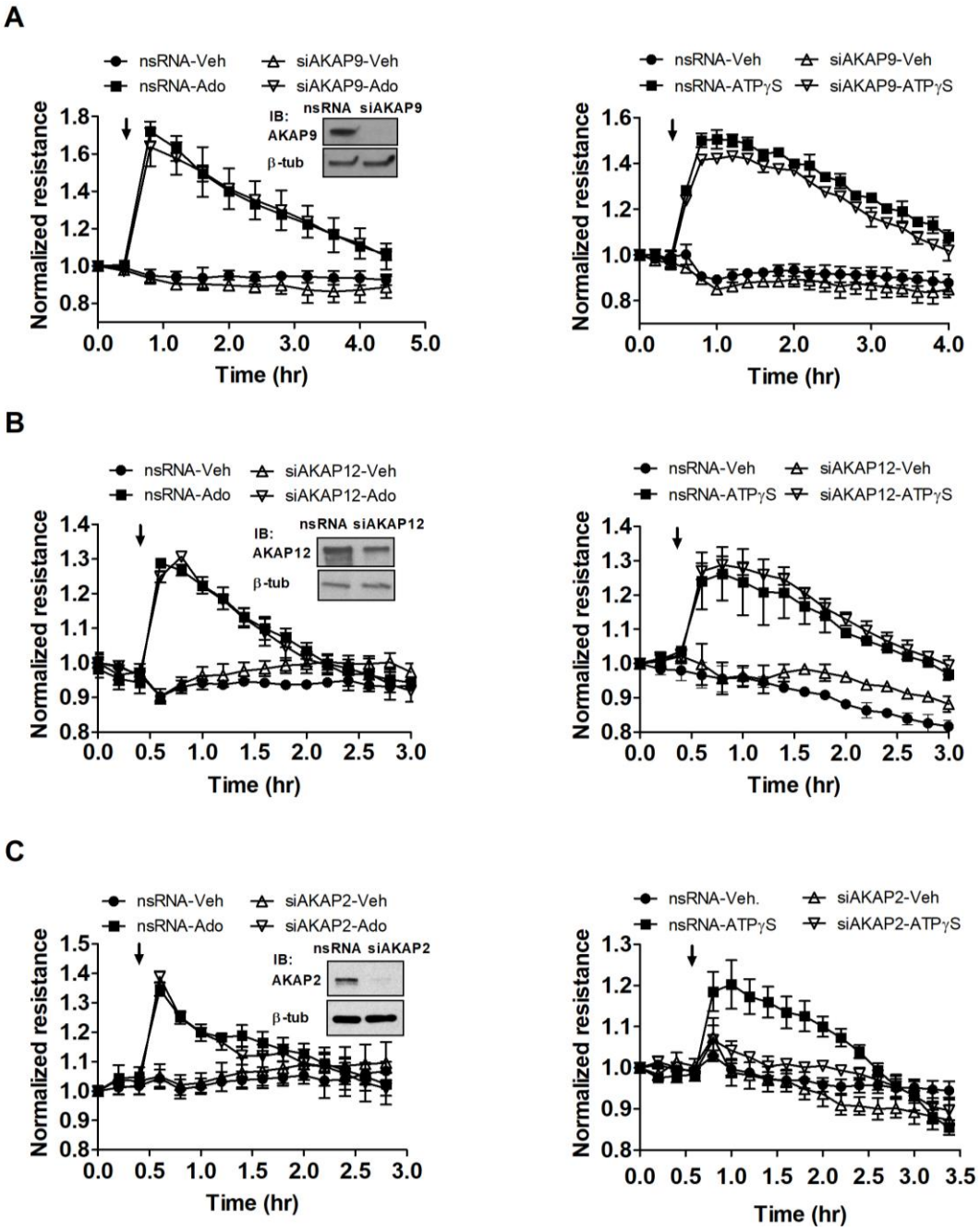

Figure 28. AKAP2 contributes to ATPγS-induced HLMVEC barrier enhancement. HLMVECs were transfected with non-specific siRNA (nsRNA) or AKAP9 (**A**), AKAP12 (**B**) and AKAP2 (**C**) specific silencing RNA. Three days after transfection HLMVECs were treated with 50 μM ATPγS (right panels) or 50 μM Ado (left panels) and changes in TER was recorded. Arrows indicate the time points of ATPγS and Ado administration. Depletion of AKAPs (**insets**) were confirmed by Western blotting. Data are presented as mean ± SEM of four independent experiments.

Scaffolding PKA-binding AKAP proteins exert their activities mainly via directing PKA to specific subcellular location (targets) and serve as a platform for biochemical interactions [267]. It has also been shown that cAMP-independent PKA activation may involve AKAPs [157]. Furthermore, specific AKAPs namely AKAP9 and -12 are involved in EC barrier regulation, although in a cAMP-dependent manner [158-159]. Thus, in the next set of experiments, we examined whether depletion of AKAPs influences the Ado- and ATPγS-induced TER increases, and MLC20 phosphorylation. Our data indicate that neither depletion of AKAP9 (Fig. 28A) nor AKAP12 (Fig. 28B) attenuated ATPγS or Ado-induced barrier enhancing effects in HLMVEC. However, depletion of AKAP2 attenuated the effect of ATPγS, but not Ado on TER, suggesting a dominant role for AKAP2 in ATPγS induced, cAMP-independent PKA activation.

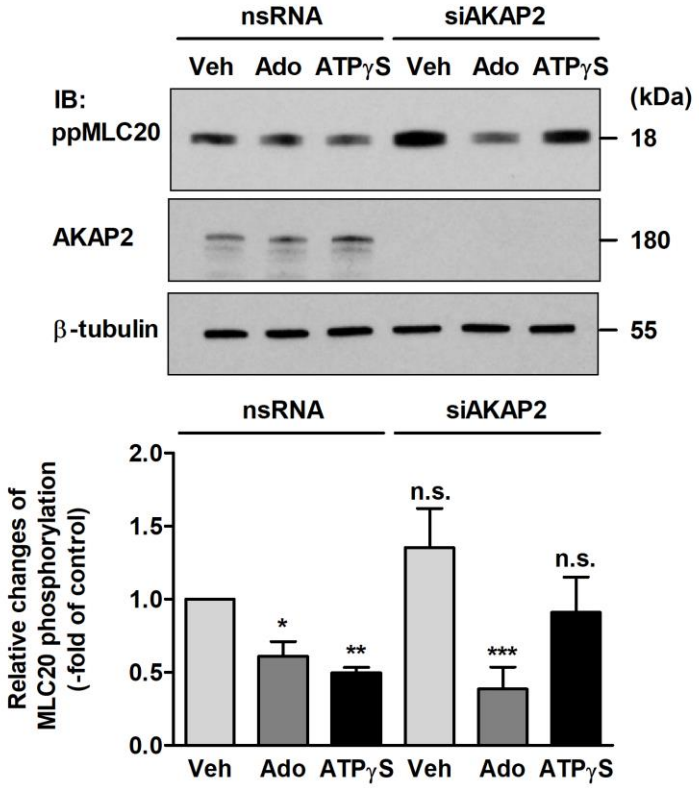

Figure 29. ***Effect of AKAP2 depletion on Ado- and ATPγS-induced MLC20 dephosphorylation.*** HLMVECs were transfected with non-specific siRNA (nsRNA) and AKAP2 specific silencing RNA. Three days after transfection the cells were treated with vehicle, 50 μM Ado or ATPγS for 30 minutes and the level of ppMLC20, further depletion of AKAP2 was determined by Western blotting. The bar graphs represent the changes in the level of ppMLC20. Densitometric analysis of blots from four independent experiments (mean ± SEM, n.s.= not-significant, *p<0.05, **p<0.01, ***p<0.001 versus non-specific siRNA treated vehicle control, one-way ANOVA, Newman-Keuls post-hoc testing).

To investigate the direct involvement of AKAP2 in ATPγS-, and Ado-induced MLC20 dephosphorylation gene silencing experiments were performed (Fig. 29.). Our data show, that AKAP2 has a prominent role in ATPγS-, but not in Ado-induced MLC20 dephosphorylation.

Direct interaction of AKAPs and PP1-containing holoenzymes has been previously reported [268]; however, the interaction of AKAP(s) with MYPT1 has not been described in the literature. Therefore, we investigated whether AKAP2 or other AKAPs could interact with MYPT1. HEK293 cells were transfected with c-myc-MYPT1 [269], and co-immunoprecipitation experiments were performed. Our results (Fig. 30A) demonstrate that MYPT1 can be co-immunoprecipitated with AKAP2 but not with AKAP3, AKAP9 or AKAP12, suggesting the existence of a specific functional complex between AKAP2 and MP. Reciprocal experiments where HA-AKAP2 was overexpressed (Fig. 30B) and provided co-immunoprecipitation of MYPT1 further supported an interaction (direct or indirect). Moreover, our results provided evidence of PKAc and G_{i2} co-immunoprecipitation with AKAP2 in HLMVECs (Fig. 30B) suggesting the scaffolding role of AKAP2 in G_i-mediated PKA activation.

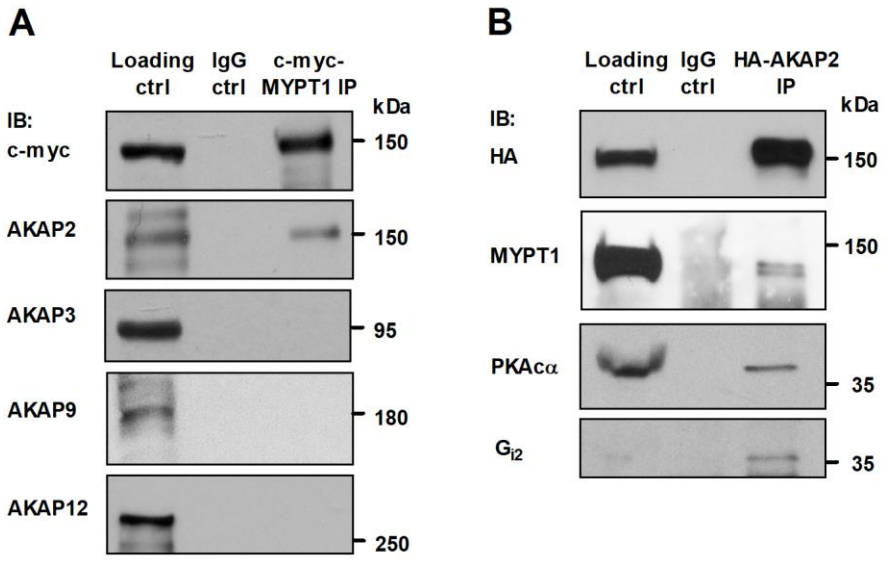

Figure 30. Identification of AKAP2-MYPT1 complex. ***(A)*** The c-myc-MYPT1-containing plasmid was transfected into HEK293 cells. After 48 hours harvested cell lysate was immunoprecipitated (IP) with control IgG or anti-myc antibody. IPs were subjected to Western blot analysis with specific antibodies to myc-tag (MYPT1) and AKAP2, 3, 9, and 12. (**B**) AKAP2 with HA-tag was overexpressed in HEK293 cells, and after 48 hours the IP was carried out as described in Materials and Methods. The samples were subjected to immunoblotting with antibodies against HA-tag (AKAP2), MYPT1, PKAc, and G_{i2}.

DISCUSSION

Investigation of the regulation of eNOS via MP

Phosphorylation/dephosphorylation of eNOS at Thr495 is a crucial factor in the mediation of eNOS activity, and it is also involved in balancing whether eNOS generates NO or superoxide [270]. PKC and ROCK are the kinase candidates to target Thr495 under physiological conditions [271], while the dephosphorylating phosphatase is not unambiguously identified. There appears to be a consensus in the literature that PP1 type phosphatase acts on eNOS phosphorylated at Thr495 ($eNOS^{pThr495}$) in ECs [4, 192, 272]. Surprisingly, the type of PP1 holoenzyme has not been identified yet, although this knowledge is essential to uncover physiological regulatory events in the dephosphorylation of $eNOS^{pT495}$. In the first part of our studies we identified MP, consisting of associated PP1cδ and MYPT1, as a phosphatase holoenzyme which dephosphorylates $eNOS^{pT495}$. In support of this finding are the following data: (i) MYPT1 and eNOS co-precipitated from HUVEC, and tsA201 lysates overexpressing recombinant MYPT1 and eNOS, and their colocalization was also apparent in HPAEC and BPAEC (see Fig. 9.) (ii) stable interaction between c-myc-eNOS and GST-MYPT1 was also confirmed by surface plasmon resonance based binding assays using purified proteins (iii) the PP1cδ-MYPT1 complex dephosphorylated $eNOS^{pT495}$ effectively in which MYPT1 had a targeting role increasing the activity of PP1cδ toward $eNOS^{pT495}$ (see Fig. 12.) (iv) depletion of PP1cδ-MYPT1 or both in BPAECs increased the level of $eNOS^{pT495}$ (see Fig. 13.). We also provide evidence that overexpression of MYPT1 in eNOS expressing tsA201 cells or in HEK293-eNOS cells increased eNOS activity without changing the expression level of eNOS. However, in a recent paper of Lubomirov *et al.* [273] it was shown that MYPT1 may also influence eNOS expression as in basilar arteries of old, heterozygous MYPT1-Thr696Ala knock-in mice eNOS-mRNA was lower in knock-in compared to the wild-type animal. We speculate that the observed differences might be due to the distinct experimental models applied.

It has been established that regulation of MP activity occurs via inhibitors (toxins, inhibitory proteins) interacting with the PP1cδ catalytic subunit [104, 111, 274] or by inhibitory phosphorylation of MYPT1 at Thr696 and Thr850 residues [275]. In our study regulation of $eNOS^{pT495}$ level by MP was modeled with cell-permeable phosphatase inhibitory toxins (CLA and TM) at concentrations assumed to be specific for PP2A and PP1, respectively [102-104]. It should be

emphasized that the viability of ECs limits the applied toxin concentrations. Therefore, only partial inhibition of PP2A or PP1 could be assumed, as it was shown previously [104]. Our present data demonstrate that PP1 specific inhibition by TM moderately increased eNOS^{pT495} and MYPT1^{pT696} levels. In contrast, CLA enhanced both eNOS^{pT495} and MYPT1^{pT696} more profoundly via predominant inhibition of PP2A as validated by phosphatase assays of BPAEC lysates (see Fig. 15.). These results are correlated with previous findings demonstrating that inhibition of PP2A [275] or PP2B [250], enzymes which dephosphorylate MYPT1^{pT696}, leads to increased level of MYPT1^{pT696}. The latter is accompanied by MP inhibition and as a consequence enhanced phosphorylation level of MLC20, a dedicated substrate of MP. The above data establish a mechanism implying an interplay of PP2A and MP in the regulation of eNOS^{pT495} dephosphorylation, however, the physiological significance of these events await further clarification.

Previous work of Michell et al. [4] has shown that forskolin treatment of ECs stimulated dephosphorylation of eNOS^{pThr495} by PP1, suggesting the involvement of a signaling pathway via cAMP/PKA in PP1 activation, however, the detailed mechanism of this process still remained to be elucidated. Our present results highlight another signaling mechanism for physiological stimulation of eNOS^{pT495} dephosphorylation (Fig. 31.) which involves EGCG, as an agonist interacting with the 67LR and signaling downstream to activate PKA and PP2A. It has been proven in melanoma cell lines that EGCG stimulates the activity of PP2A via the 67LR in a cAMP/PKA-dependent manner, and the activated PP2A dephosphorylated both phosphorylated CPI-17 and MYPT1^{pT696} resulting in MP activation and dephosphorylation of merlin, another MP substrate [15]. Therefore, it seemed to be reasonable to assume that the EGCG→ 67LR→PKA→ PP2A pathway also operates in ECs and induces PP2A activation. It is apparent that PP2A activated along this pathway results in marked dephosphorylation of MYPT1^{pT696} coupled with activation of MP (see Figs. 17-19.) and subsequent dephosphorylation of eNOS^{pT495} and ppMLC20 in ECs.

Our present data support the existence of a novel pathway via EGCG→67LR→PKA→PP2A→MP activation for efficient dephosphorylation of both eNOS^{pT495} and ppMLC20 (see Fig. 30.). EGCG and structurally related other catechins may have a plethora of intracellular targets, and they may exert distinct physiological influences. In the previous work of Kiss et al., [276] it has been shown that EGCG interact with and inhibit PP1c activity at micromolar concentrations in *in vitro* phosphatase assays. The binding of EGCG to the hydrophobic groove of

the PP1c substrate binding region was also established [276]. However, only moderate extent of phosphatase inhibition occurred when intact cells were incubated with relatively high EGCG concentration (100-500 μM), and it was presumably due to the low penetration of EGCG through the cell membranes [277]. These data suggest a distinct action of EGCG on cells depending upon its applied concentrations. Thus, at low concentration (1-20 μM) EGCG exerts its effect through binding to 67LR initiating a signaling pathway leading to phosphatase activation. In contrast, at high concentration EGCG might also permeate cells to a certain extent and binds to PP1c causing phosphatase inhibition. However, regarding the assumed EGCG concentration (~1 μM) after regular green tea consumption only the previous process (EGCG→67LR signaling) might have physiological relevance.

In agreement with previous studies [110, 278], we found that PKC activation by PMA, or phosphatase inhibition with CLA, caused a decrease in TER of EC monolayers. The TER and NO suppressing effect of PMA were attenuated by EGCG which helped to restore, at least partially, the barrier integrity and eNOS activity. There are apparent controversies concerning how changes in NO level influence endothelial permeability (reviewed by Durán et al. [212]). It appears that hyperpermeability induced by inflammatory agents required eNOS activation and increased NO production [279]. However, light and electron microscopic studies of Predescu at al. [3] revealed that eNOS inhibition by L-NAME treatment resulted in opening of IEJs (i.e. increased EC permeability) of capillaries and venules within few minutes and had widespread effect within 30 minutes. Furthermore, they observed 35% increase in the transendothelial transport of dinitrophenylated albumin tracer, in mouse lungs and other organs [3], demonstrating that eNOS-derived NO is crucial to ECs integrity and serves to maintain the low basal permeability of continuous endothelia. Our results also indicate that EGCG induced enhancement of NO, and this is accompanied by stabilization and improvement of EC barrier function. This might be due to widespread influences of EGCG on the signaling pathways in ECs. On one hand, EGCG may also stimulate phosphorylation of Ser1177 in eNOS that is required to enhanced eNOS activity in ECs [16, 253-254] via a pathway distinct from that of operates during phosphatase activation. On the other hand, EGCG induced phosphatase activation is not limited only to enhanced dephosphorylation and stimulation of eNOS, but also has a “relaxing” effect on the contractile machinery of ECs by inducing ppMLC20 dephosphorylation decreasing the number of stress fibres and restoring EC barrier integrity. These events may also lead to reduced permeability as a consequence of

endothelial barrier improvement. Moreover, EGCG induced increase of NO level was also observed in rat aortic rings [16] or mesenteric vascular beds [253] causing a dose- and endothelium-dependent vasorelaxation of the smooth muscles, which was suppressed by L-NAME indicating the direct role of eNOS in these events.

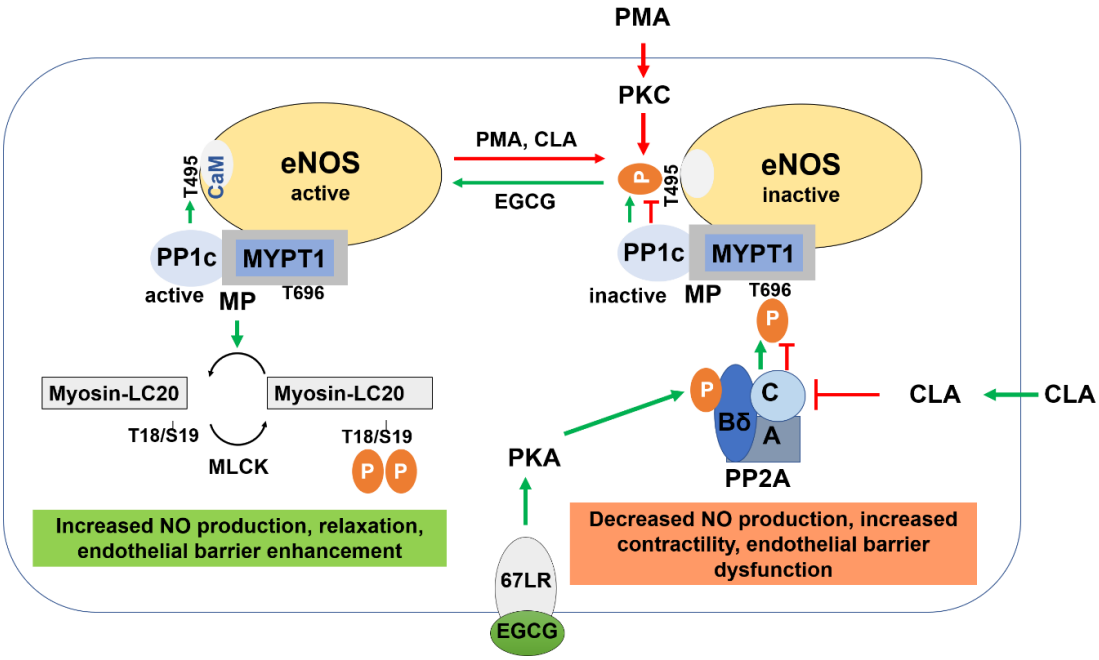

Figure 31. Regulation of eNOS activity and endothelial barrier function by phosphorylation-dephosphorylation. We have shown that myosin phosphatase (MP) interacts with eNOS via its myosin phosphatase target subunit-1 (MYPT1) which directs protein phosphatase-1 catalytic subunit (PP1c) for dephosphorylation of phospho-Thr497 allowing binding of Ca^{2+}-calmodulin (CaM) and activation of eNOS. PMA and/or calyculin-A (CLA) increases the phosphorylation level of eNOS-Thr497 by activation of protein kinase C (PKC) and/or inhibition of PP2A, respectively (red lines). Suppression of PP2A activity results in increased phosphorylation of MYPT1 at Thr696 and inhibition of MP. Both PKC activation and MP inhibition contributes to the inactivation of eNOS via increased phosphorylation at Thr497 and thus interfering with CaM binding. Inactivation of eNOS accompanies by decreased NO production while the enhanced LC20 phosphorylation leads to increased contractility and thereby endothelial barrier dysfunction. Our present data suggest that the reactivation of eNOS and dephosphorylation of LC20 may be accomplished by an EGCG induced activation of both PP2A and MP involving the 67 kDa laminin receptor (67LR) and protein kinase A (PKA) in this phosphatase activation. The 67LR mediated action of EGCG implies activation of PKA which phosphorylates the Bδ subunit of PP2A resulting in PP2A activation and subsequent dephosphorylation of MYPT1 (at phospho-Thr696) and activation of MP (green lines). Then, the activated MP dephosphorylates both phospho-Thr497 in eNOS and phospho-Thr18/Ser19 in LC20 resulting in increased NO production and decreased contractility (relaxation) with endothelial barrier enhancement.

The first part of the present study contributes to the understanding of the regulation of eNOS activity in EC from an aspect less frequently studied so far. Activation of eNOS requires dephosphorylation of $eNOS^{pT495}$, therefore, identification of the phosphatases involved may shed

light on novel regulatory pathways. We have shown here that MP (the complex of PP1c and MYPT1) dephosphorylates eNOS^{pT495} and the inhibitory phosphorylation of MYPT1 at Thr696 is a significant regulatory event in eNOS dephosphorylation. The pathways regulating inhibitory MYPT1 phosphorylation have been described [111, 274], and among these signaling RhoA/ROCK is involved in the phosphorylation of MYPT1 at Thr696 [250], eNOS at Thr495 [7], and MLC20 at both Thr18 and Ser19 sites in ECs [8]. It also has been established that mono- and diphosphorylation of MLC20 is involved in the fine tuning of barrier disruption in ECs [280]. Thus, ROCK can act in a concerted manner in simultaneous phosphorylation of Thr495 in eNOS and Thr696 in MYPT1 that is leading to a sustained level of eNOS^{pT495}, suppression of NO production, and increased level of ppMLC20 and EC barrier disruption. Another novel aspect of our present finding is that we identified a signaling pathway in ECs which operates via interaction of EGCG with 67LR leading to PP2A-driven activation of MP which accompanies with dephosphorylation (and activation) of eNOS and ppMLC20 (see Fig. 30.). In addition to increasing eNOS activity and NO production EGCG is stimulating ppMLC20 dephosphorylation decreases the contractility of ECs thereby restoring and improving barrier function. Because, the NO synthesized in ECs plays crucial roles in the regulation of distinct cardiovascular events, uncovering the molecular background of the regulation of NO production may also have relevance with regards of cardiovascular pharmacology.

Investigation of barrier protective role of purinergic signaling in endothelial barrier enhancement

ECs form the inner layer of the blood vessels, and as such the barrier integrity of EC is essential for controlling the passage of fluids, macromolecules and immune cells between the inner space of blood vessels and the surrounding interstitial space [1]. The role of extracellular purines, ATP and its degradation product, Ado, in the preservation of EC barrier integrity in pulmonary artery EC (PAEC) has been previously shown [17-18, 153]. It has also been demonstrated previously that Ado and the very slowly hydrolyzable ATP analog, ATPγS, attenuated LPS-induced lung inflammation and vascular leak in murine models of acute lung injury (ALI) [151, 281]. Furthermore, there is increasing scientific evidence supporting the barrier enhancement induced by Ado or ATP in HPAEC which involves the activation of PKA and MP leading to decreased contractile responses in ECs (MLC20 dephosphorylation, stress fibers dissolution), an increase in cortical actin

and the strengthening of intercellular contacts [17-18, 269]. However, the upstream signaling pathways leading to PKA and MP activation induced by purinergic agonists has not been explored. These pathways are diverse and include activation of the A2A receptors, G_s engagement and cAMP increases (for Ado) and P2Y-mediated G_{i2} and G_q activation leading to PKA/MP activation in a cAMP-independent manner (for ATPγS) [17-18].

In the second part of our studies we characterized and compared the signaling pathways in HLMVECs mediating Ado- and ATPγS-induced EC barrier-strengthening. Our data demonstrate that both Ado and ATPγS have similar functional effects on the EC barrier *in vitro*. Since ATPγS is very slowly hydrolyzable, it cannot activate Ado receptors. Further, the formation of pro-inflammatory "inflammasomes" apparently requires ATP hydrolysis [282], and therefore, ATPγS is unlikely to increase EC inflammatory responses. Indeed, Kolosova et al. have previously shown that ATPγS decreases LPS-induced inflammatory responses in a murine model of ALI [151].

Interestingly, there are no prior comprehensive studies in the literature reporting on the mRNA expression profile of adenosine (P1) and P2 receptors in HLMVEC. Thus, to provide a broad analysis, we measured the mRNA expression of each receptor subtype using qRT-PCR. A2B was found to be the most abundant P1 receptor in HLMVECs, while the expression of other receptors is very low or none. In contrast, the large vessel ECs (HPAEC) predominantly express A2A and A2B receptors with A2A expression approximately two times lower compared to the A2B isotype [17]. Differential expression of P1 receptors has also been observed in human macro- (HUVEC) and microvascular ECs where they are proposed to contribute to the functional heterogeneity of human macro- and microvascular ECs [261]. The results of Umapathy et al. [17] also demonstrate that A2A, but not A2B is functionally crucial in Ado-induced barrier enhancement in HPAEC. A2B is considered a low-affinity receptor and is ~ 50 times less sensitive than other receptors requiring supraphysiological conditions for its activation [283]. However, Qing et al. provided evidence that both A2A and A2B, but not A1 or A3 receptors are involved in the barrier-enhancing effects of Ado in bovine PAECs [153]. Genetic ablation of the A2B receptor exacerbated the loss of barrier function and increased pulmonary inflammation in bleomycin-induced ALI model, but decreased inflammatory responses in a chronic model of lung injury [284-285]. Taken together, these findings strongly suggest that the expression level and functional significance of P1 receptor subtypes is different in various disease states and highly dependent on the vascular bed where the EC were obtained from and further emphasizes the importance to examine the

signaling mechanisms of P1-mediated barrier-enhancement in HLMVEC. A2 (but not A1 or A3) adenosine receptors are coupled to G_s trimeric G-protein, which activate adenylyl cyclase [286]. Our results demonstrate that the Ado-induced increases in TER are accompanied by increased cAMP production (see Fig. 25A) supporting the involvement of the G_s-coupled A2B receptors in HLMVEC barrier strengthening.

Our qPCR analysis demonstrated that all eight P2Y receptors are expressed in HLMVECs to different ratios. Five P2Y receptors (P2Y 1, 2, 4, 11 and 12) can be activated by different concentrations of ATPγS in mammals [287]. However, there are inconsistencies in the literature about the selectivity of P2Y receptors towards their agonists. Molecular cloning and characterization of human P2Y4 (hP2Y4) and rat P2Y4 (rP2Y4) receptors revealed that these proteins share ~83% sequence homology. Furthermore, it was apparent that ATP and ATPγS are potent agonists of rP2Y4 receptors [288]. Kennedy et al. [289] demonstrated that ATP did not activate hP2Y4, and behaved more as a competitive antagonist of hP2Y4 and a potent agonist of rP2Y4, although they did not investigate the effect of ATPγS against the hP2Y4. In contrast, Bilbao et al. [290] provided evidence that stimulation of P2Y2/P2Y4 receptors by ATP increased the proliferation rate of human breast cancer MCF-7 cells by a PI3K/Akt-dependent signaling mechanism indicating the involvement of these receptors and demonstrating that ATP can activate them in human cells. The latter results are consistent with our findings on P2Y receptor-depleted cells. We show that depletion of P2Y4 and P2Y12 receptors resulted in a significant decrease in TER following ATPγS stimulation. This data demonstrates a primary role of both receptors in ATPγS induced HLMVEC barrier enhancement. Since both receptors are coupled to G_i-proteins [287], it was anticipated that they would decrease or at least would not influence the cAMP levels following agonist stimulation. However, endothelial barrier preservation is often associated with the elevated cAMP level [17, 291] followed by PKA activation [292]. These findings led us to measure the cAMP levels, and PKA activity of Ado and ATPγS treated HLMVECs. Upon Ado stimulation, we detected a significant elevation in cAMP levels and increased PKA activity which is consistent with the expression of G_s-coupled A2B receptors. At the same time, ATPγS treatment resulted in a slight, but significant decrease in cAMP levels further supporting the involvement of G_i-coupled P2Y4 and P2Y12 receptors in ATPγS response. We need to emphasize that the modest reduction in cAMP may be explained by the fact that ATPγS also can activate the G_s-coupled P2Y11 receptors. However, based on our gene silencing experiments (see Fig. 24.) P2Y11 receptors are not involved in the ATPγS-induced

EC barrier enhancement but may contribute to the net effect of ATPγS on the cAMP level. It also needs to be emphasized, that despite the observed decrease in cAMP levels, the activity of PKA was increased upon ATPγS treatment (see Fig. 25C) in accord with some published studies supporting the existence of a cAMP-independent model of PKA activation [18, 157, 293-294].

The signaling mechanisms of PKA-mediated EC barrier protection are not fully understood but likely involve PKA-mediated MYPT1 phosphorylation that leads to MP activation [18]. Using a dual phospho-MYPT1 specific antibody to MYPT1$^{pS695/pT696}$, we showed that PKA activation upon both, Ado and ATPγS treatment led to increased MYPT1 phosphorylation, thus promoting MP-mediated dephosphorylation of its substrate, the MLC20. Furthermore, Ado and ATPγS equally induced MLC20 dephosphorylation. Unexpectedly, depletion of PKA abolished ATPγS-, but not Ado-induced MLC20 dephosphorylation suggesting the involvement of additional signaling mechanisms. The cAMP-mediated signaling mechanisms involve two primary downstream targets, PKA [292] and EPAC1 [152, 295]. Recent publications indicate that EPAC1 activation leads to ROCK1 inactivation through a Rap1-RhoA-ROCK1 pathway [156] which is known to result in decreased phosphorylation of MYPT1 at its inhibitory phosphorylation sites (Thr696 and Thr853) [275]. Therefore, it seemed to be plausible to test the effect of EPAC1 depletion on Ado and ATPγS responses. Our data (see Fig. 26.) demonstrated that EPAC1 depletion alone does not prevent the decrease in MLC20 phosphorylation induced by either Ado or ATPγS in HLMVEC, while combined depletion of both PKAc and EPAC1 had a significant effect. These data indicate that Ado-induced MLC20 dephosphorylation requires both PKA- and EPAC1-mediated signaling. We hypothesize that both of these signaling pathways promoted increases in MYPT1 phosphorylation at PKA-specific sites accompanied by decreases in MYPT1 phosphorylation at ROCK1 sites coupled with MP de-inhibition and decreased ROCK1-mediated MLC20 phosphorylation. In contrast, PKA, but not EPAC1, is involved in the regulation of ATPγS-induced dephosphorylation of MLC20 which is consistent with the ability of ATPγS to induce HLMVEC cytoskeletal remodeling in a cAMP-independent manner (Fig. 32.).

Consistent with the data on MLC20 phosphorylation, TER measurements indicate that depletion of PKAc attenuated ATPγS-, but not Ado-induced EC barrier enhancement, while depletion of EPAC1 alone had no effect on Ado- or ATPγS-induced TER increases, but simultaneous depletion of PKA and EPAC1 attenuated the TER increase after treatment with both

agonists. We found that there was not much difference between PKAc depletion and PKAc/EPAC1 depletion in response to ATPγS, suggesting that increases in TER are EPAC1-independent, and consistent with the ability of ATPγS to enhance the HLMVEC barrier in a cAMP-independent manner.

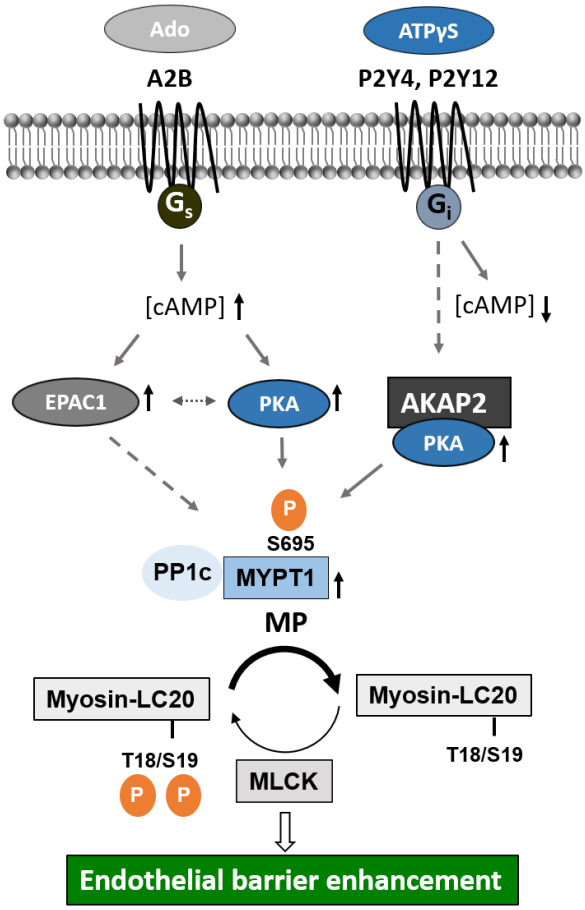

Figure 32. Schematic representation of PKA-, EPAC1- and AKAP2-PKA mediated signaling pathways induced by Ado and ATPγS in HLMVECs. Ado stimulates cAMP level increase in HLMVECs through A2B receptors which leads to the activation of two downstream targets, PKA and EPAC1. In contrast, ATPγS dependent signaling is mediated by P2Y4 and P2Y12 receptors leading to the cAMP-independent activation of PKA that requires AKAP2 expression. The effect of both, Ado and ATPγS converge at the level of MP via increased phosphorylation of the regulatory subunit MYPT1 at Ser695 residue, resulting in MP de-inhibition, which leads to MLC20 dephosphorylation and finally to EC barrier strengthening.

In accordance with previous report of Kolosova et al. [18], our results indicate that ATPγS induced cAMP-independent activation of PKA in HLMVEC. Models for cAMP-independent PKA activation have been proposed by other groups. One possible pathway is through the PAR-1 mediated association of NF-κB with PKA [296]. While another pathway proposed by Niu J. et al. [157] involves the G13/AKAP110 axis. AKAPs are known to be involved in the temporal and spatial

regulation of PKA activity via their interactions with different subcellular targets [267]. Specific AKAPs (e.g. AKAP79/150) interact with calcineurin (PP2B) [297], while interactions of PP1c/MYPT1 with AKAP220 contribute to the regulation, of the catalytic activity of MP [268]. Thus, it was plausible to test whether AKAP2 can interact with MYPT1, the regulatory subunit of MP, in a HEK293 model system. The ectopically expressed c-myc-MYPT1 co-immunoprecipitated with AKAP2, but not AKAP3, 9 or 12 suggesting the existence of a specific AKAP2/MYPT1 complex. Our data indicate that AKAP2 is involved in ATPγS-induced HLMVEC barrier enhancement and suggest a novel AKAP2-dependent mechanism which regulates the activation of PKA that is independent of the intracellular cAMP levels. We speculate that AKAP2 serves as an adapter protein facilitating PKA-induced phosphorylation of MYPT1 leading to MP activation and that this mechanism mediates the cAMP-independent strengthening of the EC barrier in response to ATPγS, however, this hypothesis requires further investigation.

This part of our studies has clarified the signaling pathways involved in actions of Ado and ATPγS to promote barrier strengthening in microvascular ECs. Our data strongly suggest that both Ado and ATPγS utilize PKA-dependent mechanisms and MP-mediated MLC20 dephosphorylation. While Ado-induced barrier-enhancing signaling is cAMP-dependent, ATPγS-induced HLMVEC barrier enhancement is cAMP-independent and likely involves AKAP2-mediated activation of PKA. Characterization of these two distinct mechanisms of EC barrier strengthening induced by extracellular purines might contribute to the development of new therapeutic tools in the treatment of ALI.

SUMMARY

The importance of eNOS to cardiovascular homeostasis has been well established. A major regulator of the activity of eNOS is post-translational phosphorylation and in particular the inhibitory phosphorylation at Thr495. Through the use of various biochemical and molecular biological techniques we have demonstrated that the myosin phosphatase (MP) holoenzyme, comprised of protein phosphatase-1 catalytic subunit (PP1c) and the MP target subunit-1 (MYPT1), is a bona fide eNOS^{pThr495} phosphatase. MYPT1 plays a regulatory role by guiding PP1c toward the eNOS^{pThr495} substrate. Inhibitory phosphorylation of MYPT1 at Thr696 can thus impact the action of MP on eNOS^{pThr495}. Phosphatase inhibitors were shown to suppress NO production and decrease barrier function, both of which are important functions in ECs. Epigallocatechin-3-gallate (EGCG) treatment induced protein kinase A (PKA) -dependent activation of protein phosphatase-2A (PP2A) which increased MP activity. Activated MP dephosphorylated both eNOS^{pThr495} and the 20 kDa myosin II light chains at Thr18/Ser19 (ppMLC20) which resulted in relaxation of ECs. Our results suggest that the coordinated interplay between PP2A and MP accounts for the physiological regulation of eNOS activity. EGCG dependent activation of these phosphatases leads to eNOS pT495 dephosphorylation, eNOS activation, enhanced NO production and EC barrier strengthening.

Loss of EC barrier integrity results in increased vascular permeability, which often has severe consequences including the flooding of alveolar space that occurs in pneumonia. We have shown that Ado and ATPγS exert their profound barrier protecting effects on HLMVEC via distinct signaling mechanisms. ATPγS induced P2Y4 and P2Y12 mediated cAMP independent PKA activation, resulting in MP activation and ppMLC20 dephosphorylation. This pathway involves protein kinase A-anchor protein 2 (AKAP2). However, Ado-induced strengthening of the HLMVEC barrier required the coordinated activation of PKA and EPAC1 in cAMP-dependent manner.

In summary our studies shed light on the receptor-mediated phosphorylation-dephosphorylation of key endothelial proteins and identified kinases and phosphatases as well as the signaling pathways implicated in these modifications. We also show the importance of these phosphorylation-dephosphorylation events in the regulation of the physiological functions of the endothelial cells, therefore, our results may possible have pharmacological relevance.

ÖSSZEFOGLALÁS

Az eNOS számos kardiovaszkuláris funkció szabályozásában fontos szerepet játszik. Az eNOS aktivitásának szabályozásában a Thr495 aminosavon történő gátló foszforiláció kitüntetett szereppel bír. Munkánk során különböző biokémiai és molekuláris biológiai technikák alkalmazásával kimutattuk, hogy a miozin foszfatáz (MP) holoenzim, amely egy protein foszfatáz-1 (PP1c) katalitikus és egy MP regulátor alegységből (MYPT1) áll, az $eNOS^{pT495}$ oldalláncot defoszforiláló foszfatáz. A $MYPT1^{Thr696}$ gátló foszforilációja szabályozza az $eNOS^{pT495}$ MP általi defoszforilációját. Foszfatáz gátlószerek alkalmazása csökkentette a NO képződését és gátló hatással volt az endotél sejtek barrier funkiójára, amely kulcsfontosságú az erek homeosztázisának fenntartásában. Az (-)-epigallokatekin-3-gallát (EGCG) kezelés protein kináz A (PKA) által mediált protein foszfatáz 2A (PP2A) aktivációt eredményezett, amely hatására növekedett a MP aktivitása. Az aktivált MP defoszforilálta az $eNOS^{pThr495}$-t, valamint a 20 kDa molekulatömegű miozin II könnyűláncot (MLC20) a pThr18/pSer19 oldalláncokon, amely az endotél sejtek kontraktilis apparátusának relaxációját idézte elő. Eredményeink arra utalnak, hogy a PP2A és a MP koordinált aktivációjának szerepe van az eNOS fiziológiai aktivációjának szabályozásában. E foszfatázok EGCG általi aktivációja a NO szint emelkedését és az endotél barrier funkció fokozódását is elősegíti.

Az endotél sejtek barrier funkciójának elvesztése az erek permeabilitásának növekedéséhez vezet, amely gyakran súlyos következményekkel jár. Munkánk során kimutattuk, hogy az Ado és ATPγS különböző jelátviteli útvonalakon fejtik ki hatásukat a HLMVEC sejteken. Az ATPγS a P2Y4 és P2Y12 receptorok közvetítésével cAMP független útvonalon PKA aktivációt idéz elő, amely a ppMLC20 foszforilációs szintjének csökkenéséhez vezet a MP által történő defoszforilációval. Eredményeink alapján ebben a jelátviteli útvonalban az AKAP2-nek is szerepe van. Ezzel szemben az Ado indukálta endotél barrier funkció növekedéséhez a PKA és EPAC1 koordinált cAMP függő aktivációja szükséges.

Összefoglalva, eredményeink kulcsfontosságú endotél fehérjék receptor-mediált foszforilációs-defoszforilációs folyamataira, valamint ezek szabályozásában szerepet játszó kinázok, foszfatázok és jelátviteli útvonalak szabályozására derítenek fényt. Azt is bemutatjuk, hogy e foszforilációs-defoszforilációs folyamatok mennyire fontosak az endotél sejtek fiziológiai funkciójának szabályozásában, ezért eredményeink farmakológiai jelentőséggel bírhatnak.

REFERENCES

1. Mehta, D.; Malik, A. B., Signaling mechanisms regulating endothelial permeability. *Physiol Rev* **2006,** *86* (1), 279-367.
2. Qian, J.; Fulton, D., Post-translational regulation of endothelial nitric oxide synthase in vascular endothelium. *Frontiers in Physiology* **2013,** *4* (347).
3. Predescu, D.; Predescu, S.; Shimizu, J.; Miyawaki-Shimizu, K.; Malik, A. B., Constitutive eNOS-derived nitric oxide is a determinant of endothelial junctional integrity. *American Journal of Physiology - Lung Cellular and Molecular Physiology* **2005,** *289* (3), L371-L381.
4. Michell, B. J.; Chen, Z.; Tiganis, T.; Stapleton, D.; Katsis, F.; Power, D. A.; Sim, A. T.; Kemp, B. E., Coordinated control of endothelial nitric-oxide synthase phosphorylation by protein kinase C and the cAMP-dependent protein kinase. *J Biol Chem* **2001,** *276* (21), 17625-8.
5. Park, J.-H.; Sung, H. Y.; Lee, J. Y.; Kim, H. J.; Ahn, J.-H.; Jo, I., B56α subunit of protein phosphatase 2A mediates retinoic acid-induced decreases in phosphorylation of endothelial nitric oxide synthase at serine 1179 and nitric oxide production in bovine aortic endothelial cells. *Biochemical and Biophysical Research Communications* **2013,** *430* (2), 476-481.
6. Harris, M. B.; Ju, H.; Venema, V. J.; Liang, H.; Zou, R.; Michell, B. J.; Chen, Z. P.; Kemp, B. E.; Venema, R. C., Reciprocal phosphorylation and regulation of endothelial nitric-oxide synthase in response to bradykinin stimulation. *J Biol Chem* **2001,** *276* (19), 16587-91.
7. Ruan, L.; Torres, C. M.; Buffett, R. J.; Kennard, S.; Fulton, D.; Venema, R. C., Calcineurin-mediated Dephosphorylation of eNOS at Serine 116 Affects eNOS Enzymatic Activity Indirectly by Facilitating c-Src Binding and Tyrosine 83 Phosphorylation. *Vascul Pharmacol* **2013,** *59* (0).
8. Amano, M.; Ito, M.; Kimura, K.; Fukata, Y.; Chihara, K.; Nakano, T.; Matsuura, Y.; Kaibuchi, K., Phosphorylation and activation of myosin by Rho-associated kinase (Rho-kinase). *J Biol Chem* **1996,** *271* (34), 20246-9.
9. Garcia, J. G.; Lazar, V.; Gilbert-McClain, L. I.; Gallagher, P. J.; Verin, A. D., Myosin light chain kinase in endothelium: molecular cloning and regulation. *Am J Respir Cell Mol Biol* **1997,** *16* (5), 489-94.
10. Alessi, D.; MacDougall, L. K.; Sola, M. M.; Ikebe, M.; Cohen, P., The control of protein phosphatase-1 by targetting subunits. The major myosin phosphatase in avian smooth muscle is a novel form of protein phosphatase-1. *Eur J Biochem* **1992,** *210* (3), 1023-35.
11. Feng, J.; Ito, M.; Ichikawa, K.; Isaka, N.; Nishikawa, M.; Hartshorne, D. J.; Nakano, T., Inhibitory phosphorylation site for Rho-associated kinase on smooth muscle myosin phosphatase. *J Biol Chem* **1999,** *274* (52), 37385-90.
12. Wooldridge, A. A.; MacDonald, J. A.; Erdodi, F.; Ma, C.; Borman, M. A.; Hartshorne, D. J.; Haystead, T. A., Smooth muscle phosphatase is regulated in vivo by exclusion of phosphorylation of threonine 696 of MYPT1 by phosphorylation of Serine 695 in response to cyclic nucleotides. *J Biol Chem* **2004,** *279* (33), 34496-504.
13. Kolozsvari, B.; Bako, E.; Becsi, B.; Kiss, A.; Czikora, A.; Toth, A.; Vamosi, G.; Gergely, P.; Erdodi, F., Calcineurin regulates endothelial barrier function by interaction with and dephosphorylation of myosin phosphatase. *Cardiovasc Res* **2012,** *96* (3), 494-503.
14. Lontay, B.; Kiss, A.; Gergely, P.; Hartshorne, D. J.; Erdődi, F., Okadaic acid induces phosphorylation and translocation of myosin phosphatase target subunit 1 influencing myosin phosphorylation, stress fiber assembly and cell migration in HepG2 cells. *Cellular Signalling* **2005,** *17* (10), 1265-1275.

15. Tsukamoto, S.; Huang, Y.; Umeda, D.; Yamada, S.; Yamashita, S.; Kumazoe, M.; Kim, Y.; Murata, M.; Yamada, K.; Tachibana, H., 67-kDa laminin receptor-dependent protein phosphatase 2A (PP2A) activation elicits melanoma-specific antitumor activity overcoming drug resistance. *J Biol Chem* **2014,** *289* (47), 32671-81.
16. Lorenz, M.; Wessler, S.; Follmann, E.; Michaelis, W.; Dusterhoft, T.; Baumann, G.; Stangl, K.; Stangl, V., A constituent of green tea, epigallocatechin-3-gallate, activates endothelial nitric oxide synthase by a phosphatidylinositol-3-OH-kinase-, cAMP-dependent protein kinase-, and Akt-dependent pathway and leads to endothelial-dependent vasorelaxation. *J Biol Chem* **2004,** *279* (7), 6190-5.
17. Umapathy, N. S.; Fan, Z.; Zemskov, E. A.; Alieva, I. B.; Black, S. M.; Verin, A. D., Molecular mechanisms involved in adenosine-induced endothelial cell barrier enhancement. *Vascul Pharmacol* **2010,** *52* (5-6), 199-206.
18. Kolosova, I. A.; Mirzapoiazova, T.; Adyshev, D.; Usatyuk, P.; Romer, L. H.; Jacobson, J. R.; Natarajan, V.; Pearse, D. B.; Garcia, J. G.; Verin, A. D., Signaling pathways involved in adenosine triphosphate-induced endothelial cell barrier enhancement. *Circ Res* **2005,** *97* (2), 115-24.
19. Pries, A. R.; Secomb, T. W.; Gaehtgens, P., The endothelial surface layer. *Pflügers Archiv* **2000,** *440* (5), 653-666.
20. Baldwin, A. L.; Thurston, G., Mechanics of Endothelial Cell Architecture and Vascular Permeability. *Crit Rev Biomed Eng.* **2001,** *29* (2), 247-278.
21. Yuan, S. Y.; Rigor, R. R., In *Regulation of Endothelial Barrier Function*, Morgan & Claypool Life Sciences: San Rafael (CA), **2010**, Chapter 2, Structure and Function of Exchange Microvessels; pp 3-5.
22. Florey, The endothelial cell. *British Medical Journal* **1966,** *2* (5512), 487-90.
23. Kibria, G.; Heath, D.; Smith, P.; Biggar, R., Pulmonary endothelial pavement patterns. *Thorax* **1980,** *35* (3), 186-191.
24. Hirata, A.; Baluk, P.; Fujiwara, T.; McDonald, D. M., Location of focal silver staining at endothelial gaps in inflamed venules examined by scanning electron microscopy. *American Journal of Physiology - Lung Cellular and Molecular Physiology* **1995,** *269* (3), L403-L418.
25. Aird, W. C., Phenotypic Heterogeneity of the Endothelium. *I. Structure, Function, and Mechanisms* **2007,** *100* (2), 158-173.
26. Rostgaard, J.; Qvortrup, K., Electron Microscopic Demonstrations of Filamentous Molecular Sieve Plugs in Capillary Fenestrae. *Microvascular Research* **1997,** *53* (1), 1-13.
27. Wisse, E., An electron microscopic study of the fenestrated endothelial lining of rat liver sinusoids. *Journal of Ultrastructure Research* **1970,** *31* (1), 125-150.
28. Siflinger-Birnboim, A.; del Vecchio, P. J.; Cooper, J. A.; Blumenstock, F. A.; Shepard, J. M.; Malik, A. B., Molecular sieving characteristics of the cultured endothelial monolayer. *Journal of Cellular Physiology* **1987,** *132* (1), 111-117.
29. Aird, W. C., Vascular bed-specific hemostasis: role of endothelium in sepsis pathogenesis. *Crit Care Med* **2001,** *29* (7 Suppl), S28-34; discussion S34-5.
30. Sandoo, A.; van Zanten, J.; Metsios, G. S.; Carroll, D.; Kitas, G. D., The Endothelium and Its Role in Regulating Vascular Tone. *The Open Cardiovascular Medicine Journal* **2010,** *4*, 302-12.
31. Carmeliet, P., Molecular mechanisms and clinical applications of angiogenesis. **2011,** *473* (7347), 298-307.

32. Saba, S. R.; Mason, R. G., Studies of an activity from endothelial cells that inhibits platelet aggregation, serotonin release, and clot retraction. *Thrombosis Research* **1974,** *5* (6), 747-757.
33. Pasqualini, R.; Arap, W., Profiling the molecular diversity of blood vessels. *Cold Spring Harb Symp Quant Biol* **2002,** *67*, 223-5.
34. Crone, C., Permeability of single capillaries. *Clin Invest Med* **1985,** *8* (1), 89-95.
35. Gloor, S. M.; Wachtel, M.; Bolliger, M. F.; Ishihara, H.; Landmann, R.; Frei, K., Molecular and cellular permeability control at the blood–brain barrier. *Brain Research Reviews* **2001,** *36* (2), 258-264.
36. Khimenko, P. L.; Taylor, A. E., Segmental microvascular permeability in ischemia-reperfusion injury in rat lung. *American Journal of Physiology - Lung Cellular and Molecular Physiology* **1999,** *276* (6), L958-L960.
37. Lamm, W. J.; Luchtel, D.; Albert, R. K., Sites of leakage in three models of acute lung injury. *Journal of Applied Physiology* **1988,** *64* (3), 1079-1083.
38. Blum, M. S.; Toninelli, E.; Anderson, J. M.; Balda, M. S.; Zhou, J.; O'Donnell, L.; Pardi, R.; Bender, J. R., Cytoskeletal rearrangement mediates human microvascular endothelial tight junction modulation by cytokines. *The American Journal Of Physiology* **1997,** *273* (1 Pt 2), H286-H294.
39. Gaar KA; Taylor, A.; Owens, L.; Guyton, A., Pulmonary capillary pressure and filtration coefficient in the isolated perfused lung. *American Journal of Physiology -- Legacy Content* **1967,** *213* (4), 910-914.
40. Michiels, C., Endothelial cell functions. *Journal of Cellular Physiology* **2003,** *196* (3), 430-443.
41. Yuan, S. Y.; Rigor, R. R., In *Regulation of Endothelial Barrier Function*, Morgan & Claypool Life Sciences: San Rafael (CA), **2010,** Chapter 4, The Endothelial Barrier.; p 53.
42. Yuan, S. Y.; Rigor, R. R., In *Regulation of Endothelial Barrier Function*, Morgan & Claypool Life Sciences: San Rafael (CA), **2010,** Chapter 4, The Endothelial Barrier.; p 39.
43. Komarova, Y. A.; Kruse, K.; Mehta, D.; Malik, A. B., Protein Interactions at Endothelial Junctions and Signaling Mechanisms Regulating Endothelial Permeability. *Circ. Res.* **2017,** *120* (1), 179-206.
44. Mese, G.; Richard, G.; White, T. W., Gap junctions: basic structure and function. *J Invest Dermatol* **2007,** *127* (11), 2516-24.
45. Goodenough, D. A.; Paul, D. L., Gap Junctions. *Cold Spring Harb Perspect Biol* **2009,** *1* (1).
46. Okamoto, T.; Akita, N.; Hayashi, T.; Shimaoka, M.; Suzuki, K., Endothelial connexin 32 regulates tissue factor expression induced by inflammatory stimulation and direct cell–cell interaction with activated cells. *Atherosclerosis* **2014,** *236* (2), 430-437.
47. Okamoto, T.; Akita, N.; Kawamoto, E.; Hayashi, T.; Suzuki, K.; Shimaoka, M., Endothelial connexin32 enhances angiogenesis by positively regulating tube formation and cell migration. *Experimental Cell Research* **2014,** *321* (2), 133-141.
48. O'Donnell, J. J., III; Birukova, A. A.; Beyer, E. C.; Birukov, K. G., Gap Junction Protein Connexin43 Exacerbates Lung Vascular Permeability. *PLOS ONE* **2014,** *9* (6), e100931.
49. Yuan, S. Y.; Rigor, R. R., In *Regulation of Endothelial Barrier Function*, Morgan & Claypool Life Sciences: San Rafael (CA), **2010**, Chapter 4, The Endothelial Barrier.; p 43.
50. Bazzoni, G.; Dejana, E., Endothelial Cell-to-Cell Junctions: Molecular Organization and Role in Vascular Homeostasis. *Physiological Reviews* **2004,** *84* (3), 869-901.

51. Alema, S.; Salvatore, A. M., p120 catenin and phosphorylation: Mechanisms and traits of an unresolved issue. *Biochim Biophys Acta* **2007,** *1773* (1), 47-58.
52. Yuan, S. Y.; Rigor, R. R., In *Regulation of Endothelial Barrier Function*, Morgan & Claypool Life Sciences: San Rafael (CA), **2010,** Chapter 4, The Endothelial Barrier.; p 46.
53. Bazzoni, G., Endothelial tight junctions: permeable barriers of the vessel wall. *Thrombosis and Haemostasis* **2006,** *95* (1), 36-42.
54. Yuan, S. Y.; Rigor, R. R., In *Regulation of Endothelial Barrier Function*, Morgan & Claypool Life Sciences: San Rafael (CA), **2010**, Chapter 4, The Endothelial Barrier.; p 42.
55. Shivanna, M.; Srinivas, S. P., Microtubule Stabilization Opposes the (TNF-α)-Induced Loss in the Barrier Integrity of Corneal Endothelium. *Experimental eye research* **2009,** *89* (6), 950-9.
56. Wu, M. H., Endothelial focal adhesions and barrier function. *J Physiol* **2005,** *569* (Pt 2), 359-66.
57. Cheng, Y.-F.; Clyman, R. I.; Enenstein, J.; Waleh, N.; Pytela, R.; Kramer, R. H., The integrin complex αvβ3 participates in the adhesion of microvascular endothelial cells to fibronectin. *Experimental Cell Research* **1991,** *194* (1), 69-77.
58. Avraham, H. K.; Lee, T. H.; Koh, Y.; Kim, T. A.; Jiang, S.; Sussman, M.; Samarel, A. M.; Avraham, S., Vascular endothelial growth factor regulates focal adhesion assembly in human brain microvascular endothelial cells through activation of the focal adhesion kinase and related adhesion focal tyrosine kinase. *J Biol Chem* **2003,** *278* (38), 36661-8.
59. Chen, X. L.; Nam, J. O.; Jean, C.; Lawson, C.; Walsh, C. T.; Goka, E.; Lim, S. T.; Tomar, A.; Tanjoni, I.; Uryu, S.; Guan, J. L.; Acevedo, L. M.; Weis, S. M.; Cheresh, D. A.; Schlaepfer, D. D., VEGF-induced vascular permeability is mediated by FAK. *Developmental Cell* **2012,** *22* (1), 146-57.
60. Fletcher, D. A., Cell mechanics and the cytoskeleton. **2010,** *463* (7280), 485-92.
61. Holmes, K. C.; Popp, D.; Gebhard, W.; Kabsch, W., Atomic model of the actin filament. **1990,** *347*, 44.
62. Yuan, S. Y.; Rigor, R. R., In *Regulation of Endothelial Barrier Function*, Morgan & Claypool Life Sciences: San Rafael (CA), **2010**, Chapter 4, The Endothelial Barrier.; p 52.
63. Vouret-Craviari, V.; Boquet, P.; Pouysségur, J.; Van Obberghen-Schilling, E., Regulation of the Actin Cytoskeleton by Thrombin in Human Endothelial Cells: Role of Rho Proteins in Endothelial Barrier Function. *Mol Biol Cell* **1998,** *9* (9), 2639-53.
64. Dudek, S. M.; Garcia, J. G., Cytoskeletal regulation of pulmonary vascular permeability. *J Appl Physiol (1985)* **2001,** *91* (4), 1487-500.
65. Yuan, S. Y.; Rigor, R. R., In *Regulation of Endothelial Barrier Function*, Morgan & Claypool Life Sciences: San Rafael (CA), **2010,** Chapter 4, The Endothelial Barrier.; p 51.
66. Birukova, A. A.; Smurova, K.; Birukov, K. G.; Usatyuk, P.; Liu, F.; Kaibuchi, K.; Ricks-Cord, A.; Natarajan, V.; Alieva, I.; Garcia, J. G.; Verin, A. D., Microtubule disassembly induces cytoskeletal remodeling and lung vascular barrier dysfunction: role of Rho-dependent mechanisms. *J Cell Physiol* **2004,** *201* (1), 55-70.
67. Birukova, A. A.; Liu, F.; Garcia, J. G.; Verin, A. D., Protein kinase A attenuates endothelial cell barrier dysfunction induced by microtubule disassembly. *Am J Physiol Lung Cell Mol Physiol* **2004,** *287* (1), L86-93.
68. Sefton, B. M., Overview of protein phosphorylation. *Curr Protoc Cell Biol* **2001,** *Chapter 14*, Unit 14 1.

69. Johnson, Louise N., The regulation of protein phosphorylation. *Biochemical Society Transactions* **2009,** *37* (4), 627-641.
70. Cohen, P., The structure and regulation of protein phosphatases. *Adv Second Messenger Phosphoprotein Res* **1990,** *24*, 230-5.
71. Shi, Y., Serine/Threonine Phosphatases: Mechanism through Structure. *Cell* **2009,** *139* (3), 468-484.
72. Manning, G.; Whyte, D. B.; Martinez, R.; Hunter, T.; Sudarsanam, S., The Protein Kinase Complement of the Human Genome. *Science* **2002,** *298* (5600), 1912-1934.
73. Cohen, P., Protein kinases [mdash] the major drug targets of the twenty-first century? *Nat Rev Drug Discov* **2002,** *1* (4), 309-315.
74. Peti, W.; Nairn, A. C.; Page, R., Structural basis for protein phosphatase 1 regulation and specificity. *The FEBS journal* **2013,** *280* (2), 596-611.
75. Cohen, P. T. W., Protein phosphatase 1 – targeted in many directions. *Journal of Cell Science* **2002,** *115* (2), 241-256.
76. Alonso, A.; Sasin, J.; Bottini, N.; Friedberg, I.; Friedberg, I.; Osterman, A.; Godzik, A.; Hunter, T.; Dixon, J.; Mustelin, T., Protein tyrosine phosphatases in the human genome. *Cell* **2004,** *117* (6), 699-711.
77. Ingebritsen, T. S.; Cohen, P., The protein phosphatases involved in cellular regulation. 1. Classification and substrate specificities. *Eur J Biochem* **1983,** *132* (2), 255-61.
78. Cohen, P. T. W., Novel protein serine/threonine phosphatases: Variety is the spice of life. *Trends in Biochemical Sciences* **1997,** *22* (7), 245-251.
79. Brautigan, D. L., Protein Ser/Thr phosphatases – the ugly ducklings of cell signalling. *FEBS Journal* **2013,** *280* (2), 324-325.
80. Ceulemans, H.; Bollen, M., Functional Diversity of Protein Phosphatase-1, a Cellular Economizer and Reset Button. *Physiological Reviews* **2004,** *84* (1), 1-39.
81. Butler, T.; Paul, J.; Europe-Finner, N.; Smith, R.; Chan, E.-C., Role of serine-threonine phosphoprotein phosphatases in smooth muscle contractility. *American Journal of Physiology - Cell Physiology* **2013,** *304* (6), C485-C504.
82. Gallego, M.; Virshup, D. M., Protein serine/threonine phosphatases: life, death, and sleeping. *Curr Opin Cell Biol* **2005,** *17* (2), 197-202.
83. Lontay, B.; Serfozo, Z.; Gergely, P.; Ito, M.; Hartshorne, D. J.; Erdodi, F., Localization of myosin phosphatase target subunit 1 in rat brain and in primary cultures of neuronal cells. *J Comp Neurol* **2004,** *478* (1), 72-87.
84. Kiss, A.; Lontay, B.; Becsi, B.; Markasz, L.; Olah, E.; Gergely, P.; Erdodi, F., Myosin phosphatase interacts with and dephosphorylates the retinoblastoma protein in THP-1 leukemic cells: its inhibition is involved in the attenuation of daunorubicin-induced cell death by calyculin-A. *Cell Signal* **2008,** *20* (11), 2059-70.
85. Dohadwala, M.; da Cruz e Silva, E. F.; Hall, F. L.; Williams, R. T.; Carbonaro-Hall, D. A.; Nairn, A. C.; Greengard, P.; Berndt, N., Phosphorylation and inactivation of protein phosphatase 1 by cyclin-dependent kinases. *Proc Natl Acad Sci U S A* **1994,** *91* (14), 6408-12.
86. Kwon, Y. G.; Lee, S. Y.; Choi, Y.; Greengard, P.; Nairn, A. C., Cell cycle-dependent phosphorylation of mammalian protein phosphatase 1 by cdc2 kinase. *Proc Natl Acad Sci U S A* **1997,** *94* (6), 2168-73.
87. Jiang, Y., Regulation of the cell cycle by protein phosphatase 2A in Saccharomyces cerevisiae. *Microbiol Mol Biol Rev* **2006,** *70* (2), 440-9.

88. Ruvolo, P. P.; Qui, Y.; Coombes, K. R.; Zhang, N.; Ruvolo, V.; Konopleva, M.; Andreeff, M.; Kornblau, S. M., Role for PP2A Regulatory Subunit B55α as A Regulator of AKT and Other Signaling Pathways In AML. *Blood* **2010,** *116* (21), 1668-1668.
89. Seshacharyulu, P.; Pandey, P.; Datta, K.; Batra, S. K., Phosphatase: PP2A structural importance, regulation and its aberrant expression in cancer. *Cancer Lett* **2013,** *335* (1), 9-18.
90. Slupe, A. M.; Merrill, R. A.; Strack, S., Determinants for Substrate Specificity of Protein Phosphatase 2A. *Enzyme Res* **2011,** *2011*, 398751.
91. Kremmer, E.; Ohst, K.; Kiefer, J.; Brewis, N.; Walter, G., Separation of PP2A core enzyme and holoenzyme with monoclonal antibodies against the regulatory A subunit: abundant expression of both forms in cells. *Mol Cell Biol* **1997,** *17* (3), 1692-701.
92. Janssens, V.; Goris, J., Protein phosphatase 2A: a highly regulated family of serine/threonine phosphatases implicated in cell growth and signalling. *Biochem J* **2001,** *353* (Pt 3), 417-39.
93. Kamibayashi, C.; Estes, R.; Lickteig, R. L.; Yang, S. I.; Craft, C.; Mumby, M. C., Comparison of heterotrimeric protein phosphatase 2A containing different B subunits. *J Biol Chem* **1994,** *269* (31), 20139-48.
94. Chen, J.; Martin, B.; Brautigan, D., Regulation of protein serine-threonine phosphatase type-2A by tyrosine phosphorylation. *Science* **1992,** *257* (5074), 1261-1264.
95. Ahn, J. H.; McAvoy, T.; Rakhilin, S. V.; Nishi, A.; Greengard, P.; Nairn, A. C., Protein kinase A activates protein phosphatase 2A by phosphorylation of the B56delta subunit. *Proc Natl Acad Sci U S A* **2007,** *104* (8), 2979-84.
96. Leulliot, N.; Quevillon-Cheruel, S.; Sorel, I.; Li de La Sierra-Gallay, I.; Collinet, B.; Graille, M.; Blondeau, K.; Bettache, N.; Poupon, A.; Janin, J.; van Tilbeurgh, H., Structure of protein phosphatase methyltransferase 1 (PPM1), a leucine carboxyl methyltransferase involved in the regulation of protein phosphatase 2A activity. *J Biol Chem* **2004,** *279* (9), 8351-8.
97. Ikehara, T.; Ikehara, S.; Imamura, S.; Shinjo, F.; Yasumoto, T., Methylation of the C-terminal leucine residue of the PP2A catalytic subunit is unnecessary for the catalytic activity and the binding of regulatory subunit (PR55/B). *Biochemical and Biophysical Research Communications* **2007,** *354* (4), 1052-1057.
98. Tachibana, K.; Scheuer, P. J.; Tsukitani, Y.; Kikuchi, H.; Van Engen, D.; Clardy, J.; Gopichand, Y.; Schmitz, F. J., Okadaic acid, a cytotoxic polyether from two marine sponges of the genus Halichondria. *Journal of the American Chemical Society* **1981,** *103* (9), 2469-2471.
99. Zhang, M.; Yogesha, S. D.; Mayfield, J. E.; Gill, G. N.; Zhang, Y., Viewing serine/threonine protein phosphatases through the eyes of drug designers. *The FEBS journal* **2013,** *280* (19), 4739-60.
100. Pereira, S. R.; Vasconcelos, V. M.; Antunes, A., Computational study of the covalent bonding of microcystins to cysteine residues – a reaction involved in the inhibition of the PPP family of protein phosphatases. *FEBS Journal* **2013,** *280* (2), 674-680.
101. Kato, Y.; Fusetani, N.; Matsunaga, S.; Hashimoto, K.; Fujita, S.; Furuya, T., Bioactive marine metabolites. Part 16. Calyculin A. A novel antitumor metabolite from the marine sponge Discodermia calyx. *Journal of the American Chemical Society* **1986,** *108* (10), 2780-2781.
102. Yan, Y.; Mumby, M. C., Distinct roles for PP1 and PP2A in phosphorylation of the retinoblastoma protein. PP2a regulates the activities of G(1) cyclin-dependent kinases. *J Biol Chem* **1999,** *274* (45), 31917-24.

103. Favre, B.; Turowski, P.; Hemmings, B. A., Differential inhibition and posttranslational modification of protein phosphatase 1 and 2A in MCF7 cells treated with calyculin-A, okadaic acid, and tautomycin. *J Biol Chem* **1997,** *272* (21), 13856-63.
104. Dedinszki, D.; Kiss, A.; Márkász, L.; Márton, A.; Tóth, E.; Székely, L.; Erdődi, F., Inhibition of protein phosphatase-1 and -2A decreases the chemosensitivity of leukemic cells to chemotherapeutic drugs. *Cellular Signalling* **2015,** *27* (2), 363-372.
105. Hartshorne, D. J.; Ito, M.; Erdodi, F., Myosin light chain phosphatase: subunit composition, interactions and regulation. *J Muscle Res Cell Motil* **1998,** *19* (4), 325-41.
106. Arimura, T.; Suematsu, N.; Zhou, Y. B.; Nishimura, J.; Satoh, S.; Takeshita, A.; Kanaide, H.; Kimura, A., Identification, characterization, and functional analysis of heart-specific myosin light chain phosphatase small subunit. *J Biol Chem* **2001,** *276* (9), 6073-82.
107. Matsumura, F.; Hartshorne, D. J., Myosin phosphatase target subunit: Many roles in cell function. *Biochem Biophys Res Commun* **2008,** *369* (1), 149-56.
108. Moorhead, G.; Johnson, D.; Morrice, N.; Cohen, P., The major myosin phosphatase in skeletal muscle is a complex between the β-isoform of protein phosphatase 1 and the MYPT2 gene product. *FEBS Letters* **1998,** *438* (3), 141-144.
109. Yamashiro, S.; Yamakita, Y.; Totsukawa, G.; Goto, H.; Kaibuchi, K.; Ito, M.; Hartshorne, D.; Matsumura, F., Myosin phosphatase targeting subunit1 regulates mitosis by antagonizing polo-like kinase1. *Developmental Cell* **2008,** *14* (5), 787-97.
110. Verin, A. D.; Patterson, C. E.; Day, M. A.; Garcia, J. G., Regulation of endothelial cell gap formation and barrier function by myosin-associated phosphatase activities. *Am J Physiol* **1995,** *269* (1 Pt 1), L99-108.
111. Hartshorne, D. J.; Ito, M.; Erdodi, F., Role of protein phosphatase type 1 in contractile functions: myosin phosphatase. *J Biol Chem* **2004,** *279* (36), 37211-4.
112. Takahashi, N.; Ito, M.; Tanaka, J.; Nakano, T.; Kaibuchi, K.; Odai, H.; Takemura, K., Localization of the gene coding for myosin phosphatase, target subunit 1 (MYPT1) to human chromosome 12q15-q21. *Genomics* **1997,** *44* (1), 150-2.
113. Dirksen, W. P.; Vladic, F.; Fisher, S. A., A myosin phosphatase targeting subunit isoform transition defines a smooth muscle developmental phenotypic switch. *American Journal of Physiology - Cell Physiology* **2000,** *278* (3), C589-C600.
114. Terrak, M.; Kerff, F.; Langsetmo, K.; Tao, T.; Dominguez, R., Structural basis of protein phosphatase 1 regulation. *Nature* **2004,** *429* (6993), 780-4.
115. Tóth, A.; Kiss, E.; Herberg, F. W.; Gergely, P.; Hartshorne, D. J.; Erdödi, F., Study of the subunit interactions in myosin phosphatase by surface plasmon resonance. *European Journal of Biochemistry* **2000,** *267* (6), 1687-1697.
116. Wu, Y.; Murányi, A.; Erdődi, F.; Hartshorne, D. J., Localization of Myosin Phosphatase Target Subunit and its Mutants. *Journal of Muscle Research & Cell Motility* **2005,** *26* (2), 123.
117. Kimura, K.; Ito, M.; Amano, M.; Chihara, K.; Fukata, Y.; Nakafuku, M.; Yamamori, B.; Feng, J.; Nakano, T.; Okawa, K.; Iwamatsu, A.; Kaibuchi, K., Regulation of Myosin Phosphatase by Rho and Rho-Associated Kinase (Rho-Kinase). *Science* **1996,** *273* (5272), 245-248.
118. Khromov, A.; Choudhury, N.; Stevenson, A. S.; Somlyo, A. V.; Eto, M., Phosphorylation-dependent autoinhibition of myosin light chain phosphatase accounts for Ca2+ sensitization force of smooth muscle contraction. *J Biol Chem* **2009,** *284* (32), 21569-79.
119. Kiss, E.; Murányi, A.; Csortos, C.; Gergely, P.; Ito, M.; Hartshorne, D. J.; Erdodi, F., Integrin-linked kinase phosphorylates the myosin phosphatase target subunit at the inhibitory site in platelet cytoskeleton. *Biochem J* **2002,** *365* (Pt 1), 79-87.

120. Murányi, A.; Zhang, R.; Liu, F.; Hirano, K.; Ito, M.; Epstein, H. F.; Hartshorne, D. J., Myotonic dystrophy protein kinase phosphorylates the myosin phosphatase targeting subunit and inhibits myosin phosphatase activity. *FEBS Letters* **2001,** *493* (2-3), 80-84.
121. Niiro, N.; Ikebe, M., Zipper-interacting protein kinase induces Ca(2+)-free smooth muscle contraction via myosin light chain phosphorylation. *J Biol Chem* **2001,** *276* (31), 29567-74.
122. Broustas, C. G.; Grammatikakis, N.; Eto, M.; Dent, P.; Brautigan, D. L.; Kasid, U., Phosphorylation of the myosin-binding subunit of myosin phosphatase by Raf-1 and inhibition of phosphatase activity. *J Biol Chem* **2002,** *277* (4), 3053-9.
123. Takizawa, N.; Koga, Y.; Ikebe, M., Phosphorylation of CPI17 and myosin binding subunit of type 1 protein phosphatase by p21-activated kinase. *Biochemical and Biophysical Research Communications* **2002,** *297* (4), 773-778.
124. Velasco, G.; Armstrong, C.; Morrice, N.; Frame, S.; Cohen, P., Phosphorylation of the regulatory subunit of smooth muscle protein phosphatase 1M at Thr850 induces its dissociation from myosin. *FEBS Letters* **2002,** *527* (1-3), 101-104.
125. Shin, H. M.; Je, H. D.; Gallant, C.; Tao, T. C.; Hartshorne, D. J.; Ito, M.; Morgan, K. G., Differential association and localization of myosin phosphatase subunits during agonist-induced signal transduction in smooth muscle. *Circ Res* **2002,** *90* (5), 546-53.
126. Ito, M.; Nakano, T.; Erdődi, F.; Hartshorne, D. J., Myosin phosphatase: Structure, regulation and function. *Molecular and Cellular Biochemistry* **2004,** *259* (1), 197-209.
127. Surks, H. K.; Mochizuki, N.; Kasai, Y.; Georgescu, S. P.; Tang, K. M.; Ito, M.; Lincoln, T. M.; Mendelsohn, M. E., Regulation of Myosin Phosphatase by a Specific Interaction with cGMP- Dependent Protein Kinase Iα. *Science* **1999,** *286* (5444), 1583-1587.
128. Grassie, M. E.; Sutherland, C.; Ulke-Lemee, A.; Chappellaz, M.; Kiss, E.; Walsh, M. P.; MacDonald, J. A., Cross-talk between Rho-associated kinase and cyclic nucleotide-dependent kinase signaling pathways in the regulation of smooth muscle myosin light chain phosphatase. *J Biol Chem* **2012,** *287* (43), 36356-69.
129. Sutherland, C.; MacDonald, J. A.; Walsh, M. P., Analysis of phosphorylation of the myosin targeting subunit of myosin light chain phosphatase by Phos-tag SDS-PAGE. *American Journal of Physiology - Cell Physiology* **2016**, C681-C691.
130. Zagórska, A.; Deak, M.; Campbell, D. G.; Banerjee, S.; Hirano, M.; Aizawa, S.; Prescott, A. R.; Alessi, D. R., New Roles for the LKB1-NUAK Pathway in Controlling Myosin Phosphatase Complexes and Cell Adhesion. *Science Signaling* **2010,** *3* (115), ra25-ra25.
131. Totsukawa, G.; Yamakita, Y.; Yamashiro, S.; Hosoya, H.; Hartshorne, D. J.; Matsumura, F., Activation of Myosin Phosphatase Targeting Subunit by Mitosis-specific Phosphorylation. *J Cell Biol* **1999,** *144* (4), 735-44.
132. Eto, M.; Ohmori, T.; Suzuki, M.; Furuya, K.; Morita, F., A novel protein phosphatase-1 inhibitory protein potentiated by protein kinase C. Isolation from porcine aorta media and characterization. *J Biochem* **1995,** *118* (6), 1104-7.
133. Hayashi, Y.; Senba, S.; Yazawa, M.; Brautigan, D. L.; Eto, M., Defining the structural determinants and a potential mechanism for inhibition of myosin phosphatase by the protein kinase C-potentiated inhibitor protein of 17 kDa. *J Biol Chem* **2001,** *276* (43), 39858-63.
134. Eto, M.; Senba, S.; Morita, F.; Yazawa, M., Molecular cloning of a novel phosphorylation-dependent inhibitory protein of protein phosphatase-1 (CPI17) in smooth muscle: its specific localization in smooth muscle 1. *FEBS Letters* **1997,** *410* (2-3), 356-360.

135. Koyama, M.; Ito, M.; Feng, J.; Seko, T.; Shiraki, K.; Takase, K.; Hartshorne, D. J.; Nakano, T., Phosphorylation of CPI-17, an inhibitory phosphoprotein of smooth muscle myosin phosphatase, by Rho-kinase. *FEBS Letters* **2000,** *475* (3), 197-200.
136. Eto, M.; Brautigan, D. L., Endogenous inhibitor proteins that connect Ser/Thr kinases and phosphatases in cell signaling. *IUBMB life* **2012,** *64* (9), 732-9.
137. Woodsome, T. P.; Eto, M.; Everett, A.; Brautigan, D. L.; Kitazawa, T., Expression of CPI-17 and myosin phosphatase correlates with Ca2+ sensitivity of protein kinase C-induced contraction in rabbit smooth muscle. *The Journal of Physiology* **2001,** *535* (2), 553-564.
138. Kolosova, I. A.; Ma, S.-F.; Adyshev, D. M.; Wang, P.; Ohba, M.; Natarajan, V.; Garcia, J. G. N.; Verin, A. D., Role of CPI-17 in the regulation of endothelial cytoskeleton. *American Journal of Physiology - Lung Cellular and Molecular Physiology* **2004,** *287* (5), L970-L980.
139. Birukova, A. A.; Smurova, K.; Birukov, K. G.; Kaibuchi, K.; Garcia, J. G.; Verin, A. D., Role of Rho GTPases in thrombin-induced lung vascular endothelial cells barrier dysfunction. *Microvasc Res* **2004,** *67* (1), 64-77.
140. Kaneko-Kawano, T.; Takasu, F.; Naoki, H.; Sakumura, Y.; Ishii, S.; Ueba, T.; Eiyama, A.; Okada, A.; Kawano, Y.; Suzuki, K., Dynamic regulation of myosin light chain phosphorylation by Rho-kinase. *PLoS One* **2012,** *7* (6), e39269.
141. Vicente-Manzanares, M.; Ma, X.; Adelstein, R. S.; Horwitz, A. R., Non-muscle myosin II takes centre stage in cell adhesion and migration. *Nature reviews. Molecular cell biology* **2009,** *10* (11), 778-90.
142. Somlyo, A. P.; Somlyo, A. V., Ca^{2+} Sensitivity of Smooth Muscle and Nonmuscle Myosin II: Modulated by G Proteins, Kinases, and Myosin Phosphatase. *Physiological Reviews* **2003,** *83* (4), 1325-1358.
143. Rigor, R. R.; Shen, Q.; Pivetti, C. D.; Wu, M. H.; Yuan, S. Y., Myosin Light Chain Kinase Signaling in Endothelial Barrier Dysfunction. *Med Res Rev* **2013,** *33* (5), 911-33.
144. Garcia, J. G.; Davis, H. W.; Patterson, C. E., Regulation of endothelial cell gap formation and barrier dysfunction: role of myosin light chain phosphorylation. *J Cell Physiol* **1995,** *163* (3), 510-22.
145. Miller, J. R.; Silver, P. J.; Stull, J. T., The role of myosin light chain kinase phosphorylation in beta-adrenergic relaxation of tracheal smooth muscle. *Molecular Pharmacology* **1983,** *24* (2), 235-242.
146. Birukov, K. G.; Csortos, C.; Marzilli, L.; Dudek, S.; Ma, S. F.; Bresnick, A. R.; Verin, A. D.; Cotter, R. J.; Garcia, J. G., Differential regulation of alternatively spliced endothelial cell myosin light chain kinase isoforms by p60(Src). *J Biol Chem* **2001,** *276* (11), 8567-73.
147. Vinet, R.; Cortés, M. P.; Álvarez, R.; Delpiano, M. A., Bradykinin and histamine-induced cytosolic calcium increase in capillary endothelial cells of bovine adrenal medulla. *Cell Biology International* **2014,** *38* (9), 1023-1031.
148. Petrache, I.; Verin, A. D.; Crow, M. T.; Birukova, A.; Liu, F.; Garcia, J. G. N., Differential effect of MLC kinase in TNF-α-induced endothelial cell apoptosis and barrier dysfunction. *American Journal of Physiology - Lung Cellular and Molecular Physiology* **2001,** *280* (6), L1168-L1178.
149. Stasek, J. E.; Patterson, C. E.; Garcia, J. G. N., Protein kinase C phosphorylates caldesmon77 and vimentin and enhances albumin permeability across cultured bovine pulmonary artery endothelial cell monolayers. *Journal of Cellular Physiology* **1992,** *153* (1), 62-75.

150. Kimura, K.; Ito, M.; Amano, M.; Chihara, K.; Fukata, Y.; Nakafuku, M.; Yamamori, B.; Feng, J.; Nakano, T.; Okawa, K.; Iwamatsu, A.; Kaibuchi, K., Regulation of myosin phosphatase by Rho and Rho-associated kinase (Rho-kinase). *Science* **1996,** *273* (5272), 245-8.
151. Kolosova, I. A.; Mirzapoiazova, T.; Moreno-Vinasco, L.; Sammani, S.; Garcia, J. G.; Verin, A. D., Protective effect of purinergic agonist ATPgammaS against acute lung injury. *Am J Physiol Lung Cell Mol Physiol* **2008,** *294* (2), L319-24.
152. Birukova, A. A.; Burdette, D.; Moldobaeva, N.; Xing, J.; Fu, P.; Birukov, K. G., Rac GTPase is a hub for protein kinase A and Epac signaling in endothelial barrier protection by cAMP. *Microvasc Res* **2010,** *79* (2), 128-38.
153. Lu, Q.; Harrington, E. O.; Newton, J.; Casserly, B.; Radin, G.; Warburton, R.; Zhou, Y.; Blackburn, M. R.; Rounds, S., Adenosine protected against pulmonary edema through transporter- and receptor A2-mediated endothelial barrier enhancement. *Am J Physiol Lung Cell Mol Physiol* **2010,** *298* (6), L755-67.
154. Nerlich, A.; Rohde, M.; Talay, S. R.; Genth, H.; Just, I.; Chhatwal, G. S., Invasion of endothelial cells by tissue-invasive M3 type group A streptococci requires Src kinase and activation of Rac1 by a phosphatidylinositol 3-kinase-independent mechanism. *J Biol Chem* **2009,** *284* (30), 20319-28.
155. Shibata, K.; Sakai, H.; Huang, Q.; Kamata, H.; Chiba, Y.; Misawa, M.; Ikebe, R.; Ikebe, M., Rac1 regulates myosin II phosphorylation through regulation of myosin light chain phosphatase. *J Cell Physiol* **2015,** *230* (6), 1352-64.
156. Lakshmikanthan, S.; Zieba, B. J.; Ge, Z. D.; Momotani, K.; Zheng, X.; Lund, H.; Artamonov, M. V.; Maas, J. E.; Szabo, A.; Zhang, D. X.; Auchampach, J. A.; Mattson, D. L.; Somlyo, A. V.; Chrzanowska-Wodnicka, M., Rap1b in smooth muscle and endothelium is required for maintenance of vascular tone and normal blood pressure. *Arterioscler Thromb Vasc Biol* **2014,** *34* (7), 1486-94.
157. Niu, J.; Vaiskunaite, R.; Suzuki, N.; Kozasa, T.; Carr, D. W.; Dulin, N.; Voyno-Yasenetskaya, T. A., Interaction of heterotrimeric G13 protein with an A-kinase-anchoring protein 110 (AKAP110) mediates cAMP-independent PKA activation. *Curr Biol* **2001,** *11* (21), 1686-90.
158. Sehrawat, S.; Ernandez, T.; Cullere, X.; Takahashi, M.; Ono, Y.; Komarova, Y.; Mayadas, T. N., AKAP9 regulation of microtubule dynamics promotes Epac1-induced endothelial barrier properties. *Blood* **2011,** *117* (2), 708-18.
159. Weissmuller, T.; Glover, L. E.; Fennimore, B.; Curtis, V. F.; Macmanus, C. F.; Ehrentraut, S. F.; Campbell, E. L.; Scully, M.; Grove, B. D.; Colgan, S. P., HIF-dependent regulation of AKAP12 (gravin) in the control of human vascular endothelial function. *FASEB journal : official publication of the Federation of American Societies for Experimental Biology* **2014,** *28* (1), 256-64.
160. Dudzinski, D. M.; Igarashi, J.; Greif, D.; Michel, T., The regulation and pharmacology of endothelial nitric oxide synthase. *Annu Rev Pharmacol Toxicol* **2006,** *46*, 235-76.
161. Sessa, W. C., The nitric oxide synthase family of proteins. *J Vasc Res* **1994,** *31* (3), 131-43.
162. Förstermann, U.; Closs, E. I.; Pollock, J. S.; Nakane, M.; Schwarz, P.; Gath, I.; Kleinert, H., Nitric oxide synthase isozymes. Characterization, purification, molecular cloning, and functions. *Hypertension* **1994,** *23* (6 Pt 2), 1121-1131.
163. Bredt, D. S.; Hwang, P. M.; Snyder, S. H., Localization of nitric oxide synthase indicating a neural role for nitric oxide. *Nature* **1990,** *347* (6295), 768-70.

164. Stuehr, D. J.; Gross, S. S.; Sakuma, I.; Levi, R.; Nathan, C. F., Activated murine macrophages secrete a metabolite of arginine with the bioactivity of endothelium-derived relaxing factor and the chemical reactivity of nitric oxide. *The Journal of Experimental Medicine* **1989,** *169* (3), 1011-1020.
165. Kröncke, K.; Fehsel, K.; Kolb-Bachofen, V., Inducible nitric oxide synthase in human diseases. *Clinical and Experimental Immunology* **1998,** *113* (2), 147-56.
166. Pollock, J. S.; Nakane, M.; Buttery, L. D.; Martinez, A.; Springall, D.; Polak, J. M.; Forstermann, U.; Murad, F., Characterization and localization of endothelial nitric oxide synthase using specific monoclonal antibodies. *American Journal of Physiology-Cell Physiology* **1993,** *265* (5), C1379-C1387.
167. Förstermann, U.; Sessa, W. C., Nitric oxide synthases: regulation and function. *European Heart Journal* **2012,** *33* (7), 829-37.
168. Marsden, P. A.; Schappert, K. T.; Chen, H. S.; Flowers, M.; Sundell, C. L.; Wilcox, J. N.; Lamas, S.; Michel, T., Molecular cloning and characterization of human endothelial nitric oxide synthase. *FEBS Letters* **1992,** *307* (3), 287-293.
169. Janssens, S. P.; Shimouchi, A.; Quertermous, T.; Bloch, D. B.; Bloch, K. D., Cloning and expression of a cDNA encoding human endothelium-derived relaxing factor/nitric oxide synthase. *J Biol Chem* **1992,** *267* (21), 14519-22.
170. Chen, P. F.; Tsai, A. L.; Berka, V.; Wu, K. K., Mutation of Glu-361 in human endothelial nitric-oxide synthase selectively abolishes L-arginine binding without perturbing the behavior of heme and other redox centers. *J Biol Chem* **1997,** *272* (10), 6114-8.
171. Fleming, I.; Busse, R., Signal transduction of eNOS activation. *Cardiovasc Res.* **1999,** *43* (3), 532-541.
172. List, B. M.; Klösch, B.; Völker, C.; Gorren, A. C. F.; Sessa, W. C.; Werner, E. R.; Kukovetz, W. R.; Schmidt, K.; Mayer, B., Characterization of bovine endothelial nitric oxide synthase as a homodimer with down-regulated uncoupled NADPH oxidase activity: tetrahydrobiopterin binding kinetics and role of haem in dimerization. *Biochemical Journal* **1997,** *323* (1), 159-165.
173. Fulton, D.; Gratton, J.-P.; Sessa, W. C., Post-Translational Control of Endothelial Nitric Oxide Synthase: Why Isn't Calcium/Calmodulin Enough? *Journal of Pharmacology and Experimental Therapeutics* **2001,** *299* (3), 818-824.
174. Pfeiffer, S.; Leopold, E.; Schmidt, K.; Brunner, F.; Mayer, B., Inhibition of nitric oxide synthesis by NG-nitro-L-arginine methyl ester (L-NAME): requirement for bioactivation to the free acid, NG-nitro-L-arginine. *Br J Pharmacol* **1996,** *118* (6), 1433-40.
175. Church, J. E.; Fulton, D., Differences in eNOS activity because of subcellular localization are dictated by phosphorylation state rather than the local calcium environment. *J Biol Chem* **2006,** *281* (3), 1477-88.
176. Chen, P. F.; Wu, K. K., Structural elements contribute to the calcium/calmodulin dependence on enzyme activation in human endothelial nitric-oxide synthase. *J Biol Chem* **2003,** *278* (52), 52392-400.
177. Hemmens, B.; Goessler, W.; Schmidt, K.; Mayer, B., Role of bound zinc in dimer stabilization but not enzyme activity of neuronal nitric-oxide synthase. *J Biol Chem* **2000,** *275* (46), 35786-91.
178. List, B. M.; Klösch, B.; Völker, C.; Gorren, A. C.; Sessa, W. C.; Werner, E. R.; Kukovetz, W. R.; Schmidt, K.; Mayer, B., Characterization of bovine endothelial nitric oxide synthase as a

homodimer with down-regulated uncoupled NADPH oxidase activity: tetrahydrobiopterin binding kinetics and role of haem in dimerization. *Biochem J* **1997,** *323* (Pt 1), 159-65.
179. Stuehr, D.; Pou, S.; Rosen, G. M., Oxygen reduction by nitric-oxide synthases. *J Biol Chem* **2001,** *276* (18), 14533-6.
180. Fleming, I., Molecular mechanisms underlying the activation of eNOS. *Pflügers Archiv - European Journal of Physiology* **2010,** *459* (6), 793-806.
181. Searles, C. D., Transcriptional and posttranscriptional regulation of endothelial nitric oxide synthase expression. *American Journal of Physiology - Cell Physiology* **2006,** *291* (5), C803-C816.
182. Yoshizumi, M.; Perrella, M. A.; Burnett, J. C., Jr.; Lee, M. E., Tumor necrosis factor downregulates an endothelial nitric oxide synthase mRNA by shortening its half-life. *Circ Res* **1993,** *73* (1), 205-9.
183. Gibson, P. R., Increased gut permeability in Crohn's disease: is TNF the link? *Gut* **2004,** *53* (12), 1724-1725.
184. Yan, G.; You, B.; Chen, S.-P.; Liao, J. K.; Sun, J., Tumor Necrosis Factor-α Downregulates Endothelial Nitric Oxide Synthase mRNA Stability via Translation Elongation Factor 1-α 1. *Circ Res.* **2008,** *103* (6), 591-597.
185. Anderson, H. D.; Rahmutula, D.; Gardner, D. G., Tumor necrosis factor-alpha inhibits endothelial nitric-oxide synthase gene promoter activity in bovine aortic endothelial cells. *J Biol Chem* **2004,** *279* (2), 963-9.
186. Ramseyer, V.; Hong, N.; Garvin, J. L., Tumor necrosis factor alpha decreases NOS3 expression primarily via Rho/Rho kinase in the thick ascending limb. *Hypertension* **2012,** *59* (6), 1145-50.
187. Sugimoto, M.; Nakayama, M.; M Goto, T.; Amano, M.; Komori, K.; Kaibuchi, K., *Rho-kinase phosphorylates eNOS at threonine 495 in endothelial cells*. 2007; Vol. 361, p 462-7.
188. Mount, P. F.; Kemp, B. E.; Power, D. A., Regulation of endothelial and myocardial NO synthesis by multi-site eNOS phosphorylation. *Journal of Molecular and Cellular Cardiology* **2007,** *42* (2), 271-279.
189. Michel, T.; Li, G. K.; Busconi, L., Phosphorylation and subcellular translocation of endothelial nitric oxide synthase. *Proc Natl Acad Sci U S A* **1993,** *90* (13), 6252-6.
190. Fulton, D.; Gratton, J. P.; McCabe, T. J.; Fontana, J.; Fujio, Y.; Walsh, K.; Franke, T. F.; Papapetropoulos, A.; Sessa, W. C., Regulation of endothelium-derived nitric oxide production by the protein kinase Akt. *Nature* **1999,** *399* (6736), 597-601.
191. McCabe, T. J.; Fulton, D.; Roman, L. J.; Sessa, W. C., Enhanced electron flux and reduced calmodulin dissociation may explain "calcium-independent" eNOS activation by phosphorylation. *J Biol Chem* **2000,** *275* (9), 6123-8.
192. Fleming, I.; Fisslthaler, B.; Dimmeler, S.; Kemp, B. E.; Busse, R., Phosphorylation of Thr^{495} Regulates Ca^{2+}/calmodulin-Dependent Endothelial Nitric Oxide Synthase Activity. *Circ Res.* **2001,** *88* (11), e68-e75.
193. Boo, Y. C., Shear stress stimulates phosphorylation of protein kinase A substrate proteins including endothelial nitric oxide synthase in endothelial cells. *Exp Mol Med* **2006,** *38* (1), 63-71.
194. Matsubara, M.; Hayashi, N.; Jing, T.; Titani, K., Regulation of endothelial nitric oxide synthase by protein kinase C. *J Biochem* **2003,** *133* (6), 773-81.
195. Chen, Z.-P.; Mitchelhill, K. I.; Michell, B. J.; Stapleton, D.; Rodriguez-Crespo, I.; Witters, L. A.; Power, D. A.; Ortiz de Montellano, P. R.; Kemp, B. E., AMP-activated protein kinase phosphorylation of endothelial NO synthase. *FEBS Letters* **1999,** *443* (3), 285-289.

196. Thomas, S. R.; Chen, K.; Keaney, J. F., Jr., Hydrogen peroxide activates endothelial nitric-oxide synthase through coordinated phosphorylation and dephosphorylation via a phosphoinositide 3-kinase-dependent signaling pathway. *J Biol Chem* **2002,** *277* (8), 6017-24.
197. Michell, B. J.; Harris, M. B.; Chen, Z. P.; Ju, H.; Venema, V. J.; Blackstone, M. A.; Huang, W.; Venema, R. C.; Kemp, B. E., Identification of regulatory sites of phosphorylation of the bovine endothelial nitric-oxide synthase at serine 617 and serine 635. *J Biol Chem* **2002,** *277* (44), 42344-51.
198. Bauer, P. M.; Fulton, D.; Boo, Y. C.; Sorescu, G. P.; Kemp, B. E.; Jo, H.; Sessa, W. C., Compensatory phosphorylation and protein-protein interactions revealed by loss of function and gain of function mutants of multiple serine phosphorylation sites in endothelial nitric-oxide synthase. *J Biol Chem* **2003,** *278* (17), 14841-9.
199. Gallis, B.; Corthals, G. L.; Goodlett, D. R.; Ueba, H.; Kim, F.; Presnell, S. R.; Figeys, D.; Harrison, D. G.; Berk, B. C.; Aebersold, R.; Corson, M. A., Identification of flow-dependent endothelial nitric-oxide synthase phosphorylation sites by mass spectrometry and regulation of phosphorylation and nitric oxide production by the phosphatidylinositol 3-kinase inhibitor LY294002. *J Biol Chem* **1999,** *274* (42), 30101-8.
200. Kou, R.; Greif, D.; Michel, T., Dephosphorylation of endothelial nitric-oxide synthase by vascular endothelial growth factor. Implications for the vascular responses to cyclosporin A. *J Biol Chem* **2002,** *277* (33), 29669-73.
201. Fulton, D.; Church, J. E.; Ruan, L.; Li, C.; Sood, S. G.; Kemp, B. E.; Jennings, I. G.; Venema, R. C., Src kinase activates endothelial nitric-oxide synthase by phosphorylating Tyr-83. *J Biol Chem* **2005,** *280* (43), 35943-52.
202. Loot, A. E.; Schreiber, J. G.; Fisslthaler, B.; Fleming, I., Angiotensin II impairs endothelial function via tyrosine phosphorylation of the endothelial nitric oxide synthase. *The Journal of Experimental Medicine* **2009,** *206* (13), 2889-2896.
203. Liu, J.; Garcia-Cardena, G.; Sessa, W. C., Biosynthesis and palmitoylation of endothelial nitric oxide synthase: mutagenesis of palmitoylation sites, cysteines-15 and/or -26, argues against depalmitoylation-induced translocation of the enzyme. *Biochemistry* **1995,** *34* (38), 12333-40.
204. Lisanti, M. P.; Scherer, P. E.; Tang, Z.; Sargiacomo, M., Caveolae, caveolin and caveolin-rich membrane domains: a signalling hypothesis. *Trends in Cell Biology* **1994,** *4* (7), 231-235.
205. Smart, E. J.; Graf, G. A.; McNiven, M. A.; Sessa, W. C.; Engelman, J. A.; Scherer, P. E.; Okamoto, T.; Lisanti, M. P., Caveolins, Liquid-Ordered Domains, and Signal Transduction. *Mol Cell Biol* **1999,** *19* (11), 7289-304.
206. Gonzalez, E.; Kou, R.; Lin, A. J.; Golan, D. E.; Michel, T., Subcellular targeting and agonist-induced site-specific phosphorylation of endothelial nitric-oxide synthase. *J Biol Chem* **2002,** *277* (42), 39554-60.
207. Shaul, P. W., Regulation of endothelial nitric oxide synthase: location, location, location. *Annu Rev Physiol* **2002,** *64*, 749-74.
208. Fernández-Hernando, C.; Fukata, M.; Bernatchez, P. N.; Fukata, Y.; Lin, M. I.; Bredt, D. S.; Sessa, W. C., Identification of Golgi-localized acyl transferases that palmitoylate and regulate endothelial nitric oxide synthase. *The Journal of Cell Biology* **2006,** *174* (3), 369-377.
209. Yeh, D. C.; Duncan, J. A.; Yamashita, S.; Michel, T., Depalmitoylation of endothelial nitric-oxide synthase by acyl-protein thioesterase 1 is potentiated by Ca(2+)-calmodulin. *J Biol Chem* **1999,** *274* (46), 33148-54.

210. Liu, J.; Hughes, T. E.; Sessa, W. C., The First 35 Amino Acids and Fatty Acylation Sites Determine the Molecular Targeting of Endothelial Nitric Oxide Synthase into the Golgi Region of Cells: A Green Fluorescent Protein Study. *The Journal of Cell Biology* **1997,** *137* (7), 1525-1535.
211. Fulton, D.; Babbitt, R.; Zoellner, S.; Fontana, J.; Acevedo, L.; McCabe, T. J.; Iwakiri, Y.; Sessa, W. C., Targeting of endothelial nitric-oxide synthase to the cytoplasmic face of the Golgi complex or plasma membrane regulates Akt- versus calcium-dependent mechanisms for nitric oxide release. *J Biol Chem* **2004,** *279* (29), 30349-57.
212. Durán, W. N.; Breslin, J. W.; Sánchez, F. A., The NO cascade, eNOS location, and microvascular permeability. *Cardiovasc Res* **2010,** *87* (2), 254-61.
213. García-Cardeña, G.; Martasek, P.; Masters, B. S. S.; Skidd, P. M.; Couet, J.; Li, S.; Lisanti, M. P.; Sessa, W. C., Dissecting the Interaction between Nitric Oxide Synthase (NOS) and Caveolin: Functional significance of the NOS caveolin binding domain in vivo. *Journal of Biological Chemistry* **1997,** *272* (41), 25437-25440.
214. Garcia-Cardena, G.; Fan, R.; Shah, V.; Sorrentino, R.; Cirino, G.; Papapetropoulos, A.; Sessa, W. C., Dynamic activation of endothelial nitric oxide synthase by Hsp90. *Nature* **1998,** *392* (6678), 821-4.
215. Xu, H.; Shi, Y.; Wang, J.; Jones, D.; Weilrauch, D.; Ying, R.; Wakim, B.; Pritchard, K. A., Jr., A heat shock protein 90 binding domain in endothelial nitric-oxide synthase influences enzyme function. *J Biol Chem* **2007,** *282* (52), 37567-74.
216. Billecke, S. S.; Draganov, D. I.; Morishima, Y.; Murphy, P. J. M.; Dunbar, A. Y.; Pratt, W. B.; Osawa, Y., The Role of hsp90 in Heme-dependent Activation of Apo-neuronal Nitric-oxide Synthase. *Journal of Biological Chemistry* **2004,** *279* (29), 30252-30258.
217. Dedio, J.; Konig, P.; Wohlfart, P.; Schroeder, C.; Kummer, W.; Muller-Esterl, W., NOSIP, a novel modulator of endothelial nitric oxide synthase activity. *FASEB J* **2001,** *15* (1), 79-89.
218. Zimmermann, K.; Opitz, N.; Dedio, J.; Renné, C.; Müller-Esterl, W.; Oess, S., NOSTRIN: A protein modulating nitric oxide release and subcellular distribution of endothelial nitric oxide synthase. *Proc Natl Acad Sci U S A* **2002,** *99* (26), 17167-72.
219. Knowles, R. G.; Palacios, M.; Palmer, R. M.; Moncada, S., Formation of nitric oxide from L-arginine in the central nervous system: a transduction mechanism for stimulation of the soluble guanylate cyclase. *Proc Natl Acad Sci U S A* **1989,** *86* (13), 5159-62.
220. Ziche, M.; Morbidelli, L.; Masini, E.; Granger, H.; Geppetti, P.; Ledda, F., Nitric Oxide Promotes DNA Synthesis and Cyclic GMP Formation in Endothelial Cells from Postcapillary Venules. *Biochemical and Biophysical Research Communications* **1993,** *192* (3), 1198-1203.
221. Etter, E. F.; Eto, M.; Wardle, R. L.; Brautigan, D. L.; Murphy, R. A., Activation of myosin light chain phosphatase in intact arterial smooth muscle during nitric oxide-induced relaxation. *J Biol Chem* **2001,** *276* (37), 34681-5.
222. Garg, U. C.; Hassid, A., Nitric oxide-generating vasodilators and 8-bromo-cyclic guanosine monophosphate inhibit mitogenesis and proliferation of cultured rat vascular smooth muscle cells. *J Clin Invest* **1989,** *83* (5), 1774-7.
223. Alheid, U.; Frolich, J. C.; Forstermann, U., Endothelium-derived relaxing factor from cultured human endothelial cells inhibits aggregation of human platelets. *Thromb Res* **1987,** *47* (5), 561-71.
224. Kubes, P.; Suzuki, M.; Granger, D. N., Nitric oxide: an endogenous modulator of leukocyte adhesion. *Proc Natl Acad Sci U S A* **1991,** *88* (11), 4651-5.
225. Qian, J.; Fulton, D. J. R., Exogenous, but not Endogenous Nitric Oxide Inhibits Adhesion Molecule Expression in Human Endothelial Cells. *Front Physiol* **2012,** *3*.

226. Khan, B. V.; Harrison, D. G.; Olbrych, M. T.; Alexander, R. W.; Medford, R. M., Nitric oxide regulates vascular cell adhesion molecule 1 gene expression and redox-sensitive transcriptional events in human vascular endothelial cells. *Proc Natl Acad Sci U S A* **1996,** *93* (17), 9114-9.
227. Zampolli, A.; Basta, G.; Lazzerini, G.; Feelisch, M.; De Caterina, R., Inhibition of Endothelial Cell Activation by Nitric Oxide Donors. *Journal of Pharmacology and Experimental Therapeutics* **2000,** *295* (2), 818-823.
228. Murohara, T.; Asahara, T.; Silver, M.; Bauters, C.; Masuda, H.; Kalka, C.; Kearney, M.; Chen, D.; Symes, J. F.; Fishman, M. C.; Huang, P. L.; Isner, J. M., Nitric oxide synthase modulates angiogenesis in response to tissue ischemia. *J Clin Invest* **1998,** *101* (11), 2567-78.
229. Hippenstiel, S.; Krull, M.; Ikemann, A.; Risau, W.; Clauss, M.; Suttorp, N., VEGF induces hyperpermeability by a direct action on endothelial cells. *Am J Physiol* **1998,** *274* (5 Pt 1), L678-84.
230. Wu, H. M.; Huang, Q.; Yuan, Y.; Granger, H. J., VEGF induces NO-dependent hyperpermeability in coronary venules. *Am J Physiol* **1996,** *271* (6 Pt 2), H2735-9.
231. Six, I.; Kureishi, Y.; Luo, Z.; Walsh, K., Akt signaling mediates VEGF/VPF vascular permeability in vivo. *FEBS Letters* **2002,** *532* (1-2), 67-69.
232. Bredt, D. S., Endogenous nitric oxide synthesis: biological functions and pathophysiology. *Free Radic Res* **1999,** *31* (6), 577-96.
233. Kubes, P., Nitric Oxide Affects Microvascular Permeability in the Intact and Inflamed Vasculature. *Microcirculation* **1995,** *2* (3), 235-244.
234. Kubes, P.; Granger, D. N., Nitric oxide modulates microvascular permeability. *American Journal of Physiology - Heart and Circulatory Physiology* **1992,** *262* (2), H611-H615.
235. Ann L. Baldwin, G. T., and Hamda Al Naemi, Inhibition of nitric oxide synthesis increases venular permeability and alters endothelial actin cytoskeleton. *American Journal of Physiology-Heart and Circulatory Physiology* **1998,** *274* (5), H1776-H1784.
236. P, H.; , L. B., Curry FE., Effect of nitric oxide synthase inhibitors on endothelial [Ca2+]i and microvessel permeability. *American Journal of Physiology-Heart and Circulatory Physiology* **1997,** *272* (1), H176-H185.
237. Hoffmann, A.; Gloe, T.; Pohl, U.; Zahler, S., Nitric oxide enhances de novo formation of endothelial gap junctions. *Cardiovasc Res* **2003,** *60* (2), 421-30.
238. Yang, D.; Liu, J.; Tian, C.; Zeng, Y.; Zheng, Y.; Fang, Q.; Li, H., Epigallocatechin gallate inhibits angiotensin II-induced endothelial barrier dysfunction via inhibition of the p38 MAPK/HSP27 pathway. *Acta Pharmacologica Sinica* **2010,** *31* (10), 1401-6.
239. Erwin, P. A.; Lin, A. J.; Golan, D. E.; Michel, T., Receptor-regulated dynamic S-nitrosylation of endothelial nitric-oxide synthase in vascular endothelial cells. *J Biol Chem* **2005,** *280* (20), 19888-94.
240. Martinez-Ruiz, A.; Lamas, S., Nitrosylation of thiols in vascular homeostasis and disease. *Curr Atheroscler Rep* **2005,** *7* (3), 213-8.
241. Liu, L.; Hausladen, A.; Zeng, M.; Que, L.; Heitman, J.; Stamler, J. S., A metabolic enzyme for S-nitrosothiol conserved from bacteria to humans. *Nature* **2001,** *410* (6827), 490-4.
242. Mitchell, D. A.; Marletta, M. A., Thioredoxin catalyzes the S-nitrosation of the caspase-3 active site cysteine. *Nat Chem Biol* **2005,** *1* (3), 154-8.
243. Ravi, K.; Brennan, L. A.; Levic, S.; Ross, P. A.; Black, S. M., S-nitrosylation of endothelial nitric oxide synthase is associated with monomerization and decreased enzyme activity.

Proceedings of the National Academy of Sciences of the United States of America **2004,** *101* (8), 2619-2624.
244. Seth, D.; Stamler, J. S., The SNO-proteome: causation and classifications. *Current Opinion in Chemical Biology* **2011,** *15* (1), 129-136.
245. Sutherland, C.; MacDonald, J. A.; Walsh, M. P., Analysis of phosphorylation of the myosin-targeting subunit of myosin light chain phosphatase by Phos-tag SDS-PAGE. *Am J Physiol Cell Physiol* **2016,** *310* (8), C681-91.
246. Erdodi, F.; Toth, B.; Hirano, K.; Hirano, M.; Hartshorne, D. J.; Gergely, P., Endothall thioanhydride inhibits protein phosphatases-1 and -2A in vivo. *Am J Physiol* **1995,** *269* (5 Pt 1), C1176-84.
247. Palatka, K.; Serfőző, Z.; Veréb, Z.; Bátori, R.; Lontay, B.; Hargitay, Z.; Nemes, Z.; Udvardy, M.; Erdődi, F.; Altorjay, I., Effect of IBD sera on expression of inducible and endothelial nitric oxide synthase in human umbilical vein endothelial cells. *World Journal of Gastroenterology : WJG* **2006,** *12* (11), 1730-8.
248. Munhoz, F. C.; Potje, S. R.; Pereira, A. C.; Daruge, M. G.; da Silva, R. S.; Bendhack, L. M.; Antoniali, C., Hypotensive and vasorelaxing effects of the new NO-donor [Ru(terpy)(bdq)NO(+)](3+) in spontaneously hypertensive rats. *Nitric Oxide* **2012,** *26* (2), 111-7.
249. Nagy, D.; Gonczi, M.; Dienes, B.; Szoor, A.; Fodor, J.; Nagy, Z.; Toth, A.; Fodor, T.; Bai, P.; Szucs, G.; Rusznak, Z.; Csernoch, L., Silencing the KCNK9 potassium channel (TASK-3) gene disturbs mitochondrial function, causes mitochondrial depolarization, and induces apoptosis of human melanoma cells. *Arch Dermatol Res* **2014,** *306* (10), 885-902.
250. Kolozsvári, B.; Bakó, É.; Bécsi, B.; Kiss, A.; Czikora, Á.; Tóth, A.; Vámosi, G.; Gergely, P.; Erdődi, F., Calcineurin regulates endothelial barrier function by interaction with and dephosphorylation of myosin phosphatase. *Cardiovasc Res.* **2012,** *96* (3), 494-503.
251. Scotto-Lavino, E.; Garcia-Diaz, M.; Du, G.; Frohman, M. A., Basis for the Isoform-specific Interaction of Myosin Phosphatase Subunits Protein Phosphatase 1c β and Myosin Phosphatase Targeting Subunit 1. *J Biol Chem* **2010,** *285* (9), 6419-24.
252. Umeda, D.; Yano, S.; Yamada, K.; Tachibana, H., Green tea polyphenol epigallocatechin-3-gallate signaling pathway through 67-kDa laminin receptor. *J Biol Chem* **2008,** *283* (6), 3050-8.
253. Kim, J. A.; Formoso, G.; Li, Y.; Potenza, M. A.; Marasciulo, F. L.; Montagnani, M.; Quon, M. J., Epigallocatechin gallate, a green tea polyphenol, mediates NO-dependent vasodilation using signaling pathways in vascular endothelium requiring reactive oxygen species and Fyn. *J Biol Chem* **2007,** *282* (18), 13736-45.
254. Lorenz, M.; Urban, J.; Engelhardt, U.; Baumann, G.; Stangl, K.; Stangl, V., Green and black tea are equally potent stimuli of NO production and vasodilation: new insights into tea ingredients involved. *Basic Research in Cardiology* **2009,** *104* (1), 100-110.
255. Hasko, G.; Cronstein, B., Regulation of inflammation by adenosine. *Frontiers in immunology* **2013,** *4*, 85.
256. Patil, S.; Kaplan, J. E.; Minnear, F. L., Protein, not adenosine or adenine nucleotides, mediates platelet decrease in endothelial permeability. *Am J Physiol* **1997,** *273* (5 Pt 2), H2304-11.
257. Hasko, G.; Cronstein, B. N., Adenosine: an endogenous regulator of innate immunity. *Trends in immunology* **2004,** *25* (1), 33-9.
258. Ralevic, V.; Burnstock, G., Receptors for purines and pyrimidines. *Pharmacol Rev* **1998,** *50* (3), 413-92.

259. Sheth, S.; Brito, R.; Mukherjea, D.; Rybak, L. P.; Ramkumar, V., Adenosine receptors: expression, function and regulation. *Int J Mol Sci* **2014,** *15* (2), 2024-52.
260. Zemskov, E.; Lucas, R.; Verin, A. D.; Umapathy, N. S., P2Y receptors as regulators of lung endothelial barrier integrity. *J Cardiovasc Dis Res* **2011,** *2* (1), 14-22.
261. Feoktistov, I.; Goldstein, A. E.; Ryzhov, S.; Zeng, D.; Belardinelli, L.; Voyno-Yasenetskaya, T.; Biaggioni, I., Differential expression of adenosine receptors in human endothelial cells: role of A2B receptors in angiogenic factor regulation. *Circ Res* **2002,** *90* (5), 531-8.
262. Erb, L.; Weisman, G. A., Coupling of P2Y receptors to G proteins and other signaling pathways. *Wiley Interdiscip Rev Membr Transp Signal* **2012,** *1* (6), 789-803.
263. Filippov, A. K.; Simon, J.; Barnard, E. A.; Brown, D. A., Coupling of the nucleotide P2Y4 receptor to neuronal ion channels. *Br J Pharmacol* **2003,** *138* (2), 400-6.
264. Tasken, K.; Skalhegg, B. S.; Tasken, K. A.; Solberg, R.; Knutsen, H. K.; Levy, F. O.; Sandberg, M.; Orstavik, S.; Larsen, T.; Johansen, A. K.; Vang, T.; Schrader, H. P.; Reinton, N. T.; Torgersen, K. M.; Hansson, V.; Jahnsen, T., Structure, function, and regulation of human cAMP-dependent protein kinases. *Adv Second Messenger Phosphoprotein Res* **1997,** *31*, 191-204.
265. Nguyen, E.; Gausdal, G.; Varennes, J.; Pendino, F.; Lanotte, M.; Doskeland, S. O.; Segal-Bendirdjian, E., Activation of both protein kinase A (PKA) type I and PKA type II isozymes is required for retinoid-induced maturation of acute promyelocytic leukemia cells. *Mol Pharmacol* **2013,** *83* (5), 1057-65.
266. Zieba, B. J.; Artamonov, M. V.; Jin, L.; Momotani, K.; Ho, R.; Franke, A. S.; Neppl, R. L.; Stevenson, A. S.; Khromov, A. S.; Chrzanowska-Wodnicka, M.; Somlyo, A. V., The cAMP-responsive Rap1 guanine nucleotide exchange factor, Epac, induces smooth muscle relaxation by down-regulation of RhoA activity. *J Biol Chem* **2011,** *286* (19), 16681-92.
267. Colledge, M.; Scott, J. D., AKAPs: from structure to function. *Trends Cell Biol* **1999,** *9* (6), 216-21.
268. Schillace, R. V.; Voltz, J. W.; Sim, A. T.; Shenolikar, S.; Scott, J. D., Multiple interactions within the AKAP220 signaling complex contribute to protein phosphatase 1 regulation. *J Biol Chem* **2001,** *276* (15), 12128-34.
269. Kim, K. M.; Csortos, C.; Czikora, I.; Fulton, D.; Umapathy, N. S.; Olah, G.; Verin, A. D., Molecular characterization of myosin phosphatase in endothelium. *J Cell Physiol* **2012,** *227* (4), 1701-8.
270. Lin, M. I.; Fulton, D.; Babbitt, R.; Fleming, I.; Busse, R.; Pritchard, K. A., Jr.; Sessa, W. C., Phosphorylation of threonine 497 in endothelial nitric-oxide synthase coordinates the coupling of L-arginine metabolism to efficient nitric oxide production. *J Biol Chem* **2003,** *278* (45), 44719-26.
271. Watts, V. L.; Motley, E. D., Role of protease-activated receptor-1 in endothelial nitric oxide synthase-Thr495 phosphorylation. *Exp Biol Med (Maywood)* **2009,** *234* (2), 132-9.
272. Schmitt, C. A.; Heiss, E. H.; Aristei, Y.; Severin, T.; Dirsch, V. M., Norfuraneol dephosphorylates eNOS at threonine 495 and enhances eNOS activity in human endothelial cells. *Cardiovasc Res.* **2009,** *81* (4), 750-757.
273. Lubomirov, L. T.; Papadopoulos, S.; Putz, S.; Welter, J.; Klockener, T.; Weckmuller, K.; Ardestani, M. A.; Filipova, D.; Metzler, D.; Metzner, H.; Staszewski, J.; Zittrich, S.; Gagov, H.; Schroeter, M. M.; Pfitzer, G., Aging-related alterations in eNOS and nNOS responsiveness and smooth muscle reactivity of murine basilar arteries are modulated by apocynin and

phosphorylation of myosin phosphatase targeting subunit-1. *J Cereb Blood Flow Metab* **2017,** *37* (3), 1014-1029.
274. Grassie, M. E.; Moffat, L. D.; Walsh, M. P.; MacDonald, J. A., The myosin phosphatase targeting protein (MYPT) family: a regulated mechanism for achieving substrate specificity of the catalytic subunit of protein phosphatase type 1delta. *Arch Biochem Biophys* **2011,** *510* (2), 147-59.
275. Muranyi, A.; Derkach, D.; Erdodi, F.; Kiss, A.; Ito, M.; Hartshorne, D. J., Phosphorylation of Thr695 and Thr850 on the myosin phosphatase target subunit: inhibitory effects and occurrence in A7r5 cells. *FEBS Lett* **2005,** *579* (29), 6611-5.
276. Kiss, A.; Bécsi, B.; Kolozsvári, B.; Komáromi, I.; Kövér, K. E.; Erdődi, F., Epigallocatechin-3-gallate and penta-O-galloyl-β-d-glucose inhibit protein phosphatase-1. *FEBS Journal* **2013,** *280* (2), 612-626.
277. Bécsi, B.; Kiss, A.; Erdődi, F., Interaction of protein phosphatase inhibitors with membrane lipids assessed by surface plasmon resonance based binding technique. *Chemistry and Physics of Lipids* **2014,** *183*, 68-76.
278. Huang, F.; Subbaiah, P. V.; Holian, O.; Zhang, J.; Johnson, A.; Gertzberg, N.; Lum, H., Lysophosphatidylcholine increases endothelial permeability: role of PKCalpha and RhoA cross talk. *Am J Physiol Lung Cell Mol Physiol* **2005,** *289* (2), L176-85.
279. Sanchez, F. A.; Rana, R.; Gonzalez, F. G.; Iwahashi, T.; Duran, R. G.; Fulton, D. J.; Beuve, A. V.; Kim, D. D.; Duran, W. N., Functional significance of cytosolic endothelial nitric-oxide synthase (eNOS): regulation of hyperpermeability. *J Biol Chem* **2011,** *286* (35), 30409-14.
280. Hirano, M.; Hirano, K., Myosin di-phosphorylation and peripheral actin bundle formation as initial events during endothelial barrier disruption. *Sci Rep* **2016,** *6*.
281. Gonzales, J. N.; Gorshkov, B.; Varn, M. N.; Zemskova, M. A.; Zemskov, E. A.; Sridhar, S.; Lucas, R.; Verin, A. D., Protective effect of adenosine receptors against lipopolysaccharide-induced acute lung injury. *Am J Physiol Lung Cell Mol Physiol* **2014,** *306* (6), L497-507.
282. Baron, L.; Gombault, A.; Fanny, M.; Villeret, B.; Savigny, F.; Guillou, N.; Panek, C.; Le Bert, M.; Lagente, V.; Rassendren, F.; Riteau, N.; Couillin, I., The NLRP3 inflammasome is activated by nanoparticles through ATP, ADP and adenosine. *Cell Death Dis* **2015,** *6*, e1629.
283. Fredholm, B. B.; Irenius, E.; Kull, B.; Schulte, G., Comparison of the potency of adenosine as an agonist at human adenosine receptors expressed in Chinese hamster ovary cells. *Biochem Pharmacol* **2001,** *61* (4), 443-8.
284. Zhou, Y.; Schneider, D. J.; Morschl, E.; Song, L.; Pedroza, M.; Karmouty-Quintana, H.; Le, T.; Sun, C. X.; Blackburn, M. R., Distinct roles for the A2B adenosine receptor in acute and chronic stages of bleomycin-induced lung injury. *J Immunol* **2011,** *186* (2), 1097-106.
285. Zaynagetdinov, R.; Ryzhov, S.; Goldstein, A. E.; Yin, H.; Novitskiy, S. V.; Goleniewska, K.; Polosukhin, V. V.; Newcomb, D. C.; Mitchell, D.; Morschl, E.; Zhou, Y.; Blackburn, M. R.; Peebles, R. S., Jr.; Biaggioni, I.; Feoktistov, I., Attenuation of chronic pulmonary inflammation in A2B adenosine receptor knockout mice. *Am J Respir Cell Mol Biol* **2010,** *42* (5), 564-71.
286. Klinger, M.; Freissmuth, M.; Nanoff, C., Adenosine receptors: G protein-mediated signalling and the role of accessory proteins. *Cell Signal* **2002,** *14* (2), 99-108.
287. Burnstock, G., Introduction: P2 receptors. *Curr Top Med Chem* **2004,** *4* (8), 793-803.
288. Bogdanov, Y. D.; Wildman, S. S.; Clements, M. P.; King, B. F.; Burnstock, G., Molecular cloning and characterization of rat P2Y4 nucleotide receptor. *Br J Pharmacol* **1998,** *124* (3), 428-30.

289. Kennedy, C.; Qi, A. D.; Herold, C. L.; Harden, T. K.; Nicholas, R. A., ATP, an agonist at the rat P2Y(4) receptor, is an antagonist at the human P2Y(4) receptor. *Mol Pharmacol* **2000,** *57* (5), 926-31.
290. Bilbao, P. S.; Santillan, G.; Boland, R., ATP stimulates the proliferation of MCF-7 cells through the PI3K/Akt signaling pathway. *Arch Biochem Biophys* **2010,** *499* (1-2), 40-8.
291. Aslam, M.; Tanislav, C.; Troidl, C.; Schulz, R.; Hamm, C.; Gunduz, D., cAMP controls the restoration of endothelial barrier function after thrombin-induced hyperpermeability via Rac1 activation. *Physiol Rep* **2014,** *2* (10).
292. Patterson, C. E.; Lum, H.; Schaphorst, K. L.; Verin, A. D.; Garcia, J. G., Regulation of endothelial barrier function by the cAMP-dependent protein kinase. *Endothelium* **2000,** *7* (4), 287-308.
293. Sriwai, W.; Zhou, H.; Murthy, K. S., G(q)-dependent signalling by the lysophosphatidic acid receptor LPA(3) in gastric smooth muscle: reciprocal regulation of MYPT1 phosphorylation by Rho kinase and cAMP-independent PKA. *Biochem J* **2008,** *411* (3), 543-51.
294. Ferraris, J. D.; Persaud, P.; Williams, C. K.; Chen, Y.; Burg, M. B., cAMP-independent role of PKA in tonicity-induced transactivation of tonicity-responsive enhancer/ osmotic response element-binding protein. *Proc Natl Acad Sci U S A* **2002,** *99* (26), 16800-5.
295. Bogatcheva, N. V.; Zemskova, M. A.; Kovalenkov, Y.; Poirier, C.; Verin, A. D., Molecular mechanisms mediating protective effect of cAMP on lipopolysaccharide (LPS)-induced human lung microvascular endothelial cells (HLMVEC) hyperpermeability. *J Cell Physiol* **2009,** *221* (3), 750-9.
296. Zieger, M.; Tausch, S.; Henklein, P.; Nowak, G.; Kaufmann, R., A novel PAR-1-type thrombin receptor signaling pathway: cyclic AMP-independent activation of PKA in SNB-19 glioblastoma cells. *Biochem Biophys Res Commun* **2001,** *282* (4), 952-7.
297. Lester, L. B.; Faux, M. C.; Nauert, J. B.; Scott, J. D., Targeted protein kinase A and PP-2B regulate insulin secretion through reversible phosphorylation. *Endocrinology* **2001,** *142* (3), 1218-27.

UNIVERSITY of DEBRECEN

UNIVERSITY AND NATIONAL LIBRAY
UNIVERSITY OF DEBRECEN
H-4002 Egyetem tér 1, Debrecen
Phone: +3652/410-443, email: publikaciok@lib.unideb.hu

Registry number: DEENK/296/2018.PL
Subject: PhD Publikációs Lista

Candidate: Róbert Károly Bátori
Neptun ID: WDLNJB
Doctoral School: Doctoral School of Molecular Medicine

List of publications related to the dissertation

1. **Bátori, R. K.**, Kumar, S., Bordán, Z., Cherian-Shaw, M., Kovács-Kása, A., MacDonald, J. A., Fulton, D., Erdődi, F., Verin, A.: Differential mechanisms of adenosine- and ATPγS-induced microvascular endothelial barrier strengthening.
J. Cell. Physiol. [Epub ahead of print], 2018.
DOI: http://dx.doi.org/10.1002/jcp.26419
IF: 3.923 (2017)

2. **Bátori, R. K.**, Bécsi, B., Nagy, D., Kónya, Z., Hegedűs, C., Bordán, Z., Verin, A., Lontay, B., Erdődi, F.: Interplay of myosin phosphatase and protein phosphatase-2A in the regulation of endothelial nitric-oxide synthase phosphorylation and nitric oxide production.
Sci Rep. 7 (44698), 1-17, 2017.
DOI: http://dx.doi.org/10.1038/srep44698
IF: 4.122

List of other publications

3. Horváth, D., Sipos, A., Major, E., Kónya, Z., **Bátori, R. K.**, Dedinszki, D., Szöllősi, A. G., Tamás, I., Iván, J., Kiss, A., Erdődi, F., Lontay, B.: Myosin phosphatase accelerates cutaneous wound healing by regulating migration and differentiation of epidermal keratinocytes via Akt signaling pathway in human and murine skin.
Biochim. Biophys. Acta-Mol. Basis Dis. 1864 (10), 3268-3280, 2018.
DOI: http://dx.doi.org/10.1016/j.bbadis.2018.07.013
IF: 5.108 (2017)

4. Dedinszki, D., Sipos, A., Kiss, A., **Bátori, R. K.**, Kónya, Z., Virág, L., Erdődi, F., Lontay, B.: Protein phosphatase-1 is involved in the maintenance of normal homeostasis and in UVA irradiation-induced pathological alterations in HaCaT cells and in mouse skin.
Biochim. Biophys. Acta-Mol. Basis Dis. 1852 (1), 22-33, 2015.
DOI: http://dx.doi.org/10.1016/j.bbadis.2014.11.005
IF: 5.158

UNIVERSITY of DEBRECEN

UNIVERSITY AND NATIONAL LIBRAY
UNIVERSITY OF DEBRECEN
H-4002 Egyetem tér 1, Debrecen
Phone: +3652/410-443, email: publikaciok@lib.unideb.hu

5. Ruzsnavszky, O., Dienes, B., Oláh, T., Vincze, J., Gáll, T., Balogh, E., Szemán-Nagy, G., **Bátori, R. K.**, Lontay, B., Erdődi, F., Csernoch, L.: Differential Effects of Phosphatase Inhibitors on the Calcium Homeostasis and Migration of HaCaT Keratinocytes.
PLoS One. 8 (4), 1-10, 2013.
DOI: http://dx.doi.org/10.1371/journal.pone.0061507
IF: 3.534

6. Beyer, D., Tándor, I., Kónya, Z., **Bátori, R. K.**, Roszik, J., Vereb, G., Erdődi, F., Vasas, G., Mikóné Hamvas, M., Jambrovics, K., Máthé, C.: Microcystin-LR, a protein phosphatase inhibitor, induces alterations in mitotic chromatin and microtubule organization leading to the formation of micronuclei in Vicia faba.
Ann. Bot. 110 (4), 797-808, 2012.
DOI: http://dx.doi.org/10.1093/aob/mcs154
IF: 3.449

7. Altorjay, I., Veréb, Z., Serfőző, Z., Bacskai, I., **Bátori, R. K.**, Erdődi, F., Udvardy, M., Sipka, S., Lányi, Á., Rajnavölgyi, É., Palatka, K.: Anti-TNF-alpha antibody (infliximab) therapy supports the recovery of eNOS and VEGFR2 protein expression in endothelial cells.
Int. J. Immunopathol. Pharmacol. 24 (2), 323-335, 2011.
IF: 2.991

8. Beyer, D., Surányi, G., Vasas, G., Roszik, J., Erdődi, F., Mikóné Hamvas, M., Bácsi, I., **Bátori, R. K.**, Serfőző, Z., Máthéné Szigeti, Z., Vereb, G., Demeter, Z., Gonda, S., Máthé, C.: Cylindrospermopsin induces alterations of root histology and microtubule organization in common reed (Phragmites australis) plantlets cultured in vitro.
Toxicon. 54 (4), 440-449, 2009.
DOI: http://dx.doi.org/10.1016/J.toxicon.2009.05.008
IF: 2.128

9. Palatka, K., Serfőző, Z., Veréb, Z., **Bátori, R. K.**, Lontay, B., Hargitay, Z., Nemes, Z., Udvardy, M., Erdődi, F., Altorjay, I.: Effect of IBD sera on expression of inducible and endothelial nitric oxide synthase in human umbilical vein endothelial cells.
World J. Gastroenterol. 12 (11), 1730-1738, 2006.
DOI: http://dx.doi.org/10.3748/wjg.v12.i11.1730.

DEBRECENI EGYETEM * Egyetemi és Nemzeti Könyvtár *

Total IF of journals (all publications): 30,413
Total IF of journals (publications related to the dissertation): 8,045

The Candidate's publication data submitted to the iDEa Tudóstér have been validated by DEENK on the basis of Web of Science, Scopus and Journal Citation Report (Impact Factor) databases.

06 September, 2018

KEYWORDS

Endothelial cells (ECs)

Protein phosphorylation

Myosin phosphatase (MP)

Endothelial nitric oxide synthase (eNOS)

Endothelial barrier function

Myosin light chain 20 (MLC20)

eNOS expression level

Adenosine

ATPγS

Protein kinase A (PKA)

A-kinase anchoring protein (AKAP)

TÁRGYSZAVAK

Endotél sejtek

Fehérje foszforiláció

Miozin foszfatáz (MP)

Endoteliális nitrogén monoxid szintáz (eNOS)

Endotél barrier funkció

Miozin könnyű lánc 20 (MLC20)

eNOS expressziós szint

Adenozin

ATPγS

Protein kináz A (PKA)

A-kináz kihorgonyzó fehérje (AKAP)

ACKNOWLEDGEMENT

I would like to express my utmost gratitude to my supervisor, Prof. Ferenc Erdődi, for his continuous guidance, support, and dedication in helping me to achieve my goals during my Ph.D. years. Thank you that I could be a member of the team.

Furthermore, I would like to thank Prof. László Virág and Prof. Pál Gergely the current and previous heads of the Department of Medical Chemistry for giving me the opportunity to work in the department.

I would like to thank for the Erdődi research group (Dr. Beáta Lontay, Dr. Andrea Kiss, Dr. Bálint Bécsi, Dr. Dóra Dedinszki, Zoltán Kónya, Dr. Dénes Nagy, Andrea Docsa and Dr. Árpádné Németh), furthermore for all the former and present fellow lab members for their valuable help, friendship, and caring they provided.

I am thankful to Dr. Alexander Verin for providing me the opportunity to work in his lab for more than two years, where I enhanced my technical skills.

I also would like to express my gratitude to Dr. David Fulton for his support, thoughtful suggestions and immense help.

Thank for all members of the Department of Medical Chemistry and Vascular Biology Center for that I could get help and useful suggestion all the time.

I also would like to thank for our collaborator partner their help and contributions to our work.

I sincerely thank for Zsuzsanna Bordán for her help, persistent love and encouragement.

Last, but not least I am grateful to my Family for their unconditional love, support, and encouragement that helped me through the hard times.

APPENDIX

The thesis is based on the following publlications: